

UNCLASSIFIED

AD 434300

DEFENSE DOCUMENTATION CENTER

FOR

SCIENTIFIC AND TECHNICAL INFORMATION

CAMERON STATION, ALEXANDRIA, VIRGINIA



UNCLASSIFIED

NOTICE: When government or other drawings, specifications or other data are used for any purpose other than in connection with a definitely related government procurement operation, the U. S. Government thereby incurs no responsibility, nor any obligation whatsoever; and the fact that the Government may have formulated, furnished, or in any way supplied the said drawings, specifications, or other data is not to be regarded by implication or otherwise as in any manner licensing the holder or any other person or corporation, or conveying any rights or permission to manufacture, use or sell any patented invention that may in any way be related thereto.

434300

434300

64-11

U. S. A R M Y

TRANSPORTATION RESEARCH COMMAND
FORT EUSTIS, VIRGINIA

TRECOM TECHNICAL REPORT 63-36

THE GENERAL CHARACTERISTICS OF WINGED
GROUND EFFECT MACHINES

Task 1D121401A14203
(Formerly Task 9R38-11-009-03)
Contract DA 44-177-TC-833

October 1963

prepared by:

PRINCETON UNIVERSITY
Princeton, New Jersey

100 9 1964



DISCLAIMER NOTICE

When Government drawings, specifications, or other data are used for any purpose other than in connection with a definitely related Government procurement operation, the United States Government thereby incurs no responsibility nor any obligation whatsoever; and the fact that the Government may have formulated, furnished, or in any way supplied the said drawings, specifications, or other data is not to be regarded by implication or otherwise as in any manner licensing the holder or any other person or corporation, or conveying any rights or permission, to manufacture, use, or sell any patented invention that may in any way be related thereto.

* * *

DDC AVAILABILITY NOTICE

Qualified requesters may obtain copies of this report from

Defense Documentation Center
Cameron Station
Alexandria, Virginia 22314

* * *

This report has been released to the Office of Technical Services, U. S. Department of Commerce, Washington 25, D. C. , for sale to the general public.

* * *

The findings and recommendations contained in this report are those of the contractor and do not necessarily reflect the views of the U. S. Army Mobility Command, the U. S. Army Materiel Command, or the Department of the Army.

HEADQUARTERS
U S ARMY TRANSPORTATION RESEARCH COMMAND
FORT EUSTIS, VIRGINIA

This report is published for the exchange of information and the stimulation of thought.

Francis E. LaCasse 2/Lt.
FRANCIS E. LA CASSE, 2/Lt
Project Engineer

James G. McHugh
JAMES G. MC HUGH
Group Leader
Aeromechanics Group

APPROVED.

FOR THE COMMANDER:

Larry M. Hewin
LARRY M. HEWIN
Technical Director

Task 1D121401A14203
(Formerly Task 9R38-11-009-03)
Contract DA 44-177-TC-833
TRECOM Technical Report 63-36

October 1963

THE GENERAL CHARACTERISTICS OF WINGED
GROUND EFFECT MACHINES

Report No. 657

Prepared by
Department of Aeronautical Engineering
Princeton University

for
U. S. Army Transportation Research Command
Fort Eustis, Virginia

FOREWORD

This report covers the work of three separate but related research efforts each looking into a particular phase of the over-all task. They are as follows:

Part I - - - An Analytical Investigation of the Winged Ground Effect Machine Concept, by Dale R. Summers.

Part II - - Model Studies of the Winged Ground Effect Machine Concept, by Captains Gerald P. Carr, USMC and John J. Metzko, USMC.

Part III - - Full Scale Flight Tests of a Winged Ground Effect Machine, by W. B. Nixon and A. F. Wojciechowicz, Jr.

The free bailment to Princeton University of the Curtiss-Wright Air Car ACM 6-1 by the Curtiss-Wright Corporation, thus making possible Part III of this work, is gratefully acknowledged.

TABLE OF CONTENTS

	Page
LIST OF SYMBOLS	vi
PART I AN ANALYTICAL INVESTIGATION OF THE WINGED GROUND EFFECT MACHINE CONCEPT	1
PART II MODEL STUDIES OF THE WINGED GROUND EFFECT MACHINE CONCEPT	35
PART III FULL SCALE FLIGHT TESTS OF A WINGED GROUND EFFECT MACHINE	55
BIBLIOGRAPHY	71
APPENDIX I	73
APPENDIX II	75
APPENDIX III	77
LIST OF FIGURES	82
FIGURES	85-138
DISTRIBUTION	139

LIST OF SYMBOLS

<u>Symbol</u>		<u>Dimensions</u>
A	Augmentation ratio	-
A ₀	Augmentation ratio without wings	-
A _j	Peripheral jet area	ft ²
A'	Reduced augmentation ratio due to forward velocity	-
AR	Aspect Ratio	-
b	Wing span	ft
\bar{c}_w	Characteristic length dimension - wing chord or base width	ft
C _D	Total aerodynamic drag coefficient	-
C _D [*]	Total drag coefficient; includes aerodynamic and momentum drag	-
C _l	Hover rolling moment coefficient	$\frac{x}{w}$
C _L	Aerodynamic lift coefficient	-
C _L [*]	Total lift coefficient; includes aerodynamic lift and base lift	-
C _M	Pitching moment coefficient	-
C _N	Total base lift coefficient	-
C _p	Base pressure coefficient	-
C _μ	Blowing momentum coefficient	-
D	Total aerodynamic drag	lb
D [*]	Total drag includes aerodynamic and momentum drag	lb
D _D	Duct or momentum drag	lb
D _f	Fuselage drag component	lb
D _w	Wing drag, profile and induced	lb
d _e	Equivalent diameter; diameter of a circle enclosing the same area as the GEM planform	ft
F _x	Force acting parallel to the x axis	lb
F _z	Force acting parallel to the z axis	lb

<u>Symbols</u>		<u>Dimensions</u>
g	Acceleration due to gravity	ft/sec^2
HP	Horsepower	-
h	Altitude of the vehicle	ft
$\frac{h}{w}$	Non-dimensional altitude	-
I_y	Moment of inertia about the Y axis	$\text{lb}\cdot\text{sec}^2\text{ft}$
i_t	Tail incidence	deg
i_w	Wing incidence	deg
J	Momentum of the air mass out the jet	lb
K_y	Radius of gyration	ft
L	Total aerodynamic lift of the GEM	lb
L^*	Total lift including aerodynamic and base lift	lb
$M_{a.c.}$	Wings moment about its aerodynamic center	$\text{ft}\cdot\text{lb}$
$M_{c.g.}$	Total moment about the GEM's center of gravity	$\text{ft}\cdot\text{lb}$
m	Mass of the vehicle	$\frac{\text{lb}\cdot\text{sec}^2}{\text{ft}}$
m_j	Mass rate of flow out the jets	lb/sec
N	Total base lift	lb
P	Power; or period	$\frac{\text{ft}\cdot\text{lb}}{\text{sec}}; \text{sec}$
P	Base pressure differential	lb/ft^2
P_c	Air cushion power	$\frac{\text{ft}\cdot\text{lb}}{\text{sec}}$
P_p	Propulsive power	$\frac{\text{ft}\cdot\text{lb}}{\text{sec}}$
q	Dynamic pressure	lb/ft^2
q_j	Jet dynamic pressure	lb/ft^2
R	Rouths discriminant	-
S_b	Area of the base - measured to the centerline of the peripheral jets	ft^2
S_t	Total planform area	ft^2
S_w	Total wing area	ft^2
t	Time	sec
$T_{\frac{1}{2}}$	Time to damp to half amplitude or double amplitude for an unstable root	sec
T	Total thrust	lb
V	Forward velocity of the vehicle	ft/sec
V_j	Average velocity of the air mass at the peripheral jet	ft/sec
W	Total weight of the vehicle	lb

<u>Symbols</u>		<u>Dimensions</u>
\bar{x}	Displacement of lift center from roll axis	ft
X_1	Distance along the X axis from the c.g. to the center of the base lift	ft
$X_{a.c.}$	Distance along the X axis from the c.g. to the wing aerodynamic center	ft
$Z_{a.c.}$	Distance along the Z axis from the c.g. to the wing aerodynamic center	ft
Z_2	Distance along the Z axis from the c.g. to duct drag center	ft
A,B,..K,K ₁ ,..	Constants and constant coefficients used in various sections	-
α	Angle of attack	-
ϕ	Angle of propulsive vanes	-
h	Displacement of bottom surface of wing from model base	ft
$\frac{h}{w}$	Non-dimensional wing displacement	-
Θ	Pitch angle and angle of inclination of the peripheral jet	-
γ	Angle between the relative wind and the local horizontal	-
ρ	Mass density	$\frac{lb \cdot sec^2}{ft^4}$
τ	Parameter used to non-dimensionalize time	sec
ϕ	Angle of roll	deg
λ	Momentum recovery parameter; also roots of characteristic equations	-
ψ	Angle of yaw	deg
μ	Non-dimensional mass parameter	-
$\ddot{\theta}$	Typical notation for differentiation with respect to time, two dots indicates second derivative etc.	1/sec
$\partial()$	Operator used to indicate differentiation with respect to non-dimensional time,	-
C_{mu}	Partial derivative of moment coefficient with respect to velocity perturbation $\partial C_m / \partial \frac{\Delta v}{V}$	-
CL_α	Typical short hand notation indicating the partial derivative of C_L with respect to α	-
η_i	Internal Efficiency	-
η_p	Propulsive efficiency	-

PART I AN ANALYTICAL INVESTIGATION OF THE WINGED GROUND EFFECT MACHINE CONCEPT

INTRODUCTION

The typical ground effect machine by its very nature must remain close to the surface over which it is operating. This inherent characteristic limits the maneuverability and performance of GEMs in general since they cannot develop adequate forces for turning by tilting their thrust vector as an airplane or helicopter does. In most early GEMs control was achieved by ducting some of the air mass laterally; this resulted in less air being supplied to the cushion and the GEM would settle slightly. More recently separate engine-propeller combinations have been used to supply additional thrust, these engines are usually swiveled and have reversible propellers thus side force and braking can be obtained.

Because of this low altitude performance a GEM must be flown over relatively smooth surfaces and in clear areas if a significant forward speed is to be maintained. A higher altitude can be attained by the addition of more power, more efficient ducting, lighter base loading and other refinements, however, as the altitude is increased the stability deteriorates and the GEM may become unflyable.

Wings added to the basic GEM would seem to offer a significant improvement in both maneuverability and performance. As a result of the increased altitude capability in forward flight, due to unloading the base, a larger angle of tilt could be employed for turning, forward thrust, and initial braking action. Another advantage of the winged GEM is its ability to divert more of the mass flow to thrust, when the increased altitude is not needed, thus reducing the momentum

drag and increasing its forward speed. A vehicle of this type would have the ability to cruise at a low altitude, i.e., low angle of attack, and then by increasing its angle of attack skip over an obstacle in its path. It is not proposed in this report, however, that the winged GEM have the ability to fly out of ground effect, the wings are added to partially unload the base of the GEM and thus improve its performance.

The purpose of this paper is to investigate the effects of wings on the performance and longitudinal stability of a GEM in forward flight. In section I the performance of a winged GEM is investigated analytically in three parts; augmentation at forward speed, power required and, lift to drag ratios that may be expected. A wing in ground effect experiences an increase in its lift to drag ratio (Reference 7) due to a decrease in the induced drag but, of more significance to the GEM application is the fact that maximum L/D occurs at a much higher C_L in ground effect than out of it. The total lift to drag ratio of a winged GEM remains quite small, however, due to the high drag of the GEM. The power required for forward flight is determined by taking into account the power needed for the air cushion to support the GEM's weight and the power needed to overcome the drag in forward flight. An analytical method is presented whereby the altitude ratio of a winged GEM may be predicted at any forward speed if the wing lift coefficient is known and the static or forward flight augmentation curve for the non-winged vehicle is available.

Section II deals with the longitudinal stability of a winged GEM from hover to forward flight. The classical small perturbation theory is used to obtain the equations of motion about some prescribed initial

equilibrium condition. A set of three simultaneous, partial differential equations with constant coefficients is obtained that represents the characteristic modes of motion of the winged GEM. This set of equations is then applied to the non-winged GEM and the two characteristic equations are compared.

An appendix section is included wherein some of the analytical methods described in this report are applied to the Curtiss-Wright Air Car ACM 6-1. A prediction of its forward flight altitude is presented along with a comparison of its longitudinal modes of motion with and without wings.

FORWARD FLIGHT PERFORMANCE

A. Augmentation

It is possible to modify the hovering augmentation curve or, if it is available, the forward flight augmentation curve to take into account the affect of putting wings on a GEM. The addition of wings to the basic GEM has the effect of making the GEM lighter as forward speed is increased. It will therefore be able to fly to a higher altitude for a given mass flow or at the same altitude while directing more of the lifting power to thrust, thus increasing its forward speed.

The analysis carried out here is based on the theoretical augmentation curve given by Chaplin in Reference 1. Since it is based on the theoretical augmentation curve, this work is entirely analytical, whereas, in actual practice it becomes semi-analytical and graphical since the augmentation curve for a particular vehicle is dealt with.

From Reference 1 the theoretical augmentation ratio of a peripheral jet of rectangular planform with zero initial jet angle is given by

$$A = 1 + \frac{1}{(1+\lambda)^{1/2} a_0} \quad (1)$$

where

a = rectangular width

b = rectangular length

λ = aspect ratio, a/b

a_0 = rectangular semi-width, a/2

The augmentation ratio, A, can be thought of as the total lift

coefficient needed to support the vehicle C_L^* . At any forward speed, that is $q > 0$, the total lift coefficient becomes,

$$C_L^* = \frac{W}{q S_w} \quad (2)$$

W = vehicles gross weight

S_w = total wing area of the GEM

q = dynamic pressure

and a new augmentation ratio can be calculated based on the apparent decrease in the vehicles weight due to the wing lift.

$$A' = \left(1 - \frac{C_L}{C_L^*}\right) A \quad (3)$$

C_L = wing lift coefficient

The term $\frac{C_L}{C_L^*}$ is simply the percentage by which the base is unloaded due to the aerodynamic lift created by the wing.

Equation (1) is rewritten expressing the altitude ratio, $\frac{h}{a_o}$ as a function of the augmentation.

$$\frac{h}{a_o} = \frac{1}{(1+\lambda)(A-1)} \quad (4)$$

The augmentation ratio, A , can now be replaced by its forward flight counter part A' , and the altitude of a winged GEM in forward flight is obtained as a function of its hovering augmentation ratio A , its total lift coefficient C_L^* , and its wing lift coefficient C_L ,

$$\frac{h}{a_o} = \frac{1}{(1+\lambda) \left[\left(1 - \frac{C_L}{C_L^*}\right) A - 1 \right]} \quad (5)$$

Equation (5) is plotted in Figure 4 for a vehicle with an aspect ratio of 3 and wing loadings of 20 and 40 lb/ft² at several forward speeds and a wing lift coefficient of unity. This plot clearly shows the effect of wing loading on the increase in $\frac{h}{a_0}$ at a constant q , the increase being five times as great for a wing loading of 20 lb/ft² over a wing loading of 40 lb/ft² at a q of 15 lb/ft².

In appendix I this method is used to predict the altitude capability of the Curtiss-Wright Air Car ACM 6-1, Reference 2, from its static augmentation curve for wing to base area ratios of 1.0 and 2.0. Also included in this appendix is a plot of absolute altitude versus velocity for $C_L=1.0$, and a range of wing to base area ratios. Unlike the augmentation plot this figure takes into account the loss in altitude of the air car as it gets under way.

B. Power Required

The total power required for a GEM, winged or non-winged, in forward flight is made up of two basic components; the air cushion power and the propulsive power. In mathematical terms,

$$P_{req.} = P_c + P_p \quad (6)$$

P_c = air cushion power required

P_p = propulsive power required

The air cushion power is derived in terms of the augmentation needed to support the vehicles weight not supported by the wing,

$$A = \frac{W-L}{m_j V_j} \quad (7)$$

L = aerodynamic lift.

Rewriting equation (7) and substituting $\rho A_j V_j$ for the mass flow,

$$\rho A_j V_j^2 = \frac{W-L}{A} \quad (8)$$

A_j = peripheral jet area.

Using the assumption that the jet static pressure is approximately one-half the base pressure, the jet power is given by

$$P_e = \frac{1}{2} \rho A_j V_j^3 + A_j V_j \frac{(W-L) - \frac{W}{A} \cos \Theta_0}{2 S_b} \quad (9)$$

Substituting equation (8) into equation (9)

$$P_e = \frac{1}{2} V_j (W-L) \left(\frac{1}{A} + \frac{A_j}{S_b} \right) - \frac{A_j V_j}{2 S_b} \frac{W}{A} \cos \Theta_0 \quad (10)$$

or in terms of horsepower

$$HP_e = \frac{1}{1100} V_j (W-L) \left(\frac{1}{A} + \frac{A_j}{S_b} \right) - \frac{W A_j V_j}{1100 A S_b} \cos \Theta_0 \quad (11)$$

The propulsive power is simply the power needed to overcome the total drag at a given velocity and can be expressed by,

$$P_p = D^* V \quad (12)$$

D^* = total drag.

The total drag D^* is given approximately by the following expression,

$$D^* = C_D q S_w + m_j V (1-\lambda) \quad (13)$$

C_D = aerodynamic drag coefficient, accounting for all drag except the momentum drag.

$m_j V$ = momentum drag.

λ = momentum drag recovery parameter.

The term λ also accounts for reduction in the drag due to the flow attachment effect of the fan which acts as a sink and thrust from the ejected air mass which is construed as momentum recovery.

The propulsive horsepower required becomes,

$$HP_p = \frac{V}{550} [C_D q S_w + m_j V (1-\lambda)] \quad (14)$$

and the total horsepower required as given by equation (6) is,

$$HP_{req.} = -\frac{W A_j V_j \cos \theta_0}{1100 A S_b} + \frac{1}{1100} V_j (W-L) \left(\frac{1}{A} + \frac{A_j}{S_b} \right) + \frac{V}{550} [C_D q S_w + m_j V (1-\lambda)] \quad (15)$$

Equation (15) can now be rearranged to show directly the effects of aerodynamic lift on the horsepower required.

$$HP_{req.} = \frac{1}{1100} V_j W \left(\frac{1}{A} + \frac{A_j}{S_b} \right) + \frac{V}{550} [C_D q S_w + m_j V (1-\lambda)] - \frac{1}{1100} V_j L \left(\frac{1}{A} + \frac{A_j}{S_b} \right) - \frac{W A_j V_j \cos \theta_0}{1100 A S_b} \quad (16)$$

This equation is of the form,

$$HP_{req.} = K - K_1 L$$

$$\text{where } K = -\frac{W A_j V_j \cos \theta_0}{1100 A S_b} + \frac{1}{1100} V_j W \left(\frac{1}{A} + \frac{A_j}{S_b} \right) + \frac{V}{550} [C_D q S_w + m_j V (1-\lambda)] \quad (17)$$

$$\text{and } K_1 = \frac{1}{1100} V_j \left(\frac{1}{A} + \frac{A_j}{S_b} \right)$$

which shows clearly the effect of the aerodynamic lift on reducing the total power required.

The above derivations are based on efficiency factors of one, thus the power required as given by equation (16) should be divided by the product of the various efficiency factors to obtain the true power required. Equation (16) is plotted in Fig. 5 which shows the horsepower required versus velocity of a vehicle having the following typical characteristics:

$$W = 4000 \text{ lb}$$

$$S_b = 100 \text{ ft}^2$$

$$S_w = 100 \text{ ft}^2$$

$$C_D = .20$$

$$S_j = 11.0 \text{ ft}^2$$

$$A = 6.25$$

In these plots the augmentation is held constant so that the jet momentum requirements decrease as the wings unload the base. Also λ is arbitrarily chosen to be .40 and is considered constant over the range of velocities investigated. Since a determination of the induced drag of the wings in ground effect is very difficult, the change in drag coefficient with wing lift coefficient is neglected. As can be seen in Figure 5, the wings substantially decrease the power requirements when the augmentation is held constant. Equation 15 also predicts power savings of a lesser degree when the base augmentation requirements are decreased by holding the jet momentum constant as the wing unloads the base. The reason for this is that with constant jet momentum, the total jet pressure requirements decrease as the wings unload the base.

C. Lift to Drag Ratio

One of the important advantages of adding wings to a GEM is to gain an increase in the lift to drag ratio. Since the total lift must always be equal to the weight this increase is accomplished by a reduction in the total drag. Drag reduction is accomplished by converting more of the air mass flow into thrust as the wings become effective, thus gaining more momentum recovery and supporting the vehicle on the more efficient wing.

The total lift can be expressed as follows,

$$L^* = q S_w C_L + \Delta P_b S_b + J \cos \Theta \cos \beta \quad (18)$$

S_b = base area enclosed by the jet, measured to the centerline of the jet.

ΔP_b = base pressure rise.

J = air mass momentum at the jet.

Θ = angle of inclination of the jet. (see Figure 3)

β = angle of thrust vanes in the jet. (see Figure 3)

Equation (18) is non-dimensionalized by dividing out $q S_t$, which yields,

$$C_L^* = C_L \frac{S_w}{S_t} + C_P \frac{S_b}{S_t} + C_\mu \cos \Theta \cos \beta \quad (19)$$

C_P = base pressure coefficient.

C_μ = momentum flux coefficient.

S_t = total planform area.

Next the total drag equation is examined. Equation (13) which gives the total drag is rewritten here,

$$D = C_D q S_w + m_j V (1 - \lambda) \quad (13)$$

which is non-dimensionalized as with the lift equation above,

$$C_D^* = C_D \frac{S_w}{S_t} + \frac{2 A_j V_j}{S_t V} (1 - \lambda) \quad (20)$$

and the lift to drag ratio becomes,

$$\frac{C_L^*}{C_D^*} = \frac{C_L \frac{S_w}{S_t} + C_p \frac{S_b}{S_t} + C_M \cos \beta \cos \theta}{C_D \frac{S_w}{S_t} + \frac{2 A_j V_j}{S_t V} (1 - \lambda)} \quad (21)$$

This equation can be expressed in a manner similar to equation (17) for horsepower which shows directly the effect of the aerodynamic lift in increasing the L/D ratio.

$$\frac{C_L^*}{C_D^*} = K_2 C_L + K_3 \quad (22)$$

$$K_2 = \frac{\frac{S_w}{S_t}}{C_D \frac{S_w}{S_t} + \frac{2 A_j V_j}{S_t V} (1 - \lambda)}$$

$$K_3 = \frac{C_p \frac{S_b}{S_t} + C_M \cos \theta \cos \beta}{C_D \frac{S_w}{S_t} + \frac{2 A_j V_j}{S_t V} (1 - \lambda)}$$

Equation (21) is plotted in Fig. 6 for the same typical parameters used in the plot of Fig. 5, and also for $\theta = \beta = 0$. The fact that the curves tend toward infinity at zero velocity is merely an illustration of the fact that the total drag is zero at zero velocity while the lift is finite and equal to the vehicles weight.

LONGITUDINAL STABILITY ANALYSIS

An analysis of the static and dynamic longitudinal stability of a winged GEM will be discussed in this section. Comparisons of the various stability derivatives for a winged and non-winged GEM in forward flight will be attempted. Hover stability will also be dealt with briefly.

The static stability of a vehicle is defined as its tendency to return to its initial equilibrium position after it is disturbed. The assumption of an initial equilibrium position will be carried throughout this analysis. Dynamic stability on the other hand is concerned with the manner in which the disturbed vehicle returns to its equilibrium position - assuming a stable vehicle. Thus two areas of interest are defined; 1, whether or not the vehicle returns to its equilibrium position when disturbed; 2, the frequency and damping of the vehicle's motion as it returns to its equilibrium position.

A. Static Stability

The static stability of a winged GEM is determined by summing the moments acting about the center of gravity of the vehicle. For the vehicle to be in equilibrium flight the sum of the moments must equal zero; from Figure 1,

$$\begin{aligned}\sum M_{CG} &= 0 \\ \sum M_{CG} &= NX_1(\theta) + M_{ac} + L \cos \alpha X_{ac} - D_D Z_2 - D_W Z_{ac} \cos \alpha \\ &\quad + D_W X_{ac} \sin \alpha - L Z_{ac} \sin \alpha = 0\end{aligned}$$

(23)

X and Z are measured from the center of gravity and are positive forward and down respectively. The aerodynamic forces are positive as shown in Fig. 1. Equation (23) is non-dimensionalized by dividing by $Q S \bar{c}$ and the small angle assumption is introduced, where $\sin \alpha \cong \alpha$; $\cos \alpha \cong 1$, in arriving at equation (24).

$$C_{m_{c.g.}} = C_N \frac{X_1(\theta)}{\bar{c}} + C_{m_{a.c.}} + C_L \frac{X_{a.c.}}{\bar{c}} + C_{D_b} \frac{Z_2}{\bar{c}} - C_{D_w} \frac{Z_{a.c.}}{\bar{c}} + C_{D_w} \frac{X_{a.c.}}{\bar{c}} \alpha - C_L \frac{Z_{a.c.}}{\bar{c}} \alpha = 0 \quad (24)$$

There are three possible static stability derivatives that are of interest; $\frac{\partial C_m}{\partial \alpha}$; $\frac{\partial C_m}{\partial \theta}$; $\frac{\partial C_m}{\partial V}$; , for any given machine all three may or may not exist. To evaluate the static angle of attack stability, equation (24) is differentiated with respect to α yielding,

$$\frac{\partial C_m}{\partial \alpha} = C_{m\alpha} = C_{N\alpha} \frac{X_1(\theta)}{\bar{c}} + C_{L\alpha} \frac{X_{a.c.}}{\bar{c}} - C_{D_w\alpha} \frac{Z_{a.c.}}{\bar{c}} + C_{D_w\alpha} \frac{X_{a.c.}}{\bar{c}} \alpha_o + C_{D_w} \frac{X_{a.c.}}{\bar{c}} - C_{L\alpha} \frac{Z_{a.c.}}{\bar{c}} \alpha_o - C_L \frac{Z_{a.c.}}{\bar{c}} \quad (25)$$

Some simplifications can be made immediately based on the following assumptions, which may or may not be valid depending on the particular vehicle. The center of aerodynamic lift is assumed to be on the X axis

and the initial angle of attack is assumed to be zero, thus,

$$\alpha_0 \equiv \frac{Z_{a.c.}}{\bar{c}} \equiv 0$$

This leaves finally equation (26) for static stability derivative, $C_{m\alpha}$,

$$C_{m\alpha} = C_{N\alpha} \frac{\lambda_1(\theta)}{\bar{c}} + C_{L\alpha} \frac{\lambda_{a.c.}}{\bar{c}} + C_{Dw} \frac{\lambda_{a.c.}}{\bar{c}} \quad (26)$$

It may not be readily apparent that the derivative $C_{N\alpha}$ exists and in fact for a non-winged GEM where the only lift acting on the vehicle is N it would not exist. Here, however, the vehicle may be assumed to be flying at some angle of attack and equilibrium altitude with a portion of total weight supported by the wing. It may also be assumed that the vehicle can change its angle of attack slightly thus increasing the wing lift and decreasing the value of N needed for the equilibrium altitude. $C_{N\alpha}$ will therefore have a negative slope and in fact should be very close in absolute value to $C_{L\alpha}$ by the above argument.

Equation (26) indicates a stable $C_{m\alpha}$ for a wing that is mounted with its aerodynamic center behind the center of gravity and for $\lambda_1(\theta)$ positive. For a GEM that relies solely on its base lift to support its weight this derivative does not exist except possibly as a small change in the momentum drag due to the angle the air mass is turned.

An investigation of the velocity stability is carried out to determine the vehicles behaviour to a sudden small increase or decrease in velocity. To exhibit positive velocity stability, the GEM when disturbed from its equilibrium velocity should show a tendency to return to its equilibrium velocity.

Equation (24) is differentiated with respect to the velocity,

$$\frac{\partial C_m}{\partial V} = C_{mv} = C_{Ddr} \frac{Z_2}{c} . \quad (27)$$

This is the major term affecting C_{mv} , however, there may be a small contribution to this derivative due to deformation of the jet curtain and thus a change in the center of base lift. This effect if it exists would be small and is neglected along with all the other terms of equation (24) which are independent of velocity. The velocity stability given by equation (27) is seen to be a function of the momentum drag and the distance from the center of gravity to the duct inlet. This derivative will be about the same for a winged or non-winged GEM and should be positive for positive velocity stability, thus an increase in the velocity will cause a nose up moment which will tend to reduce the velocity back to its equilibrium value.

The third static stability derivative is the attitude stability and is caused by a change in the GEM's center of lift when its pitch angle is changed. This derivative has often been called $C_{m\alpha}$ in the literature for hover experiments, however, the term $C_{m\theta}$ will be employed here to distinguish it from the true $C_{m\alpha}$.

Equation (24) is again differentiated, this time with respect to the pitch angle, θ ,

$$\frac{\partial C_m}{\partial \theta} = C_{m\theta} = C_N \frac{X_1}{c} . \quad (28)$$

Where X_1 is a function of θ and includes possible differences in jet reaction forces between the high and low end.

X_1 is simply the distance from the Z axis to the center of the base lift. This derivative is most significant as a hovering parameter since for the GEM in forward flight the angle of attack is almost always equal to the pitch angle. To be stabilizing the sign of this derivative should be negative thus, if the pitch angle is disturbed, a restoring moment will be created tending to return the vehicle to its equilibrium position. Most work published dealing with hover stability, however, shows the vehicle to be stable only at very low altitudes although the addition of wings to the basic GEM appears to provide stability at a useable altitude, $h/c > .5$, Ref. 6.

B. Hover Stability

For the hovering GEM with or without wings the static stability derivatives are the same except possibly for the sign of $C_{m\theta}$ as discussed above. Equation (23) is rewritten for the hovering GEM in equilibrium,

$$\sum M_{CG} = N X_1(\theta) = 0. \quad (29)$$

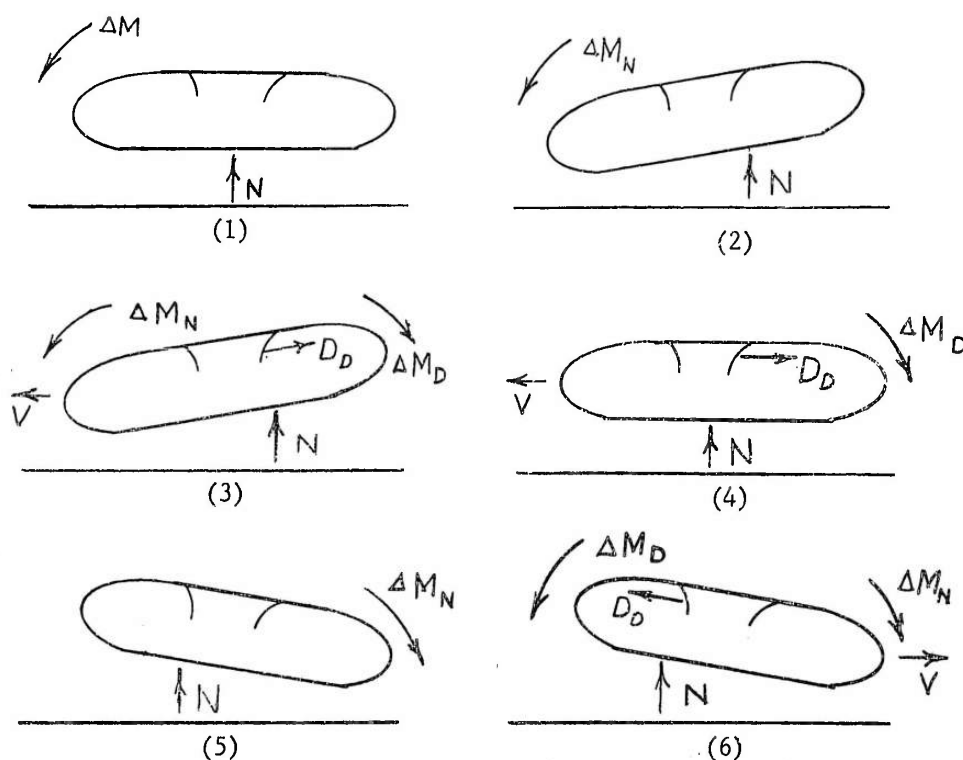
Since at hover $q=0$ this equation is non-dimensionalized by dividing it by $(q + \Delta P) S \bar{c}$ which results in the non-dimensional moment equation in coefficient form,

$$C'_{m_{CG}} = C'_N \frac{X_1(\theta)}{\bar{c}} = 0. \quad (30)$$

Differentiating this expression with respect to the pitch angle θ results in the same expression for $C_{m\theta}$ as in forward flight,

$$\frac{\partial C_m}{\partial \theta} = C_{m\theta} = C_N \frac{x_i}{c} \quad (31)$$

Experimental data seems to indicate that this is the important stability parameter for a hovering GEM, however, as the forward speed is increased the aerodynamic forces become predominant. In attempting to measure moments in a wind tunnel or on a full scale machine this derivative would be absorbed in the $C_{m\alpha}$ derivative. Before leaving this subject there is one other possibility that should be explored. If $C_{m\theta}$ above is positive there will be a coupling between the pitch and the velocity equations that will cause an oscillation in pitch angle and velocity. This may be seen physically by the following sequence of pictures.



Hovering GEM with positive $C_{m\theta}$ and C_{mv} .

This sequence shows qualitatively the motions of a hovering GEM with a positive $C_{m\theta}$ and $C_{m\dot{\theta}}$ derivatives. The GEM in equilibrium at hover is disturbed by a force causing the moment ΔM . The GEM then pitches over and since $C_{m\theta}$ is positive continues to pitch and picks up a translational velocity component from the base lift. This velocity causes a momentum drag on the duct which creates a moment, ΔM_D , to oppose the positive $C_{m\theta}$ and when it becomes large enough to overcome the, ΔM_N , the GEM tips in the opposite direction and the process is repeated as often as the damping will allow. This is actually a dynamic stability and results in an oscillation in pitch angle and velocity.

The heave mode has not been dealt with in this brief analysis since it is felt that nothing could be presented that is not already in the extensive literature on this subject (Ref. 3). This mode is usually a heavy convergence for a GEM at constant power and becomes more heavily damped as the base loading is increased.

C. Dynamic Longitudinal Stability

The dynamics of a GEM, similar to the dynamics of an airplane, involve translation along three mutually perpendicular axes and rotations about them. The axis system used in this analysis, Fig. 1, is the standard NASA system of body axes. The positive X direction is along the vehicles longitudinal axis and in its direction of motion. The positive Y axis is out the right wing and perpendicular to X, while Z is positive downward and perpendicular to both X and Y. The origin of the coordinate system is the vehicles center of gravity. In this analysis the motion in the vertical plane and about the Y axis will be

assumed to be uncoupled from the motion in the horizontal plane. This simplification, used in most air-craft stability analyses, immediately reduces the problem from one of solving six simultaneous differential equations to one solving a set of three.

The method used to obtain the equations of motion is the classical small perturbation theory. This involves the assumptions that initially the vehicle is flying at some steady equilibrium condition and that small deviations from this equilibrium may be assumed linear and thus may be examined using a linear theory. There are three separate types of forces acting on the vehicle; 1, aerodynamic forces; 2, gravity forces; 3, inertia reaction forces. The forces are summed along the X and Z axes and moments are taken about the Y axis. The aerodynamic forces are then expanded by a Taylors series about the steady state equilibrium value and only the linear first order terms are retained. These expanded forces are then substituted into the equations of motion, the steady state terms are subtracted out and the dynamic equations of longitudinal motion remain.

Summing the three types of forces and moments acting on the winged GEM and equating to zero, using d'Alembert's inertia-resistance principle, yields

Lift equation

$$F_z = F_z \text{ aero.} + F_z \text{ gravity} + F_z \text{ inertia} = 0 \quad (a)$$

Drag equation

$$F_x = F_x \text{ aero.} + F_x \text{ gravity} + F_x \text{ inertia} = 0 \quad (b) \quad (32)$$

Moment equation

$$M_y = M_y \text{ aero.} + M_y \text{ inertia} = 0 \quad (c)$$

Resolving the aerodynamic and gravity forces acting on the winged GEM as shown in Fig. 1 and equating to zero results in the equations of motion for the initial equilibrium condition.

Lift equation

$$F_{Z(A+G)} = W \cos \theta - L \cos \alpha - N - D \sin \alpha = 0 \quad (a)$$

Drag equation

$$F_{X(A+G)} = T - D_b - D \cos \alpha - W \sin \theta - L \sin \alpha = 0 \quad (b) \quad (33)$$

Moment equation

$$M_{Y(A)} = N X_1(\theta) + M_{a.c.} - L X_{a.c.} - D_b Z_2 + D_w (X_{a.c.} \alpha - Z_{a.c.}) - L Z_{a.c.} \alpha = 0 \quad (c)$$

Introducing the small angle approximation where;

$$\begin{aligned} \sin \alpha &\cong \alpha & \cos \alpha &\cong 1 \\ \sin \theta &\cong \theta & \cos \theta &\cong 1 \end{aligned}$$

and denoting initial conditions by the subscript o, equations (33)

become,

$$\begin{aligned} W_o - L_o - N_o - D_o \alpha &= 0 \quad (a) \\ T_o - D_{b_o} - D_o - W_o \theta - L_o \alpha &= 0 \quad (b) \\ N_o X_1(\theta) + M_{a.c.o} + L_o X_{a.c.} - D_{b_o} Z_2 + D_{w_o} X_{a.c.} \alpha - Z_{a.c.} - L_o Z_{a.c.} \alpha &= 0 \quad (c) \end{aligned} \quad (34)$$

The inertia resistance terms from Fig. 2 are introduced into equations (33) to give the longitudinal dynamic equations of motion for the winged GEM.

Lift equation

$$W - L - N - D \alpha + m V \ddot{\gamma} - m \dot{V} \alpha = 0 \quad (a)$$

Drag equation

$$T - D_b - D - W \theta - L \alpha - m \dot{V} - m V \ddot{\gamma} \alpha = 0 \quad (b) \quad (35)$$

Moment equation

$$N X_1(\theta) + M_{a.c.} + L X_{a.c.} - D_b Z_2 + D_w (X_{a.c.} \alpha - Z_{a.c.}) - L Z_{a.c.} \alpha - I_y \ddot{\theta} = 0 \quad (c)$$

Now the lift equation will be examined in detail. Expanding the aerodynamic forces in terms of the variables of interest, α , V and, θ yields,

$$\begin{aligned} L &= L_o + \frac{\partial L}{\partial V} \Delta V + \frac{\partial L}{\partial \alpha} \Delta \alpha + \dots \\ N &= N_o + \frac{\partial N}{\partial V} \Delta V + \frac{\partial N}{\partial \alpha} \Delta \alpha + \dots \\ D &= D_o + \frac{\partial D}{\partial V} \Delta V + \frac{\partial D}{\partial \alpha} \Delta \alpha + \dots \end{aligned} \quad (36)$$

These values are substituted into the lift equation and with some rearranging it becomes,

$$\begin{aligned} W_o - L_o - N_o - D_o \alpha - \left(\frac{\partial L}{\partial V} + \frac{\partial N}{\partial V} + \frac{\partial D}{\partial V} \alpha \right) \Delta V \\ - \left(\frac{\partial L}{\partial \alpha} + \frac{\partial N}{\partial \alpha} + \frac{\partial D}{\partial \alpha} \alpha \right) \Delta \alpha + m V \ddot{\gamma} - m \dot{V} \dot{\alpha} = 0 \end{aligned} \quad (37)$$

Separating the variables into their steady state and perturbation quantities, yields;

$$\begin{aligned} \alpha &= \alpha_o + \Delta \alpha & \dot{\alpha} &= \dot{\alpha}_o + \Delta \dot{\alpha} \\ \theta &= \theta_o + \Delta \theta & \dot{\theta} &= \dot{\theta}_o + \Delta \dot{\theta} \\ V &= V_o + \Delta V & \dot{V} &= \dot{V}_o + \Delta \dot{V} \end{aligned}$$

and defining the following terms,

$$\frac{\Delta V}{V} = u, \quad \gamma = \theta - \alpha, \quad \dot{\gamma} = \dot{\theta} - \dot{\alpha},$$

from the initial conditions,

$$\dot{V}_o \equiv \alpha_o \equiv \dot{\alpha}_o \equiv \dot{\theta}_o \equiv 0.$$

Introducing these terms into equation (37) and subtracting out the steady state flight condition yields the following,

$$\begin{aligned} - \left(\frac{\partial L}{\partial V} + \frac{\partial N}{\partial V} \right) \Delta V - \left(\frac{\partial L}{\partial \alpha} + \frac{\partial N}{\partial \alpha} + D_o \right) \Delta \alpha \\ + m [V(\dot{\theta} - \dot{\alpha}) - \dot{V} \Delta \alpha] = 0 \end{aligned} \quad (38)$$

The aerodynamic terms are written in coefficient form and the indicated derivatives taken.

$$\begin{aligned}
 L &= \frac{1}{2} \rho S V^2 C_L \\
 N &= \frac{1}{2} \rho S V^2 C_N \\
 D &= \frac{1}{2} \rho S V^2 C_D \\
 \frac{\partial L}{\partial V} &= \rho S V C_L & \frac{\partial L}{\partial \alpha} &= \frac{1}{2} \rho S V^2 C_{L\alpha} \\
 \frac{\partial N}{\partial V} &= \rho S V C_N & \frac{\partial N}{\partial \alpha} &= \frac{1}{2} \rho S V^2 C_{N\alpha} \\
 \frac{\partial D}{\partial V} &= \rho S V C_D & \frac{\partial D}{\partial \alpha} &= \frac{1}{2} \rho S V^2 C_{D\alpha}
 \end{aligned}$$

Substitution of these partials into equation (38) and dividing out ρS yields,

$$-2(C_L + C_N) \frac{\Delta V}{V} - (C_{L\alpha} + C_{N\alpha} + C_D) \Delta \alpha + \frac{2m}{\rho S V^2} [V(\dot{\theta} - \dot{\alpha}) - \dot{V} \Delta \alpha], \quad (39)$$

all that remains now is to rewrite the inertia reaction term and the lift equation will be completely non-dimensionalized.

$$\frac{2m}{\rho S V^2} [V(\dot{\theta} - \dot{\alpha}) - \dot{V} \Delta \alpha] = \frac{2m}{\rho S V^2} [V(\Delta \dot{\theta} - \Delta \dot{\alpha}) - \dot{V} \Delta \alpha]. \quad (40)$$

The second term in the brackets is zero by the assumption that products of perturbations are zero. Introducing the non-dimensional time parameter, τ , and the operator $\bar{d}()$ where,

$$\tau = \frac{m}{\rho S V^2},$$

and,

$$\bar{d}() = \frac{d()} {d(\frac{t}{\tau})},$$

the inertia reaction term becomes,

$$\begin{aligned}
 \frac{2m}{\rho S V^2} V(\Delta \dot{\theta} - \Delta \dot{\alpha}) &= 2\tau(\Delta \dot{\theta} - \Delta \dot{\alpha}) \\
 2\tau(\Delta \dot{\theta} - \Delta \dot{\alpha}) &= 2[\bar{d}(\Delta \theta) - \bar{d}(\Delta \alpha)]
 \end{aligned}$$

and finally the lift equation is reduced to a non-dimensional partial differential equation with constant coefficients,

$$2(C_L + C_N)u + (C_{L\alpha} + C_{N\alpha} + C_0 + 2d)\Delta\alpha - 2d\Delta\theta = 0 \quad (41)$$

The drag and moment equations are derived in a similar manner.

Drag equation

$$(C_L - C_{D\alpha})\Delta\alpha - 2(C_{D_0} + C_0 + d)u - C_W\Delta\theta = 0 \quad (42)$$

Moment equation

$$(C_{m\alpha} - C_{m\alpha d}d)\Delta\alpha + (C_{mu})u + (C_{m\theta} + C_{m\theta d}d - h d^2)\Delta\theta = 0 \quad (43)$$

This set of three simultaneous differential equations contain many terms that look familiar and in fact some that are identical for a winged GEM or an airplane. Some of them are different, however, and a discussion of all the terms comprising the coefficients will be undertaken:

$C_L + C_N$ This combination of terms is the aerodynamic lift coefficient and the base lift coefficient. Since the GEM is in steady flight and the total lift must equal the total weight of the vehicle, this combination of terms is simply C_W and will be the same for a winged or non-winged GEM.

$C_{L\alpha} + C_{N\alpha}$ Another combination of terms, however, this set is only found in the winged GEM. This combination of terms should be equal to zero or at least negligible by an argument similar to the above. The total weight of the vehicle is supported by the wings and the base lift and since the

total lift must always equal the weight an increase in the angle of attack which increases the wing lift must be accompanied by a decrease in the base lift to remain at the equilibrium altitude. This term could be considered $C_{W\alpha}$ which obviously does not depend on angle of attack.

C_D

This term is the aerodynamic drag coefficient and takes into account all GEM's drag except the duct or momentum drag. The drag coefficient will be approximately the same for a winged or non-winged GEM.

$C_{D\alpha}$

This is simply the slope of drag versus angle of attack curve. For the angles considered in this analysis $C_{D\alpha}$ will be assumed negligible for either a winged or non-winged GEM.

C_{D_D}

This term is peculiar to GEM's, it is the momentum drag which comes from turning the air mass into the plenum chamber. The air is assumed to be turned through 90 degrees and stopped in the plenum. Whether or not the GEM has wings will have no effect on this parameter.

C_W

This is the so-called weight coefficient. In airplane investigations where lift is always equal to the weight this term is replaced by C_L . This term will be essentially the same whether the GEM has wings or not.

$C_{m\alpha}$

The classical angle of attack stability. This derivative

was derived in the static stability section where it was shown to be a function of the wing placement on the fuselage. For a non-winged GEM α has no meaning, therefore, $C_{m\alpha}$ would have no meaning and would be replaced by $C_{m\theta}$.

$C_{m\dot{\alpha}}$

This is the angle of attack damping from airplane dynamics, which comes from the fact that the angle of attack of the wing may change and it takes a finite time for this change to be effective at the tail. For a GEM without a horizontal tail this term is negligible whether the GEM has wings or not.

$C_{m\dot{u}}$

This derivative is the velocity stability term derived in the static stability section. The principle component of this derivative is the duct or momentum drag, however, if the GEM has thrust vanes in the slot the force on these vanes when combined with the duct drag forms a couple. At the same time the overall momentum drag is reduced as the thrust is momentum recovery. Wings would have no effect on this term.

$C_{m\theta}$

This is the third static stability parameter, the attitude stability, and was also derived in the static section. It comes from the fact that the center of the base lift changes with pitch angle, and is not dependent on whether the vehicle has wings except as discussed in the static section. For this analysis this term will be assumed to be negligible.

$C_{m\dot{\alpha}\theta}$

This term is the pitch damping and in airplane stability is due primarily to the horizontal tail. For the winged GEM considered here, with no horizontal tail, this term will be assumed negligible although some pitch damping will undoubtedly occur especially at low altitudes due to the curtain action. Also with the wing behind the center of gravity some contribution to the damping will result.

h

This is the non-dimensional mass parameter which comes from the inertia reaction term.

A solution for the three equations of motion is assumed to have the following form,

$$\begin{aligned}u &= u_1 e^{\lambda t/\tau} \\ \alpha &= \alpha_1 e^{\lambda t/\tau} \\ \theta &= \theta_1 e^{\lambda t/\tau}\end{aligned}$$

making these substitutions into the three equations along with the simplifications indicated above and writing in matrix form results in,

$$\begin{bmatrix} \frac{u}{2 C_W} & \frac{\alpha}{C_D + \lambda} & \frac{\theta}{-2\lambda} \\ -2(C_{D_0} + C_D + \lambda) & C_L & -C_W \\ C_{m\dot{u}} & C_{m\dot{\alpha}} & -h\lambda^2 \end{bmatrix} . \quad (44)$$

The fourth order equation resulting from the expansion of the determinate of this matrix when set equal to zero yields the characteristic modes of motion for the winged GEM.

$$\begin{vmatrix} \frac{u}{2C_W} & \frac{\alpha}{C_D+2\lambda} & \frac{\theta}{-2\lambda} \\ -2(C_{D_0}+C_D+\lambda) & C_L & -C_W \\ C_{mu} & C_{m\alpha} & -h\lambda^2 \end{vmatrix} = 0 \quad (45)$$

$$\begin{aligned} & \lambda^4 + \left(\frac{3}{2}C_D + C_D\right)\lambda^3 + \left(\frac{C_L C_W}{2} + \frac{C_D C_{D_0}}{2} + \frac{C_D^2}{2} - \frac{C_{m\alpha}}{h}\right)\lambda^2 \\ & + \left(\frac{C_W C_{mu}}{2h} - \frac{C_{m\alpha} C_{D_0}}{h} - \frac{C_{m\alpha} C_D}{h} - \frac{C_L C_{mu}}{2h}\right)\lambda \\ & + \left(\frac{C_W C_{mu} C_D}{4h} - \frac{C_W^2 C_{m\alpha}}{2h}\right) = 0 \end{aligned} \quad (46)$$

Much valuable information can be obtained about the stability of the system represented by the characteristic equation from examining the signs of the coefficients. This is best done by applying Rouths discriminant. Rouths discriminant for a fourth order system is given by, (Ref. 5)

$$BCD - AD^2 - B^2E = R. \quad (47)$$

If all the coefficients A to E have the same sign there can be no pure divergent root, however, there may be an oscillatory divergence. If there is one sign change there will be either a pure divergent root or a divergent oscillation. If Rouths discriminant is positive there cannot be a divergent oscillation, if negative, there will be a divergent oscillation. Finally, if Rouths discriminant is zero one of the roots will be an undamped oscillation.

The coefficients listed in descending order of their powers are,

$$A = 1$$

$$\begin{aligned}
B &= \frac{3}{2} C_D + C_{D0} \\
C &= \frac{C_L C_W}{2} + \frac{C_D C_{D0}}{2} + \frac{C_D^2}{2} - \frac{C_{m\alpha}}{h} \\
D &= \frac{C_W C_{m_u}}{2h} - \frac{C_{m\alpha} C_{D0}}{h} - \frac{C_{m\alpha} C_D}{h} - \frac{C_L C_{m_u}}{2h} \\
E &= \frac{C_W C_{m_u} C_D}{4h} - \frac{C_W^2 C_{m\alpha}}{2h}
\end{aligned}$$

Coefficients A and B will always be positive; C will be positive for negative $C_{m\alpha}$. E will probably be positive also for negative $C_{m\alpha}$, since C_W^2 is the dominant term of this coefficient. This leaves only the D coefficient to be examined. If C_{m_u} is positive (stabilizing) and $C_{m\alpha}$ is negative (also stabilizing) the sign of the D coefficient will always be positive since C_W is always greater than C_L or at most if the winged GEM were allowed to fly C_W would equal C_L . Therefore with all coefficients positive a pure divergent root is not possible but an unstable oscillation is possible.

This equation is solved in Appendix II for a "typical" winged GEM based on the Curtiss-Wright Air Car ACM 6-1 for a range of values for $C_{m\alpha}$ and C_{m_u} .

The characteristic equation for the non-winged GEM can be developed directly from the determinate of coefficients for the winged GEM. Since the GEM has no wings there will be no aerodynamic lift thus the base lift must always equal the weight of the vehicle. Flight can be conducted at only one altitude, for a given power setting, therefore the lift equation and the perturbation in angle of attack are meaningless. The determinate of coefficients then reduces to,

$$\begin{vmatrix} u & \\ -2(C_{D_p} + C_D + \lambda) & -C_w \\ C_{m_u} & -h\lambda^2 \end{vmatrix} = 0 \quad (48)$$

Expanding this characteristic determinate yields the characteristic equation of longitudinal motion for the non-winged GEM,

$$\lambda^3 + (C_{D_p} + C_D)\lambda^2 + \frac{C_w C_{m_u}}{2h} = 0 \quad (49)$$

Examining the coefficients of this characteristic equation as with the quartic for the winged GEM,

$$A = 1$$

$$B = C_{D_p} + C_D$$

$$C = 0$$

$$D = \frac{C_w C_{m_u}}{2h}$$

It is apparent that all the signs of the coefficients will be positive if C_{m_u} is positive and the only sign that can change is the sign of D, which is dependent on C_{m_u} . Thus as before a pure divergent root is impossible for a stable C_{m_u} while an oscillatory divergence is possible.

Again applying Routh's discriminant, which, for a third order system is, $BC - AD = R$.

Using this criterion it is possible to state that for a stable C_{m_u} , R will be negative, therefore, the roots of the characteristic equation will be a divergent oscillation and a convergent real root. Conversely if C_{m_u} is unstable the characteristic equation (49) will yield an unstable real root and a stable oscillation. A "typical" example of this characteristic equation is also worked out in appendix II and compared to the winged GEM case.

DISCUSSION

Placing wings on a ground effect machine appears likely to offer many advantages, especially when operating at moderate forward speeds. There are also some disadvantages associated with the winged GEM the chief of which is probably the planform size and shape which might be considered cumbersome and unwieldy. The winged GEM would indeed have to be operated over relatively clear areas because of its size, however, the non-winged GEM is restricted to clear areas also for maneuverability if it is to travel at moderate forward speeds. If foldable wings were employed on the GEM the size of the planform could be suited to the area of operation.

It should come as no surprise to anyone that a winged GEM would be able to cruise at higher altitudes than its predecessor the non-winged GEM. The actual altitude attainable is however, strongly dependent on the wing loading, as indicated by Figure 4, and also of course on the forward speed of the GEM. A good altitude gain, however, can be expected for a reasonable wing area at moderate speeds for almost any GEM.

One of the big advantages of putting wings on the GEM is a decrease in the total power required for forward flight. The curves shown in Figure 5 illustrate how the aerodynamic lift affects the total power required for forward flight. This plot is based on a constant total augmentation which means the GEM must gain some altitude as its forward speed is increased, Figure 4. Thus if the altitude was held constant more of the air mass could be directed rearward increasing the momentum drag recovery and enabling the GEM to go faster.

Significant increases in the lift to drag ratios are indicated as the lift coefficient or the velocity is increased. Since the total lift remains the same, this increased L/D is the result of decreasing the drag, principally the momentum drag, as the wing assumes support of a larger and larger portion of the vehicles gross weight. This simply indicates that the wing is more efficient than the air cushion as the forward speed builds up.

There are three static stability derivatives that should be considered in the stability analysis of GEMs. These are the conventional angle of attack stability and velocity stability and, the attitude stability which is peculiar to GEM type vehicles. For the winged GEM the angle of attack stability derivative appears to be the most significant of the three. The attitude stability term is of significance only for hover studies since in all probability it will be included in the angle of attack stability term for forward flight investigations. The angle of attack stability is as with the airplane primarily dependent on the location of wing with respect to the vehicles center of gravity.

The velocity stability parameter is a function of the air mass that is ingested by the GEM, the position of its air intakes and its forward velocity. In computing this term the air is assumed to be turned 90° and its velocity slowed to zero in the plenum chamber. The drag at the intake duct resulting from the change in momentum of the air mass is the main source of this moment, however, as the air mass leaves the peripheral jet and is deflected rearward as thrust by the β vanes another component is introduced. These two components will form a couple

tending to produce a nose up moment. Two other smaller effects may be present; one the jet flap action of the rear curtain as the front curtain washes back and the sink effect of the fan pulling the air into the plenum.

Position or attitude stability is unique to the GEM class of vehicles and arises from the fact that as the pitch angle of the vehicle changes, the center of base lift also changes. There are two primary causes of this action; the first, a destabilizing effect, is due to a trapped vortex under the base just inside the jet curtain. The strength of this vortex increases on the low side of the vehicle allowing it to settle lower which increases the vortex strength etc. The second effect occurs at very low altitudes. When one side of the GEM gets very close to the surface the jet reaction on the surface resists the downward movement and a restoring force results. Thus GEMs are stable at low altitudes and unstable at high altitudes which has been born out experimentally.

The dynamic equations of motion for the winged GEM were simplified by neglecting the angle of attack and pitch damping. These assumptions appear to be reasonable for the winged GEM since the angle of attack damping is usually associated with the horizontal tail and wing down wash. This term is zero since the winged GEM in question has no horizontal tail and the down wash in ground effect is negligible. Pitch damping would result from the action of the jet curtain on the surface at low altitudes and some damping will likely be associated with the wing due to its position behind the center of gravity of the vehicle. These parameters are likely small and the assumptions valid at least for the winged GEM. The addition of the pitch damping term to the

equations of the non-winged GEM may be warranted on the basis that this GEM will not be at a very high altitude and thus the damping from the jet curtain may not be negligible. The inclusion of this term would tend to increase the damping of the oscillatory mode and reduce its frequency slightly.

Throughout this analysis it is assumed that the vehicle has enough control to enable it to be flown at some equilibrium condition, how this control is achieved is not of interest in this paper.

CONCLUSIONS

The conclusions that can be drawn from an analysis of this sort are rather limited and for the most part were discussed in the body of the report. They are, however, all brought together here.

1. The forward flight altitude capability of the GEM can be increased considerably by the addition of wings. This is accomplished by unloading the base with aerodynamic lift while keeping the mass flow to the air cushion constant. An alternative to this is an increase in forward speed for a constant altitude by directing the excess mass flow rearward as thrust.

2. The total horsepower required for forward flight can be reduced by the addition of wings for the same reason as stated above. The increased thrust appears as momentum drag recovery thus the total drag is decreased and less power is required at a given speed.

3. The longitudinal dynamic motions of the winged GEM appear to be more neutrally stable than the comparable motions of the non-winged GEM. That is the unstable oscillations are less unstable and the stable oscillations are less stable for the winged GEM, based on the "typical" case worked out in appendix II. This should enable easier control and better maneuverability of the winged GEM.

PART II MODEL STUDIES OF THE WINGED GROUND EFFECT MACHINE CONCEPT

INTRODUCTION

Can the performance of Ground Effect Machines be improved by the addition of wings? Can an improvement in static stability be achieved with winged GEM's?

To answer these questions the study reported on herein was undertaken at the James Forrestal Research Center, Princeton University during the academic year 1961-62. The study involves modifying the Curtiss-Wright Air Car ACM 6-1, an annular jet type GEM shown in Figure 14. Wings and aerodynamically faired nose and tail are to be added to improve cruise performance by generating aerodynamic lift. It is hoped that this lift will augment the propulsive power, or replace some of it so that power formerly used for propulsive lift might be used for horizontal thrust. The aerodynamic modifications are expected to give rise to a need for horizontal and vertical tail surfaces for pitch control and directional stability. Thus the modified C-W Air Car is to be a hybrid of GEM's and aircraft.

This report will include work done in hover model tests and wind tunnel tests to determine a desirable configuration for the modified C-W Air Car. The hover tests will be made to study the effect on lift augmentation and static roll stability brought about by the addition of wings of constant area, but of varying aspect ratio and of varying attachment height relative to the base of the machine. The hover tests will be made at several ground heights. The effect of wing dihedral will be briefly investigated.

Initial hover tests will be made with a very simple rectangular annular jet type model. The most desirable wing configuration will then

be used for hover tests and wind tunnel tests of a scaled model of the modified C-W Air Car.

The wind tunnel tests are designed to analyze the static longitudinal stability, the lift, and the drag of the modified C-W Air Car model. Horizontal tail effects and wing location effects will be studied in some detail.

From the wind tunnel investigation the most desirable configuration will be chosen for consideration in modifying the actual C-W Air Car by the Forrestal Research Center. Future testing will then be done on the full-sized modified C-W Air Car. The results can be compared with results from testing the unmodified C-W Air Car as given in Report No. 8 of Project No. XE-709 by Curtiss-Wright Corporation and Princeton University, May 31, 1961.

The tests were conducted by Captains Gerald P. Carr and John J. Metzko, USMC, graduate students at Princeton University.

The authors sincerely appreciate the advice and guidance of Mr. Thomas E. Sweeney of the Aeronautical Engineering Department of Princeton University.

EQUIPMENT AND PROCEDURE

The initial static hover tests involved determining lift augmentation (L/mv_j) and roll stability ($\frac{dC_l}{d\phi}$) of a rectangular powered annular jet model with several simulated wing surfaces attached. Three wing planforms with a common wing area, but with aspect ratios of 2, 4, and 6, were used. The wing area for the modified C-W Air Car was arbitrarily chosen to be 100 ft². Expressed as a fraction of the base area of 108 ft² it is .925. This non-dimensional area was used to determine the wing planforms for the rectangular model assuming 100 percent of the model base area between the wings was effective wing area. The wings were flat wooden cutouts and were attached midway along the length of the model. The rectangular model planform had a 2:1 length-to width ratio. Drawings of the model are shown in Figures 15 and 16.

The model was mounted inverted on three cantilever beams to which strain gages were attached. Strain readings from each beam were relayed through separate amplifiers and strain gage meters. These readings were then converted to forces by using strain-force calibration curves. The ground plane was a plexiglass disc adjustable in the vertical direction and in roll. Lift measurements were made by summing the three beam outputs. Moments for roll stability calculations were determined by multiplying the beam outputs by the appropriate moment arms.

The hover test rig and rectangular model are shown in Figure 17. The model was tested first without wings, and then with the different wing planforms attached flush to the base of the model. Then the model was tested with the most desirable wing planform attached at discreet

increments (δh) above the base. Tests were made at different heights above the ground plane (h) to obtain lift augmentation data. The heights, δh and h , were non-dimensionalized by dividing by the over-all base width (w).

At several selected ground heights the ground plane was adjusted to provide a succession of rolling attitudes from which static roll stability was determined. A final test was made of the rectangular model with wings attached at a $+5^\circ$ dihedral angle.

A simple technique for determining the nozzle thrust (mv_j) of the annular jet is introduced in Reference 9. In this relationship m is the mass flow of air (slugs/sec.) and v_j is the jet velocity ($^{ft}/sec.$). From the model geometry and a base pressure measurement the nozzle thrust can be closely calculated by

$$mv_j = \Delta p h C$$

where Δp is air cushion pressure less atmospheric pressure, h is height above ground, and C is the base circumference of the model measured along the mid-points of the jet annulus. Since the same power was used for each test, mv_j remained constant. Several measurements of mv_j were made at low h/w 's so that Δp was not affected by vortices within the air cushion.

Then the average mv_j of the several tests - in which the variation was very slight - was used as standard for the augmentation calculations.

Lift augmentation is a non-dimensional parameter expressed by

$$A = L/mv_j$$

where L is the lift measured by the beam support strain gages.

The final hover tests were made with a 1.25 inch: 1 foot scaled model of the modified C-W Air Car. The model was powered by two small direct current motors mounted in tandem. A picture of the modified C-W Air Car

model is shown in Figure 18, and a sketch showing pertinent dimensions is shown in Figure 19. The wings are of NACA 4412 section with an AR of 4, and were attached at a $\frac{sh}{w}$ of .129. A flexible skirt was attached in an attempt to match the full-scale configuration. This simulated skirt was used for the hover tests of the C-W Air Car model, but was not used on the model during the wind tunnel tests for reasons discussed in the analysis section.

The cruise testing was done in the Princeton University 4 ft. by 5 ft. wind tunnel. Forces and moments were measured by a mechanical balance. The model was mounted inverted on struts through the floor of the test section. Above the model was mounted a ground plane that could be adjusted vertically to vary h/w . No boundary layer removal was provided for the ground plane.

A tunnel dynamic pressure (q) of 13 lb/ft^2 was used for all the cruise tests except one, for which a q of 6.5 lb/ft^2 was used to determine fuselage effects. At a q of 13 lb/ft^2 the ratio q/Pt_j was approximately 4.

The first wind tunnel test was made with the C-W Air Car model modified only with aerodynamically shaped nose and tail surfaces. Then a horizontal tail was added and tests made at tail incidences (i_t) of -2, +2, +6, and +10°. An i_t of +2° was chosen for the remaining tests, the next of which were with the addition of wings at two different horizontal positions. These positions measured from the model C.G. to the wing quarter chord, and expressed as fractions of model width (l/w), were .105 forward and .455 aft of the C.G. respectively.

Fuselage effects were investigated by changing the nose shape, and by using the lower tunnel q mentioned above. Tests of the winged model configuration were made at ground heights (h/w) of .029, .058, and .117. The effects of model power were investigated by testing with power off, and with only the forward motor off and the inlet sealed so that no wind-milling could take place. Final tests were made of the model in the freestream, i.e., with the ground plane removed, both at zero yaw and at 5° of yaw. Both of these freestream tests were performed with and without model power.

Lift, drag, and pitching moment measurements were made for all wind tunnel tests. Side forces, yawing moments, and rolling moments were also measured for the yawed profile. The data were reduced, and are presented and discussed in the next section. Because several corrections are necessary for wind tunnel drag estimation, and since these corrections could not be applied with any degree of confidence, the drag data is of interest only to the extent of deducing drag trends.

RESULTS AND ANALYSIS

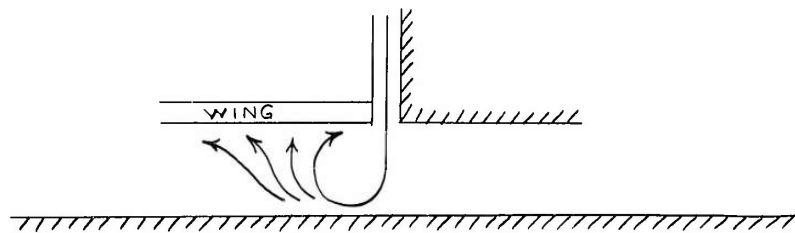
Once a winged GEM achieves enough speed so that sufficient aerodynamic lift is generated to cancel the added structural weight, wings should be a paying proposition. But until that "break-even" speed is reached, performance represented by lift augmentation (L/mv_j) versus ground height (h/w) must suffer. It was estimated that the modification to the C-W Air Car would make the machine about 5 percent heavier. If the added weight were taken as 160 lbs, and if a C_L of 1.0 is assumed, 100 ft² of wing should generate that amount of lifting force at 25 mph.

Hover Performance - Rectangular Model

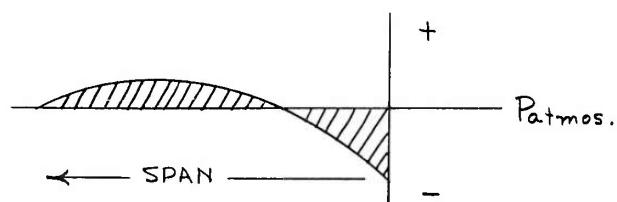
There was, however, a measurable effect on hover performance as the wing AR was varied while holding wing area constant. This effect is seen in Figure 20 where lift augmentations have been calculated and plotted against ground heights up to $h/w = 1.0$. The top curve is for the no-wing rectangular model while the lower curve resulted when AR 2 wings were added flush to the model base. Though not shown in Figure 20, hover performances with AR 4 and AR 6 wings fall between those shown; the performance of the AR 6 wings most closely approaches the no-wing performance. The same results are shown in Figure 21 for the four wing configurations, but only for a range of ground heights of more practical interest. The degradation of hover performance with decreasing AR, or with increasing chord, is quite apparent. An apt description for this phenomenon is "chord effect".

A seemingly reasonable explanation for the chord effect is that

vortex action induced by the outflowing jet results in negative pressures over areas adjacent to the annulus. A larger chord means a larger area on which the negative pressures act. Two-dimensional pressure distribution and smoke studies by Nixon and Sweeney in Reference 10 indicate that a standing vortex is formed. In static hover tests of a modified C-W Air Car model, Mr. Dale Summers of Princeton University recorded substantiating pressure distributions along the wing span. His investigation indicated that along the span beyond the area of negative pressures there exists an area of positive pressure. This might well be an area influenced by stagnation pressures as illustrated below.



The pressure distribution would then be as shown in the following sketch.



The hover performance curves in Figures 20 and 21 of this report indicate that the vorticity induced enough negative pressure over the wing root area to more than cancel the lift acting further along the span.

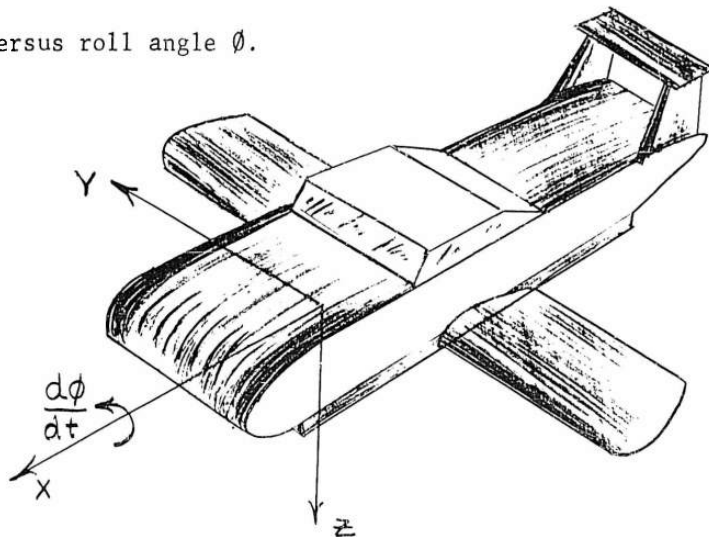
Reference 9 shows that the loss of lift augmentation due to addition

of wings can be reduced by attaching them a distance δh above the machine base. Tests were made at four $\frac{\delta h}{w}$ to investigate this effect. The results are shown in Figure 22, which indicates that as $\frac{\delta h}{w}$ increases hover performance improves toward that of the no-wing configuration. It would appear that the reason for this is that the standing vortex gets larger and slower. Correspondingly the static pressure increases.

A simple smoke study of the air flow under the wings of the rectangular model revealed just such a vorticity and stagnation as suggested above.

Static Roll Stability - Rectangular Model

For stability studies in this report the conventional aircraft axis system is used. Roll stability is given by plots of rolling moment coefficient C_l versus roll angle ϕ .



Initial stability tests were made with wings attached flush to the model base. The results are shown in Figures 23, 24, and 25. At the lower h/w 's, Figure 23 shows the model to be unstable without wings. At $h/w = .060$, the addition of wings of all three AR's made $\frac{dC_l}{d\phi}$ go negative.

As h/w was increased to .119, however, the stabilizing influence of the wings was markedly decreased. In fact the model was unstable in roll, or at best neutrally stable, up to 3° of roll with AR 2 and AR 4 wings attached. As h/w was increased still further, Figures 24 and 25 show that the presence of wings of all AR's had no effect on the roll stability.

Because only the derivative $\frac{dC_l}{d\phi}$ is of interest in the roll stability tests, no corrections for tares in the measuring apparatus were made. This explains why most of the moment coefficients are not zero at $\phi = 0^\circ$.

To determine the effect on roll stability of attaching the wings at a distance above the model base, the AR 4 wings were attached at $\delta h/w$'s of .030, .060, and .119. This was of interest since it was shown that hover performance improved as $\delta h/w$ increased. The roll stability at $h/w = .060$ is shown in Figure 26. Also at $h/w = .119$ a comparison of a no-wing configured model is made with configurations with $\delta h/w$'s of 0 and .030. At both ground heights it is seen that increasing $\delta h/w$ has a destabilizing effect.

The dihedral effect on static roll stability was investigated by testing the rectangular model with AR 4 wings attached with 5° of dihedral along the entire span. For this test $\delta h/w$ was zero. The results for $h/w = .060$ are shown in Figure 26. Roll stability for this configuration is approximately that for the no-wings configuration, so the dihedral had a pronounced destabilizing effect.

Selection of Wing

In choosing a wing planform and a wing attachment position ($\delta h/w$) for the modified C-W Air Car model, several factors were considered:

(1) The hover tests of the rectangular model indicate that of the three wing planforms AR 6 is best from the points of view of hover performance and static roll stability, (2) any $\delta h/w$ involves a trade-off between performance and roll stability, (3) wing dihedral for the modified C-W Air Car is very desirable to avoid catching a wing tip while maneuvering, (4) construction difficulties are greatest for AR 6 wings, and (5) problems of storage and maneuvering in close spaces grow with aspect ratio. Since the tests indicate that the stabilizing effect of AR 6 wings would be largely lost with dihedral incorporated, and because of the last two factors cited above, it was decided to consider the AR 2 and AR 4 wings for the modified C-W Air Car.

The hover tests to investigate the effects of $\delta h/w$ were all conducted with AR 4 wings on the model. The same tests were repeated for $\delta h/w$'s of .030 and .060 for the model with AR 2 wings. Figure 27 compares the AR 2 and AR 4 wing-configured models with $\delta h/w = .060$ in hover performance and in roll stability at $h/w = .060$. The AR 4 configuration is a shade better with respect to roll stability, while the difference in hover performance is within the magnitude of experimental error. The same comparisons are made in Figure 28, but with the wings attached at $\delta h/w = .030$. Here there is no difference in stability, and the AR 4 configuration is slightly better performance-wise at low h/w 's.

These slight advantages of using AR 4 wings, plus the advantage in cruising flight of higher C_L and lower C_D , led to choosing AR 4 wings for the modified C-W Air Car model.

In choosing a wing attachment height (δh) for the modified C-W

Air Car, a factor other than lift augmentation and static roll stability was considered. In order to ensure adequate clearance between the wing and the ground, it was felt that the modified C-W Air Car should have a δh of at least 1 ft. For the scale model tests a $\delta h/w$ of .129 was provided. Thus a gain would be accrued in hover performance at a cost of accepting some roll destabilization.

A dihedral of 6° was built into the modified model for the reason previously discussed.

Hover Tests - C-W Air Car Model

A series of hover tests were made using scaled model of the C-W Air Car - completely unmodified. Then the same tests were repeated using the same model but with wings and aerodynamically-shaped nose and tail fairings added. The nose and tail surfaces were faired tangent to the top surface of the model but were joined a distance $\delta h/w = .045$ from the model base. This was to ensure adequate ground clearance for these surfaces. It also would reduce the effect of vorticity on the nose and tail fairings so that hover performance should benefit. The disadvantage of an increment of drag as a consequence of not streamlining tangent to the base was accepted.

The C-W Air Car has a skirt that surrounds the annular jet at the base of the machine. An attempt was made to provide a scaled model skirt of like flexibility by using a simple band of pressure-sensitive tape around the outside of the model base for the hover tests. It was found to be extremely difficult to match the actual skirt. Matching the

C-W Air Car skirt flexibility at cruise was found to be even more difficult, so for the wind tunnel work the model was tested without a skirt. It was felt, though, that this would not detract from the essential results of the wind tunnel tests.

The results of these hover tests are shown in Figures 29 and 30. Hover performance in Figure 29 is very slightly better for the modified C-W Air Car model but the difference is admittedly within the range of possible experimental error. Static roll stability comparisons are made in Figure 30 at h/w 's of .029 and .058. At $h/w = .029$ the stabilities are the same, while at $h/w = .058$ the modifications appear to have been slightly destabilizing at the higher roll angles. But most interesting is that at both ground heights the models appear to have some static roll stability.

Wind Tunnel Tests - C-W Air Car Model

The first configuration to be wind tunnel tested was the modified C-W Air Car fuselage alone with no wings or horizontal tail. The test height (h/w) of .058 allowed an angle of attack variation of ± 2.5 degrees. Results of this test - lift, drag, and static longitudinal stability - are shown in Figures 31, 32, and 33. Figure 31 shows that for positive fuselage angles of attack (α) the lift curve shape is essentially linear with a slope of .11 per degree. Compared with a normal aircraft fuselage this value is high. This is because the reference area used in calculating C_L was the wing area with 100 percent fuselage carry-through. Use of an area which includes fuselage base area would produce a C_L of about 40 percent of the value presented above. It was felt, however, that there was little to be gained by comparing this vehicle with an airplane.

Pitching moment (C_m) versus angle of attack (α) curves are plotted in Figure 32 and appear to be linear up to $\alpha = 1^\circ$. In Figure 33 C_m vs C_L is non-linear but quite stable throughout.

Addition of a horizontal tail with an incidence (i_t) of $+2^\circ$ had little or no effect on the lift curve slope of the vehicle. It is clear that at this incidence angle the horizontal tail was lifting downward. In order to measure pitching moments one model support was located on the horizontal tail. For the no-wings, no-tail run the model support was attached to a $\frac{1}{4}$ -inch rod in place of the horizontal tail. It was felt that the reduction in C_D shown in Figure 31 was the result of streamlining attained by replacing this rod with a horizontal tail of about the same maximum thickness.

Figures 32 and 33 show that the addition of the horizontal tail had little effect on longitudinal stability. This was not undesirable since the tail was added only to provide control. It was noted, however, that C_m vs C_L became somewhat more linear.

For the purpose of providing trim information the data in Figure 19 was collected. From these curves

$$\frac{\Delta C_m}{\Delta i_t} = - .014/\text{deg.} \text{ average}$$

Next under consideration was the effect of addition of wings to the vehicle. The test height ($\frac{h}{w}$) was maintained at .058. Figure 31 shows that an average lift increment (ΔC_L) of about .3 was realized by this modification. It was of interest, however, to further consider the effects of horizontal wing position with respect to the C.G. of the vehicle. With the wings in the forward position the wing aerodynamic

center was ahead of the C.G., so a reduction in stability was expected. This is shown to be the case in Figures 32 and 33. Here again C_m versus C_L was non-linear. For $C_L < .9$ the static stability (dC_m/dC_L) was approximately $-.44$, and for $C_L > .9$, $dC_m/dC_L = -.14$. The lift curve slope for the wings-forward configuration was $.15/\text{deg.}$ for positive angles of attack.

With the wings shifted a good distance aft of the vehicle C.G. a stability increase was realized as shown in Figures 32 and 33. It is interesting to note that the pitching moment curves were linear up to C_L of about $.9$ which corresponded to an α of $+1^\circ$. dC_m/dC_L for this range was $-.625$. Above C_L of $.9$ an instability began to develop. Also of interest was the fact that the lift curve slope for this configuration (Figure 31), was reduced to a value of $.085/\text{deg.}$ Possibly the boundary layer growth along the side of the fuselage had progressed enough so as to increase interference at the wing root and thus reduce lift. Further, it is possible that the standing vortex from the annular jet well ahead of the wing might have rolled up and over the top of the wing near the root causing premature separation of flow. These two reasons for reduction of C_L could be looked into more closely by the use of smoke tunnel analysis or pressure distribution analysis.

It would seem appropriate at this time to consider a little more in detail the rather sudden decrease in stability or "pitch-up" which occurred at a C_L of $.9$ ($\alpha = +1^\circ$). Referring to Figure 32 it is shown that this instability began to manifest itself on all configurations at an angle of attack of about $+1^\circ$. Noteworthy is the fact that the pitch-up was accentuated in the wings aft configuration as shown in Figure 33.

At first glance it was felt that for the no-wing and wing-forward configurations, the reductions in angle of attack stability shown in Figure 32 were due to a tendency for the nose of the vehicle to begin lifting at positive angle of attack. There were no evidences of stall in the lift curves, so pitch-up due to stall was ruled out. With the wings aft it was felt that the previously mentioned annular jet vortex action ahead of the wing, which was a possible cause of the large reduction in C_{L_α} , could also be responsible for the accentuated pitch-up tendency.

Wing incidence (i_w) was varied from -5° to $+5^\circ$ in an effort to learn more about wing influences on the unstable tendency. Figures 35, 36, and 37 show the results of these tests. Angle of attack stability (C_{m_α}) and static stability (dC_m/dC_L) are shown in Figures 35 and 37 to have been essentially unaffected by i_w for angles of attack less than $+1^\circ$ and C_L less than .9. For the case where wing incidence was -5° Figure 20 and 22 show that the unstable tendency was reduced. For the $i_w = +5^\circ$ configuration the lift curve (Figure 36) indicates a decay in lift at a C_L of 1.1. The moment curves show a corresponding accentuation of the pitch-up tendency. Thus it appears that the theory of annular jet standing vortex influence is further substantiated. From the curves in

Figure 35 $\frac{\Delta C_m}{\Delta i_w \text{ average}} = -.018/\text{deg.}$

In order to investigate the fuselage influence on stability the nose fairing was "squared off" as shown below, and test runs were made with the wings aft configuration at a height (h/w) of .058. The results are presented in Figures 35, 36, and 37. Figure 36 shows that



the modification did not appreciably alter the lift curve slope or the drag curve shape, but a loss in lift and increase in drag did occur. Initially it was thought that this modification would separate the flow over the upper surface, stalling the fuselage aerodynamic lift. However, reference to Figure 31 shows that for this configuration most of the lift curve slope can be attributed to the change in fuselage lift with angle of attack. Therefore, when the fact that the lift and drag curves were not appreciably altered is taken in lieu of the results of Figure 31, it becomes reasonably clear that at the small angles of attack these runs were taken the fuselage lift was not spoiled; and the change in lift and drag can most likely be attributed to the decrease in nose camber due to the modification. It is most interesting to note as indicated in Figure 37 that this decrease in nose camber completely eliminated the pitch-up tendency at positive angles of attack. The cause of this can probably be attributed to a loss of aerodynamic lift in the vicinity of the nose coupled with a possible decrease in momentum drag due to the altered flow into the forward duct.

Vehicle power effects were then investigated, and results are shown graphically in Figures 35, 38, and 39. As a result of shutting off the forward motor and covering the inlet it was discovered in comparing Figure 36 (case of $i_W = 0^\circ$) and 38 that C_L was essentially unchanged throughout the angle of attack range. C_D was generally reduced by about .05. This reduction is considered to represent the decreases of momentum

drag and form drag connected with the annular jet air curtain. It is hoped that smoke tunnel analysis might give some insight as to the reason for the non-linearity of the lift curve (Figure 38) for positive angle of attack. Figure 39 indicates an increase of static stability (dC_m/dC_L) to -1.05, but the unstable tendency at high C_L remained.

With both engines shut off and their inlets left open Figure 38 shows a reduction in C_L and C_D of about .1 and .05 respectively compared with the wings-aft, full-power configuration (Figure 36). The reasons for C_D reduction are no doubt the same as those mentioned for shutting down only one engine. The C_L reduction can be partially attributed to loss of lift augmentation. The moment curves of Figure 35 and 38 are non-linear but stable throughout.

The final wind tunnel test at a height (h/w) of .058 was run at a reduced dynamic pressure (q) in order to get an idea of the effect of forward velocity on static stability. As seen in Figure 38 C_L was reduced by about 75 percent, C_D was halved, and though the lift curve remained linear, its slope was grossly reduced to about .02/deg. It would appear that at a reduced q the "sink" effect of the vehicle's engines is important to the cruise aerodynamics. As q decreases the sinks become stronger, and again smoke tunnel analysis may be the key to determining their effects on C_L and C_D . Additional wind tunnel tests on the modified fuselage alone at various q 's might also be useful. Figures 35 and 39 indicate a generally stable trend of pitching moments at large positive and negative angles of attack but a definite narrow instability range around zero angle of attack ($C_L = .2$).

To investigate the effects of ground height on vehicle performance the runs in ground effect at h/w of .029, .117, and free stream runs were undertaken for comparison with the $h/w = .058$ runs. Results are shown in Figures 40 through 45. In Figure 40 the lift curve slope for the lower height was found to be the same. Also a slight increase in lift and a decrease in drag were realized. These trends seem to be compatible with those indicated in Reference 7 for wings in ground effect. At the height (h/w) of .117, however, the lift curve slope increased again possibly indicating that vehicle power effects had come into play. Comparisons of stability at these three heights, considered to be in ground effect, can be drawn from Figure 41 and 42. It would appear that ground height does not materially affect the general trend of stability, but that increase in height may delay the onset of the pitch-up tendency. As shown in Figure 42 unstable trends occurred at C_L 's of .85, .9 and 1.3 as ground height was set at .029, .058, and .117 respectively. The free stream lift curve slopes shown in Figure 43 were found to be about .083, and Figures 44 and 45 indicate considerable reduction of static stability.

Also considered in the free stream tests were the effects of vehicle power and yaw. Figures 43, 44, and 45 show that a yaw of 5° has little effect on C_L , C_D , and C_L . Considering pitching moments, the yaw succeeds only in changing the trim but has no marked effect on longitudinal static stability. Vehicle power also is shown in these figures to have had little effect on lift curve slope and stability in free flight. Increases in C_L and C_D with addition of power can most likely be attributed to augmentation, momentum drag, and form drag among other things.

CONCLUSIONS AND RECOMMENDATIONS

The addition of wings to a GEM has the effect of reducing hover performance. As the chord of the wing is increased hovering performance is degraded. As the wing attachment height is increased hover performance improves toward that obtained for a wingless vehicle. With wing area kept constant static roll stability increases as wing aspect ratio increases to six. The effect of increasing attachment height is to decrease roll stability. Although dihedral is necessary for cruise maneuverability its effect is to reduce static roll stability.

In forward flight wings add lift as expected. Their contribution to static longitudinal stability, of course, depends upon their horizontal location with respect to the vehicle center of gravity. The aerodynamic shape of the nose has a profound effect on the vehicle's cruise performance and static longitudinal stability. Negative camber should be employed in order to greatly increase the angle of attack where lift from the nose causes undesirable reduction in longitudinal stability.

The wings forward configuration seems to have less of a pitch-up tendency at positive angles of attack than the wings aft configuration. The reason for this is somewhat unclear. Possibly the action of the curtain vortex system upon the wings has some bearing on the pitch-up tendency. Therefore, a better understanding might be had through flow visualization studies. However, an investigation of fuselage effects shows that the flow over the nose of the fuselage into the forward duct also has an important influence on the pitch-up tendency. In fact certain fairings of the nose can practically eliminate the pitch-up tendency over a small range of angle of attack.

PART III FULL SCALE FLIGHT TESTS OF A WINGED GROUND EFFECT MACHINE

INTRODUCTION

The altitude capability of a GEM is restricted by the base augmentation of its particular configuration and the instability which develops at the higher altitudes. This inherent characteristic limits the maneuverability and performance of GEMs in general since they cannot tilt sufficiently to obtain large control forces, as can an airplane or helicopter. Also, because of this low altitude performance, GEMs must be operated over relatively level areas which are free of obstacles if a reasonable cruise speed is to be maintained. Because of this, a great deal of thought has been given to the application of aerodynamic lift to augment the lift of GEMs and at the same time to improve their stability and control. Use of aerodynamic lift can increase the altitude capabilities of GEMs because, for constant jet momentum, it reduces the base augmentation necessary to sustain the weight of the vehicle, allowing it to rise to a greater altitude. A decrease in stability can be expected from this increase in altitude, but using aerodynamic lift to improve the stability should more than compensate for this. It is not proposed that, with increased velocity, lift builds up to such an extent that the vehicle rises out of ground effect, as in the GETOL concept, but that the aerodynamic lift is used to supplement the lift from the cushion necessary to support the weight of the vehicle. With this in mind, a few immediate conclusions can be drawn when one examines the application of this concept. First of all, the GEM will have to operate at speeds at which aerodynamic lift becomes meaningful. By this it is meant that the aerodynamic surfaces must generate enough lift to compensate for their own weight and to produce a notice-

able decrease in the base augmentation necessary to support the weight of the vehicle. Secondly, the increase in altitude with a decrease in base augmentation depends upon the part of the augmentation curve at which the GEM operates. GEMs with the higher base loadings usually operate at the lower altitudes where the slope $\frac{dA}{dh}$ of the augmentation curve is very high. This means that an appreciable decrease in the base augmentation is necessary before a significant increase in altitude is realized. On the other hand, GEMs of lighter base loadings usually operate at higher altitudes, where a decrease in the base augmentation required brings about a relatively higher increase in altitude. Thus we see that this concept is most suitable to GEMs of light base loading which are capable of cruise speeds where aerodynamic lift becomes significant.

To determine the performance and some of the handling qualities of GEMs with aerodynamic lifting surfaces, the Curtiss-Wright Air Car ACM 6-1 was modified by adding fairings, wings, and empennage surfaces; and flight tests of this vehicle were undertaken. Details of the modification appear in the text of this report. The program was conducted by the Princeton University Department of Aeronautical Engineering under the sponsorship of the United States Army Transportation Research Command. Choice of the C-W Air Car for this program was primarily due to its availability, its easy adaption to the modification, and its high speed. Also, in choosing this particular GEM it was recognized that, due to its high base loading, the altitude gain due to wing lift would be small. In spite of this, it was felt that much could be learned about the nature of the altitude increase and other fields of interest such as the use of

aerodynamic surfaces to improve the stability and control of the vehicle. In the pursuit of this knowledge through flight tests of the Modified C-W Air Car, a few interesting characteristics of this particular GEM were found which we hope will aid in a better understanding of winged GEMs in general.

THE TEST VEHICLE

The principal dimensions of the Curtiss-Wright Air Car ACM 6-1 and its modified version appear in the table following this section. For the sake of those not familiar with the C-W Air Car, both the original configuration and the modifications made to it are discussed below.

As shown in Figure 46, the ACM 6-1 is an annular jet machine having a box shape with a rectangular base. Power is provided by two Lycoming VO-360 helicopter engines situated in ducts symmetrically located fore and aft of the central pilot's compartment. The engines are mounted vertically and drive multi-bladed fans connected directly to the drive shafts. Propulsive thrust is primarily obtained by use of fully controllable bottom propulsive vanes located in both the right and the left longitudinal jet nozzles. Additional forward thrust is provided by clam-shell type louvers across the rear of the car which are coordinated with the propulsion vanes. The position of the bottom propulsive vanes and the opening of the rear thrust louvers are set by means of a control stick. As the control stick moves from positions 0 to 8, the propulsive vanes move through an angle range extending from -25° to $+55^{\circ}$. At position 3 the vehicle is in hover with the propulsive vanes set at 0 degrees. Thus, reverse thrust is obtained in control positions 0 through 2 and

forward thrust increases from position 4 to a maximum at position 8. Synchronized with these controls are vanes located in the front and rear segments of the annular jet which throttle the flow through the nozzle as the rear thrust louvers are opened. This prevents a pitch-up due to a sudden loss in chamber pressure as the rear louvers are opened.

Directional control is provided by clam-shell type louvers located at each corner of the machine. Turning the control wheel opens diagonally opposed pairs of louvers to give a yawing moment. Also, side thrust is obtained by use of symmetrically located louvers on both sides of the machine which are controlled by foot pedals. In addition to these primary controls, a reverse thrust louver located in the front of the machine and operated by a rearward movement of the control column assists in braking. Vertical louvers, located forward of the pilot's compartment on either side of the machine, augment forward and reverse thrust.

In the photograph of the modified version of the Air Car, shown in Figure 47, it is obvious that the external appearance of the machine has been altered considerably. The over-all length was increased 10 feet by the addition of nose and tail fairings; wings and a tail assembly were added; and the top of the pilot's compartment was replaced by a bubble canopy limiting its capacity to one passenger. Unpublished wind-tunnel data taken at Princeton University show that the fuselage drag coefficient can be reduced to approximately one-third of its original value by use of the nose and tail fairings. The construction of the fairings consisted of a tubular framework with balsa shaping, which was covered with sheet metal and fabric. The nose fairing completely enclosed the front end

of the original vehicle so that use of the reverse thrust louver for braking was lost. The extensive work required to duct this louver to the front of the machine was felt to be unnecessary due to the fact that adequate braking was provided by the other controls. However, since a sizeable reduction in propulsive thrust was not desired, the rear propulsive louvers were ducted through the tail fairing simply by cutting a hole in the fairing, allowing the thrusting air to pass through. It is granted that this type of ducting results in a sizeable loss in thrust, and greater thrust efficiency can be had by proper ducting. However, as a matter of expediency, it was decided that the vehicle possessed enough thrust to propel it through the speed range that could be safely conducted on the length of runway available. Outside of the changes mentioned above, no other alterations were made to the control system. Also, no changes were made to the power system or internal aerodynamics of the machine.

The wings were spares taken from a Piper PA-18 Super Cub, and they were cut down to a semi-span of 10 feet while retaining their original chord length of 5 feet. Also, the trailing edge of each wing was modified to accommodate a fixed flap extending across the entire trailing edge. Wind-tunnel studies have indicated that the stability is slightly improved with the wings forward of the center of gravity (see Reference 11). For this reason, the aerodynamic center line of each wing was placed slightly forward of the C.G., 13 feet 3 inches aft of the nose of the vehicle. To keep the wing tips from hitting the ground in rolling maneuvers, the aerodynamic center of each root section was set 1 foot above the base of the machine and the wings were given 5° dihedral. Also the wings

were set at 5° angle of incidence. However, it is difficult to say at what angle of attack the wings operated during the test runs because the root sections were most likely in a region of upwash due to the action of the jet curtain.

The empennage consisted of two vertical fins, attached at each side of the tail fairing, supporting a horizontal stabilizer. The fixed elevator was pre-set to 10° positive incidence to help compensate for the nose-up moment anticipated at the higher speeds. A controllable rudder was affixed to each of the vertical fins, and control of the rudders was tied into the primary yaw control by use of a servomechanism which followed the control stick position. The principal dimensions of the ACM 6-1 and its modified version are given in the following table:

	ACM 6-1	Modified vehicle
Over-all length	17 ft	27 ft
Over-all width	7 ft	27 ft
Over-all height	5.375 ft	7.33 ft
Base area	108 sq ft	108 sq ft
Base perimeter (at center of jet nozzle)	46.1 ft	46.1 ft
Equivalent base diameter	11.7 ft	11.7 ft
Annular jet nozzle area	11.02 sq ft	11.02 sq ft
Gross weight (dry)	3225 lb	3605 lb
Span of each wing	- - -	10 ft
Wing chord	- - -	5 ft
Stabilizer area	- - -	15.1 sq ft
Elevator area	- - -	9.75 sq ft

DISCUSSION

In the preliminary flight tests, the vehicle was first flown without wings and then with the wings attached. The vehicle displayed admirable stability and control characteristics without wings. However, when flown with the wings attached, the vehicle was unexpectedly found to experience dynamic oscillations about the roll axis at velocities exceeding approximately 10 mph. Although much has been learned about the nature of these oscillations through extensive flight testing, the cause is still unknown. Visualization of the flow in the vicinity of the wings was attempted by hovering the machine into a 10-mph headwind and injecting smoke into the flow, but it was found that the flow was so fast and turbulent that the smoke dispersed before anything definite could be seen. Next, the flow directly under the wings along the ground was observed by simply flying the machine over grass and noting the direction of the grass tips during oscillation. It was found that when the vehicle reached maximum roll angle, the flow under the higher wing suddenly rushed outward laterally and the wing began to drop. This would imply that, through some flow phenomenon, the pressure under the rising wing builds up and then suddenly "dumps" when the wing reaches maximum roll angle. This causes the wing to drop and start a repeat of this behavior on the opposite wing.

Further attempts to isolate the cause of the oscillations included an investigation into the effect of moment of inertia about the roll axis. This was done on the premise that possibly a slight but not apparent dynamic oscillation existed on the wingless vehicle, and the addi-

tional moment of inertia of the wings aggravated the situation. In this experiment the wings were replaced by 70-pound weights suspended from the sides of the vehicle at a distance to give them a moment of inertia approximating that of the wings. It was found that the added weights did not change the stability. In fact, when coaxed into an oscillation, the motions damped out in only slightly more time than with the wingless vehicle, as would be expected from the increased moment of inertia. This further supports the premise that the oscillations are most likely due to a flow phenomena about or under the wings which lie in the action of the jet curtain vortex system. Further evidence of this is found in following sections of this report. However, extensive experiments, possibly including dynamic model studies, are needed before the cause of the oscillations can be completely understood.

Initially it was feared that accurate altitude measurements could not be taken with this vehicle at the higher velocities, where major interest lies, due to the intensity of the roll oscillations during decelerations. However, the discovery that this motion could be quickly damped out by opening either set of the side gust control louvers was very encouraging. The reason why this occurs is unclear and can be the result of several factors. The louvers are located just forward of and slightly above the wing location; so the effect of ejecting a lateral flow across the wings may be the reason. Also, opening these louvers changes the internal aerodynamics, which causes the vehicle to settle slightly. A change in the curtain vortex behavior with this change in internal aerodynamics may alter the influence of the jet curtain upon the wings. Inci-

dently, it is the pilot's opinion that the gust control louvers were not used merely to hold the oscillations in control, but rather that this control action completely eliminated the motion.

By using the gust control to stabilize the vehicle when necessary, the speed-height characteristics of the Modified Air Car were determined fairly accurately. Also, the nature of the roll oscillations was investigated over a wide range of flight conditions. The results of these experiments, along with some observations on the stability and control of the vehicle, are given in the following sections.

FLIGHT TESTS

Measuring Apparatus

Altitude measurements were made by use of height sensors attached at each corner of the vehicle. The assembly of each sensor consisted of a parallelogram linkage attached to a mounting plate with a linear potentiometer installed as a diagonal of the parallelogram. Ground contact of the assembly was provided by means of a castor wheel mounted on the outer vertical member. In the case where roll angle was to be measured, readings from each sensor were fed into a separate channel of an oscillograph recorder so that a time history of each run was made. Roll angle was determined by taking the difference of the average altitudes measured on each side of the machine. In the case where altitude was to be measured, the four sensors were fed into a summing circuit to give an average reading on the recorder.

Velocity measurements were taken by means of a typical "fifth" wheel

arrangement. Assembly of the apparatus consisted of a bicycle wheel mounted at the rear of the vehicle which was geared to a calibrated d-c tachometer. Signals from the tachometer were recorded on the oscillograph so that accelerations, decelerations, and velocity could be measured during each run.

Speed-Height Characteristics

In flight experiments of a winged GEM, highest interest most likely lies in the determination of the effect of wings upon the altitude capabilities of the GEM. In order to do this, the speed-height characteristics of the vehicle were determined first with the wings attached; then for comparative purposes, the vehicle was flown without the wings. Ballast was added to the wingless vehicle to compensate for the weight of the wings. This particular comparison was made instead of a comparison with the original ACM 6-1 Air Car because it most accurately shows the direct effect of the wings upon altitude. In these tests the wing flaps were set at 30° .

The test procedure was similar to that used by Curtiss-Wright to determine the height-speed envelope of the ACM 6-1, and was as follows:

1. Control position and power were set while hovering at one end of the runway. The control position determines the position of the bottom propulsion vanes and the opening of the rear thrust louvers. The control position was varied from position 3 (hover) to position 8 (maximum thrust).
2. The machine was allowed to accelerate to maximum velocity while altitude and velocity were recorded. Altitude was taken as the

skirt to ground clearance.

3. Whenever oscillations did occur with the winged vehicle, they were damped out by use of the side thrust louvers. Measurements were made only with the louvers closed because of their effect upon altitude.

Figure 50 shows the variation in height with velocity for both the winged and the wingless vehicles at three separate power settings. The results shown in this figure represent the average measurements of several runs. Without exception, in forward flight the altitude of the winged GEM was higher than that of the wingless vehicle. As would be expected, the difference in altitude between the two configurations increased with velocity as aerodynamic lift built up. In fact, with 2625 RPM the increase in altitude was about 37 percent at 35 mph. Unfortunately, higher velocities were not obtainable in the length of runway available. But an increase of this magnitude using a vehicle of such high base loading indicates that great increases in altitude should be possible for vehicles of lighter base loadings operating at higher velocities. In any case, the results of this experiment show that the altitude capabilities of a GEM can be substantially increased by the use of wings.

The dotted curves in Figure 50 represent the computed increase in altitude due to the wings. These computations were based upon Chaplin's theoretical augmentation curve for the wingless vehicle:

$$A_0 = 1 + \frac{A_P}{h_C} \quad (50)$$

and the theoretical augmentation curve of the winged GEM:

$$A = A_0 \left(1 - \frac{L_w}{W}\right) \quad (51)$$

The wing lift at each height-velocity point was determined by assuming a constant wing lift coefficient of 2.0. This rather high lift coefficient was actually a conservative estimate when based upon the results of Reference 7, a study of the characteristics of wings of various aspect ratios in the presence of ground effect. Since the wings were pre-set at 5° positive incidence, the average angle of attack was estimated at 7° due to the presence of upwash in the vicinity of the wings. The average height-to-chord ratio of the wings was about .45; wings at this height-to-chord ratio and with an aspect ratio of 5.2 (the physical aspect ratio of the Modified Air Car) should produce a C_L of about 1.3 at 7° angle of attack. It is known that the half span flaps of the Piper PA-18 set at 30° produce an incremental C_L increase of about .60. Since the wings of the Modified Air Car have full span flaps set at 30°, a C_L increase of .70 would be a conservative estimate. Further conservative reasoning was applied by assuming only 30 percent fuselage carry-through when estimating the effective wing area.

As noted in Figure 50, in all cases the altitude increase due to the wings was higher than the theoretical prediction. Fairly good agreement is found at the higher power settings when one considers the assumptions involved in the theoretical prediction. However, the agreement diminished as power was reduced. Several reasons can be cited for this occurrence. First of all, there may be a departure of the slope of the actual augmentation curve from the theoretical at the lower altitudes. Secondly, and perhaps most important, is the fact that major attention

was focused on the accurate determination of the height-speed relationships at the higher power settings and velocities. Consequently, the data points at the higher power settings represent the average of many runs; the characteristics of 2200 RPM were only briefly examined, leaving greater room for error. For this reason, some doubt is cast upon the magnitude of the altitude increase shown by the two data points at 2200 RPM for the winged vehicle, and they are presented for general interest only. It is felt that a good degree of accuracy was maintained at the higher power settings.

One final observation based on the results of Figure 50 is that the winged vehicle achieved slightly lower velocities for each control position than did the wingless vehicle, due to the added drag of the wings. This, however, is but a small price to pay for the significant increase in altitude.

Roll Oscillations

In order to study the nature of the roll oscillations, qualitative observations and recordings of roll angle and velocity were made while flying at various control stick and power settings. The significant observations are outlined below:

1. The oscillations primarily occurred while decelerating with the control stick in reverse thrust positions and also at low velocities while the control stick was in position 4.
2. Although oscillations did occasionally occur in control settings higher than 4, the tendency to oscillate diminished as control position increased.
3. The oscillations occurred only at velocities exceeding approximately 10 mph.

4. The time period of the oscillations varied between two to three seconds.

5. The tendency to oscillate did not depend upon power setting.

6. The oscillations were divergent in nature. In almost every case the rolling would increase until the landing pads of the machine hit the ground. At this point they would dampen out slightly, then increase again.

7. There was no obvious coupling between pitch and roll. The pitch angle remained fairly constant during roll oscillations.

Since the control position determines the propulsion vane deflection, the first two observations suggest that the position of the propulsive vanes influences the oscillation. One plausible explanation for this is that the jet is swept further to the rear of the vehicle as the control position (propulsion vane deflection) is increased. Therefore, at the lower control positions (reverse thrust and position 4), the wings are more likely to be in the influence of the side jet vortex system than at higher control positions. This adds to previous evidence that the oscillations are due to a flow phenomenon about the wings which is connected to the action of the side jet vortex upon the wings. However, other factors may be involved, and this explanation is to be held tentative for consideration by others.

The typical oscillations that occurred during decelerations while using reverse thrust, and also at constant velocity with the control stick in position 4, are plotted in Figure 51. The period and divergent nature of these oscillations can be readily noted from these plots.

Comments on Stability and Control

Yaw

As compared to the original ACM 6-1 vehicle, the yaw characteristics of the Modified Air Car were quite good due to the vertical stabilizers and rudder controls. At times the yaw control of the ACM 6-1 was found to be inadequate, causing it to go into an uncontrollable divergence in yaw. This was not the case of the Modified Vehicle. The Modified Air Car was tested both with and without the rudder control. Even without the use of rudders, it was found to have good yaw stability and it could be kept on a straight track even in a moderate cross wind. Verifying the good degree of yaw control is the fact that control was never lost during the worst of the roll oscillations experienced by the vehicle. As was expected, the degree of yaw control decreased with velocity to where it was about equal to the ACM 6-1 at slow speeds. However, the very good stability and control at high speeds justify the use of airplane-like vertical stabilizer systems in GEM applications.

Pitch

Like the ACM 6-1, the Modified Air Car experienced an increasing nose-up pitch with increasing velocity. Several reasons can be cited. First, the throttling vanes in the front and rear annular jets may not have completely compensated for the opening of the rear thrust louvers. This would cause the rear of the vehicle to settle because of the reduced chamber pressure in that section of the car. Secondly, the momentum drag acting on the ducts caused a nose-up moment that increased

CONCLUSIONS

1. By using wings, the altitude capability of the Modified Air Car was significantly increased. This predicts substantial altitude increases for winged GEMs of lighter base loadings.

2. If wings are used to increase the altitude performance of GEMs while keeping constant momentum thrust, the L/D of the winged vehicle is slightly lower than without wings due to the drag of the wings. But the substantial altitude increase over-shadows the small loss in speed.

3. As compared to the original ACM 6-1 vehicle, the yaw stability and control were substantially increased by use of vertical stabilizers and rudder controls.

4. This particular winged GEM was dynamically unstable in roll, and the cause is still unknown. Experimental evidence seems to indicate that flow phenomenon about the wings which operate in the influence of the side curtain vortex system may be a reason.

5. The roll oscillation could be stopped by opening the side thrust control louvers. Since this action results in a sizable decrease in performance, use of it to control the oscillations would be intolerable for an operational vehicle.

6. Extensive research is still necessary before the cause of the roll instability can be completely understood.

BIBLIOGRAPHY

1. Chaplin, Harvey R., Theory of the Annular Nozzle in Proximity of the Ground, David Taylor Model Basin Aero. Report No. 923, July 1957.
2. Final Report on the Experimental Test of the Curtiss-Wright Air Car - ACM 6-1, Wright Aeronautical Division, Curtiss-Wright Corporation, Project No. XE-709, May 1961.
3. Dukes, T. A., Hargraves, C. R., Stability Augmentation of Ground Effect Machines, Princeton University Aero. Report No. 601, April 1962.
4. Traybar, J. J., Longitudinal Stability and Control of a Ducted Rotor Flying Platform, Princeton University Aero. Report No. 464, May 1959.
5. Perkins, C. D., Hage, R. E., Airplane Performance Stability and Control, John Wiley & Sons, Inc., 1949.
6. Knowlton, M. P., Summers, D. R., Stability and Performance Characteristics of a Cruciform GETOL, Princeton University Aero. Report No. 580, December 1961.
7. Fink, M. P., Lastinger, J. L., Aerodynamic Characteristics of Low Aspect Ratio Wings in Close Proximity to the Ground, NASA TN D926, July 1961.
8. Symposium on Ground Effect Phenomena, Princeton University, October 1959.
9. Sweeney, T. E., Nixon, W. B., Planform Characteristics of Peripheral Jet Wings, Princeton University Aero. Report No. 524, December 1961.
10. Nixon, W. B., Sweeney, T. E., Some Qualitative Characteristics of a Two-Dimensional Peripheral Jet, Princeton University Aero. Report No. 484, September 1959.
11. Carr, G. P., Metzko, J. J., Model Studies of the Winged Ground Effect Machine Concept, Princeton University Aero. Report No. 657, June 1963.
12. Summers, D. R., An Analytical Investigation of the Winged Ground Effect Machine Concept, Princeton University Aero. Report No. 657, June 1963.

with velocity. Also a nose-up contribution was caused by the propulsive thrust acting at the bottom of the vehicle. The possibility also exists that some fuselage aerodynamic lift acting ahead of the C.G. contributed to the nose-up moment.

To compensate for the nose-up moment, the fixed elevator was pre-set to 10° positive deflection. However, further compensation had to be made by the addition of 120 pounds of ballast to the nose of the machine. This caused the vehicle to be slightly unbalanced in hover. In forward flight the machine flew at nearly zero pitch angle. It is felt that the same result could have been accomplished by use of a larger elevator, which would have had a negligible effect upon the hover altitude of the machine.

APPENDIX I

PERFORMANCE

In this appendix the Curtiss-Wright Air Car ACM 6-1 is picked as a typical example on which to apply the method of section I to obtain the forward flight augmentation curves. Values for q_1 of five and ten are used along with wing to base area ratios of 1.0 and 2.0 and an aerodynamic lift coefficient of one. The total lift coefficient is calculated from equation (2) and the new augmentation ratio is found using equation (3) and the hover augmentation ratio of the air car, Reference 2. The new h/d_e is then found graphically, assuming the total augmentation remains constant, from the static augmentation plot. This example, worked out for a q_1 of five is based on the following physical dimensions of the air car.

$$W = 3650 \text{ lb}$$

$$C_L = 1.0$$

$$S_b = 108 \text{ ft}^2$$

$$A_{\text{HOVER}} = 6.19$$

$$S_w/S_b = 1.0$$

$$q_1 = 5$$

$$C_L^* = \frac{W/S}{q_1} = \frac{33.4}{5} = 6.64$$

The base of the machine is thus unloaded by the ratio of $\frac{C_L}{C_L^*}$,

$$\frac{C_L}{C_L^*} = \frac{1}{6.64} = .151$$

and the augmentation needed is reduced to:

$$A' = \left(1 - \frac{C_L}{C_L^*}\right) A = .849 A$$

This is simply a statement of the fact that for the velocity and wing loading selected 84.9 percent of the vehicles weight is supported by the base while the remaining 15.1 percent is supported by the wing. Using the static augmentation curve of Figure 7, a value of augmentation is selected from which A' is calculated using equation (3). For the first point the hover augmentation is chosen and A' becomes,

$$A' = (.849)(6.19) = 5.25$$

now going back into the static augmentation curve an h/d_e of about .035 is found using the new augmentation ratio. This point is then transferred back to the hover augmentation line and the process is repeated for several augmentation ratios and the forward flight augmentation curve is obtained.

Another plot which is probably of more interest than Figure 7, is the absolute altitude versus velocity plot shown in Figure 8. This plot was constructed from the forward flight altitude versus velocity curve and the static lift versus altitude plot of Reference 2. Several wing to base area ratios were selected for a lift coefficient of one, from which the wing lift was calculated for various velocities and subtracted from the total weight of the GEM. With this new weight a new altitude was obtained from the altitude versus lift plot and the difference in altitude is what is plotted in Figure 8.

Figure 9 is simply a plot of the ratio of wing to base lift as a function of q for a lift coefficient of one and, two wing to base area ratios. This plot is included to point out the two extremes of the winged GEM; at $q = 0$ all the weight is on the base while at $q's > 0$ the lift is divided between the wing and the base up to a q of 16.7, for wing to base area ratio of 2, where the wing is capable of supporting the entire weight.

APPENDIX II

An analytical investigation of the stability of a winged GEM is presented here using the equations of motion derived in section II. The parameters used for the calculations are based on the Curtiss-Wright Air Car ACM 6-1, Reference 2, and unpublished wind tunnel data. Equations (46) & (49) are rewritten here in the familiar root locus form in terms of the variables $C_{m\alpha}$ and $C_{m\theta}$.

$$\begin{aligned} \lambda^4 + (C_{D_D} + \frac{3}{2}C_D)\lambda^3 + \left(\frac{C_L C_W}{2} + \frac{C_D C_{D_D}}{2} + \frac{C_D^2}{2}\right)\lambda^2 \\ + \left(\frac{C_W C_{m_u}}{2h} - \frac{C_L C_{m_u}}{2h}\right)\lambda + \frac{C_W C_{m_u} C_D}{4h} \\ - C_{m\alpha} \left[\left(\frac{1}{h}\right)\lambda^2 + \left(\frac{C_{D_D}}{h} + \frac{C_D}{h}\right)\lambda + \frac{C_W^2}{2h} \right] = 0 \end{aligned} \quad (A-1)$$

and,

$$\begin{aligned} \lambda^4 + (C_{D_D} + \frac{3}{2}C_D)\lambda^3 + \left(\frac{C_L C_W}{2} + \frac{C_D C_{D_D}}{2} + \frac{C_D^2}{2} - \frac{C_{m\alpha}}{2h}\right)\lambda^2 \\ - \left(\frac{C_{m\alpha} C_{D_D}}{h} + \frac{C_{m\alpha} C_D}{h}\right)\lambda - \frac{C_W^2 C_{m\alpha}}{2h} \\ + C_{m_u} \left[\left(\frac{C_W - C_L}{2h}\right)\lambda + \frac{C_W C_D}{4h} \right] = 0 \end{aligned} \quad (A-2)$$

and for the non-winged GEM:

$$\lambda^3 + (C_{D_D} + C_D)\lambda^2 + \left(\frac{C_W}{2h}\right)C_{m_u} = 0 \quad (A-3)$$

Seven separate cases are worked out for the winged GEM for which qualitative root locus plots are presented, Figures 10 to 13. The first three cases using equation (A-1) show the effect of varying $C_{m\alpha}$ from zero to minus infinity while C_{m_u} is kept constant at three separate

values, $- .10, 0, .10$. The next four cases based on equation (A-2) show the effect of varying C_{m_u} from zero to plus and minus infinity while C_{m_α} is kept constant at 0 and $-.15$. Finally the root locus for the non-winged GEM based on equation A-3 is presented. The top half of this figure, case VIII, represents half of the complex plane for $C_{m_u} = 0$ to $-\infty$ while the lower half is half the complex plane for $C_{m_u} = 0$ to $+\infty$.

The first three cases show that for any reasonable value of C_{m_α} the period and damping will be relatively unaffected. The resulting modes of motion being two oscillations one slightly stable and one slightly unstable. Cases IV and VI show the system becoming more unstable as C_{m_u} is increased, however, the unstable mode is an oscillation. Cases V and VII on the other hand show an unstable mode as C_{m_u} is decreased towards minus infinity but this unstable mode is a pure divergence.

Case VIII for the non-winged GEM shows a pure divergent mode along with a stable oscillation or an unstable oscillation and stable real root, depending on the sign of C_{m_u} .

APPENDIX III

EXTRAPOLATED CHARACTERISTICS OF THE MODIFIED AIR CAR

Height-Speed-Power Relationships

Throughout the flight tests, it was apparent that the maximum accelerations of the Modified Air Car were somewhat less than those of the original ACM 6-1 vehicle. Although some loss in acceleration was expected from the increased weight and decreased rear louver thrust due to the modification, these causes could not account for the total decrease in acceleration. However, since 35 mph was about the maximum velocity that could be safely attained over the length of runway available, no effort was made to correct this condition. Upon completion of the test program and dismantling of the vehicle, it was found that the control system was binding in the extreme control positions, limiting the maximum propulsive vane deflection to about 35° . This vane deflection was about 18° less than the actual maximum the system was originally capable of, and accounts for the loss in maximum thrust for acceleration. By extrapolating the low-speed data to the speeds corresponding to the actual maximum vane deflection, a good estimate of the vehicle's high-speed behavior and capabilities can be made.

The method used to extrapolate the data was semianalytical. The height-speed curves shown in Figure 50 were replotted in Figure 52 using an expanded altitude scale. The slight discrepancy in hover points due to experimental error, shown in Figure 50, was eliminated in Figure 52 by slightly adjusting the curves for the winged vehicle until the hover points matched. Once the low-speed characteristics in Figure 52 were established, the curves for the wingless vehicle were extrapolated to higher velocities by simply extending

the curves. Then, on the basis of the extrapolated height-speed points for the wingless vehicle, the curves for the winged vehicle were extrapolated by theoretically determining at various height-speed points the increase in altitude due to the lift of the wings. The curve for the winged GEM at 246 BHP was determined analytically over the entire velocity range because the validity of the altitude increase shown in Figure 50 is very doubtful. The wing lift was computed by determining the amount of wing lift necessary to produce the altitude increases shown at the lower velocities where data were taken. In facilitating these calculations for wing lift and its effect upon altitude, the theoretical augmentation curves for the wingless vehicle, $A_o = 1 + \frac{S_b}{h C}$, and the winged vehicle, $A = A_o (1 - \frac{L_w}{W})$, were used. By use of these equations and the magnitude of the altitude increases at the lower velocities, it was determined that a lift coefficient of 2.2 and a fuselage carry through of 43 percent for wing area would produce the necessary lift.

The maximum speeds of the Modified Air Car were roughly estimated by referring to Reference 2 for the top speeds of the ACM 6-1 vehicle at similar power settings, and then computing the decrease in speed dictated by the change in drag coefficients and loss of thrust due to the modification. As determined by unpublished wind-tunnel data, the induced drag coefficients of the ACM 6-1 vehicle and the Modified Air Car are .20 and .29, respectively, when based upon base area. By using these drag coefficients, the top speed of the Modified Air Car was estimated to be about 50 mph.

As can be seen from the extrapolated portions of the curves, the change in altitude due to the wings does not increase substantially at velocities exceeding approximately 35 mph. The reason for this is the

altitude decay as the propulsive vane deflection increases to increase velocity. As the initial altitude decreases, the slope of the augmentation curve $\frac{dA_0}{dh}$ at which the vehicle operates becomes very high. Therefore, an increasing amount of wing lift is necessary to produce the same altitude increase. It is for this reason that the altitude gain due to the wings decreases with reduced power.

Figure 52 is cross-plotted in Figure 53 to determine the altitude versus horsepower required at constant velocity for both the winged and the wingless vehicles. These cross plots were then used to determine the horsepower required versus velocity to maintain a constant altitude of 2 inches. As seen in the bottom plot of Figure 53, the horsepower required for the winged vehicle is substantially less than that for the wingless vehicle because of the reduced momentum thrust requirements as the wings unload the base. Furthermore, as shown by the intersections of the maximum-horsepower-available with the horsepower-required curves, the winged GEM has a higher speed capability when the altitude is held constant. However, it should be noted that in order to achieve this higher maximum speed, some means must be provided to transfer lifting power to propulsive power as wing lift builds up.

Winged GEM Capability Using a Separate Propulsive System

For reasons mentioned in the previous section, much of the effectiveness of the wings for producing an altitude increase is lost when an integrated propulsion system is used. Therefore, it would be interesting, at least from an academic standpoint, to determine analytically the performance of the Modified Air Car with a separate propulsive system attached.

To facilitate the analysis, the following relationships were used:

$$A_o = 1 + \frac{S_b}{hC} \quad \text{augmentation of the wingless GEM} \quad (A-4)$$

$$A = A_o \left(1 - \frac{L_w}{W} \right) \quad \text{augmentation of the winged GEM} \quad (A-5)$$

$$HP_R = \frac{V_j}{\eta_i / 1100} (W - L) \left(\frac{1}{A} + \frac{A_j}{S_b} \right) + \frac{V}{550 \eta_p} (C_D q S_b + m_j V) \quad (A-6)$$

For use in the above equations, the following characteristics of the Modified Air Car were theoretically and experimentally determined:

$$W = 4330 \text{ lb}$$

$$S_b = 108 \text{ ft}^2$$

$$A_j = 11.02 \text{ ft}^2$$

$$A_o = 11.6 \text{ (at 356 BHP in hover, } h = 2.65 \text{ in.)}$$

$$m_j = 3.13 \text{ slugs/sec}$$

$$\eta_i = .24$$

$$C_d = .115 \text{ (no wings)}$$

$$C_d = .29 \text{ (with wings)}$$

$$V_j = 119 \text{ ft/sec}$$

$$L_w = 266 \text{ q}$$

Also, to simplify matters, it was assumed that the propulsive package was a reciprocating engine with a variable-pitch propeller so that the propeller efficiency could be held to a constant value of .7 over the range of velocities investigated. By use of equations A-4, A-5, and A-6, the following characteristics were determined:

1. Altitude increase by keeping the jet momentum constant -

In Figure 54, the altitude increase and the percentage altitude increase due to the wings are plotted versus velocity. As can be seen, the altitude increase becomes substantial with increased velocity. Thus it can

be predicted readily that use of wings on a separate propulsive system type GEM can be a powerful tool for increasing its altitude potential.

2. Brake Horsepower required versus velocity, keeping the jet momentum constant -

The most important aspect of the results shown in Figure 55 is that the lift of the wings also decreases the total power required while increasing the altitude. The reason for this is that as the wings unload the base, the static pressure requirements of the jet are reduced, which reduces the jet total pressure requirements.

3. Brake Horsepower required versus velocity, keeping the augmentation (altitude) constant -

As seen in Figure 55, the power savings due to wing lift are the greatest when the augmentation is held constant. The reason for this is twofold. First of all, as wing lift builds up, the power requirements for lift are reduced. Secondly, coupled with the decrease in power required for lift is a reduction of jet mass flow which reduces the momentum drag sizably. It is interesting to note that in this particular case where wing lift builds up rapidly and the propulsive efficiency is high, the total power required decreases with velocity, making the horsepower-required curve look somewhat similar to that of a slow-flying airplane.

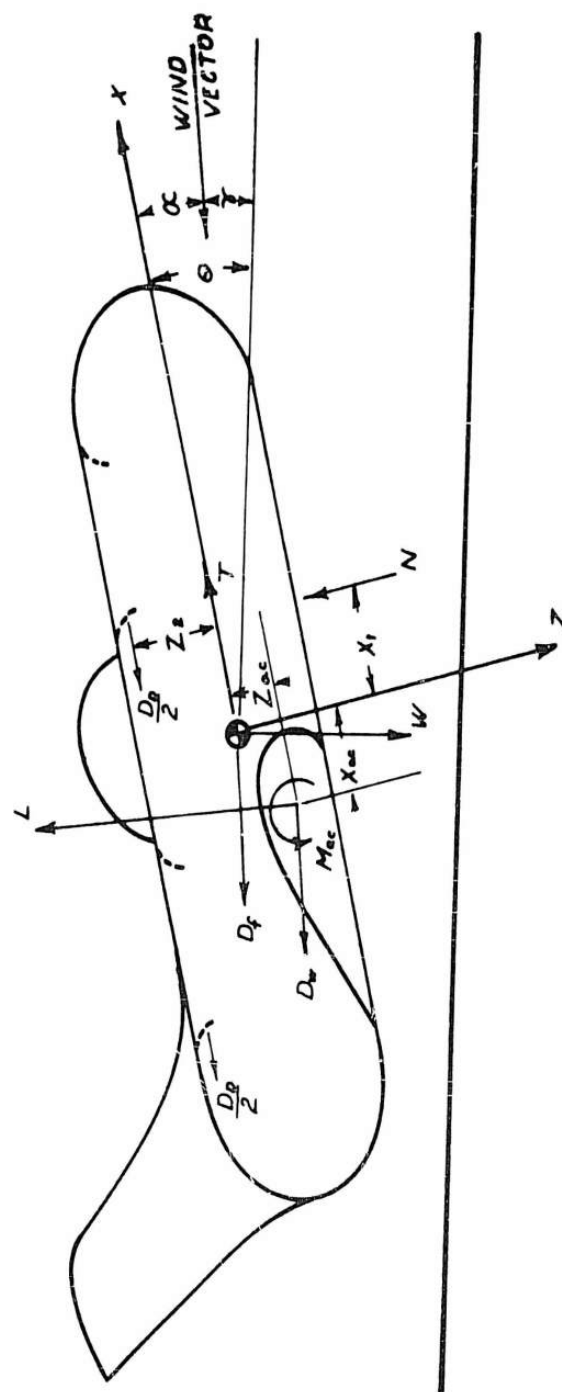
TABLE OF FIGURES

Fig. No.

- 1 Forces on a winged GEM in forward flight.
- 2 Body axis inertia reaction terms.
- 3 Definition of Θ and Φ angles.
- 4 Theoretical augmentation versus h/d_e for selected velocities.
- 5 Total power required as a function of velocity and aerodynamic lift coefficient.
- 6 Lift to drag ratios as a function of velocity and aerodynamic lift coefficient.
- 7 Augmentation ratio as a function of velocity for the Curtiss-Wright Air Car ACM 6-1.
- 8 Absolute altitude as a function of velocity for the Curtiss-Wright Air Car ACM 6-1.
- 9 Distribution of weight between the wings and base of the Curtiss-Wright Air Car ACM 6-1.
- 10 Winged GEM root locus, Case I, $C_{m\alpha} = 0$ to $-\infty$; $C_{mu} = .10$
Case II, $C_{m\alpha} = 0$ to $-\infty$; $C_{mu} = 0$
- 11 Winged GEM root locus, Case III, $C_{m\alpha} = 0$ to $-\infty$; $C_{mu} = -.10$
Case IV, $C_{m\alpha} = 0$ to $+\infty$; $C_{mu} = 0$
- 12 Winged GEM root locus, Case V, $C_{mu} = 0$ to $-\infty$; $C_{m\alpha} = 0$
Case VI, $C_{mu} = 0$ to $+\infty$; $C_{m\alpha} = -.15$
- 13 Root locus, Case VII, winged GEM $C_{mu} = 0$ to $-\infty$; $C_{m\alpha} = -.15$
Case VIII, non-winged GEM $C_{mu} = 0$ to $\pm\infty$; $C_{m\alpha} = 0$
- 14 Three quarter view, Curtiss-Wright Air Car ACM 6-1 (Photo.)
- 15 Rectangular Annular Jet Model
- 16 Rectangular Annular Jet Model fitted with wings
- 17 Static Hover Test Stand
- 18 Modified C-W Air Car Model (Photo.)
- 19 Schematic drawing of Modified C-W Air Car Model

20	Hover performance of rectangular model
21	Hover performance of rectangular model
22	Hover performance of rectangular model with wings attached
23	Static roll stability of rectangular model
24	Static roll stability of rectangular model
25	Static roll stability of rectangular model
26	Static roll stability of rectangular model with wings attached
27	Performance comparison of rectangular model with wings attached
28	Performance comparison of rectangular model with wings attached
29	Hover performance of C-W Air Car Model
30	Hover stability of C-W Air Car Model
31	C_L vs. α for several configurations (modified model)
32	C_m vs. α for several configurations (modified model)
33	C_m vs. C_L for several configurations (modified model)
34	C_m vs. α for several values of i_t (modified model)
35	C_m vs. α for several power conditions (modified model)
36	C_L, C_D vs. α for several configurations (modified model)
37	C_m vs. C_L for several values of i_t (modified model)
38	C_L, C_D vs. α for several values of q (modified model)
39	C_m vs. C_L for several values of q (modified model)
40	C_L, C_D vs. α for several values of h/w (modified model)
41	C_m vs. α for several values of h/w (modified model)
42	C_m vs. α for several values of h/w (modified model)
43	C_L, C_D vs. α for several values of ψ (modified model)
44	C_m vs. α @ $h/w = \infty$ (modified model)

- 45 $C_m \text{ vs. } \alpha @ \frac{h}{w} = \infty$ for several values of ψ (modified model)
- 46 Three quarter view, Curtiss-Wright Air Car, ACM 6-1 (Photo.)
- 47 Three quarter view, Modified Curtiss-Wright Air Car (Photo.)
- 48 Top view, Modified Curtiss-Wright Air Car (Photo.)
- 49 General layout of full scale Modified C-W Air Car
- 50 Speed-height characteristics of C-W Air Car
- 51 Typical transient roll oscillations of C-W Air Car
- 52 Extrapolated speed-height characteristics of C-W Air Car
- 53 BHP vs. velocity - C-W Air Car
- 54 Altitude capabilities of separate propulsion winged GEM
- 55 BHP required for separate propulsion winged GEM



BODY AXIS SYSTEM AND FORCES IN FORWARD FLIGHT
FIG. 1

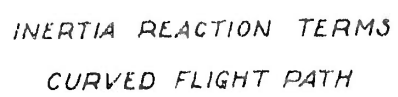
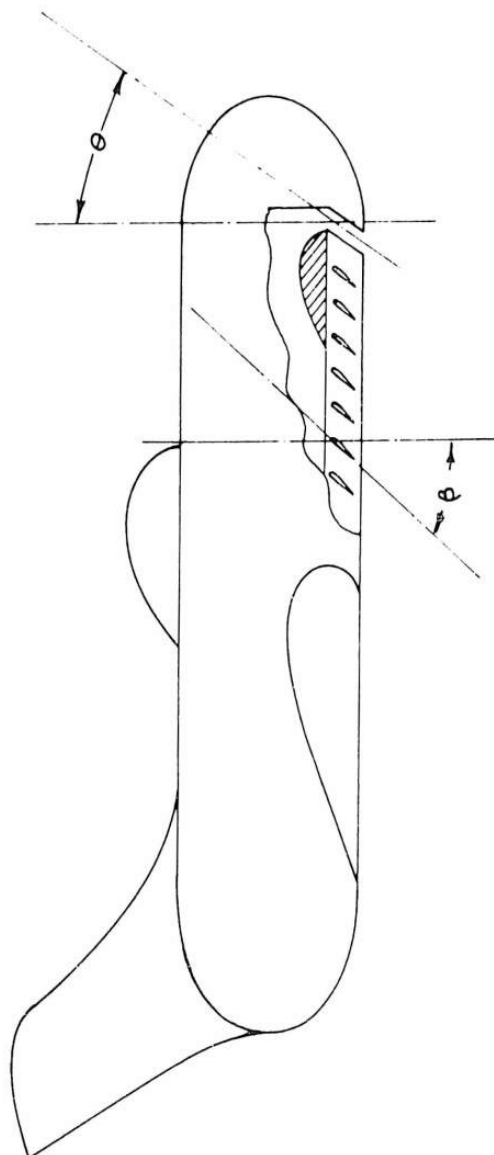
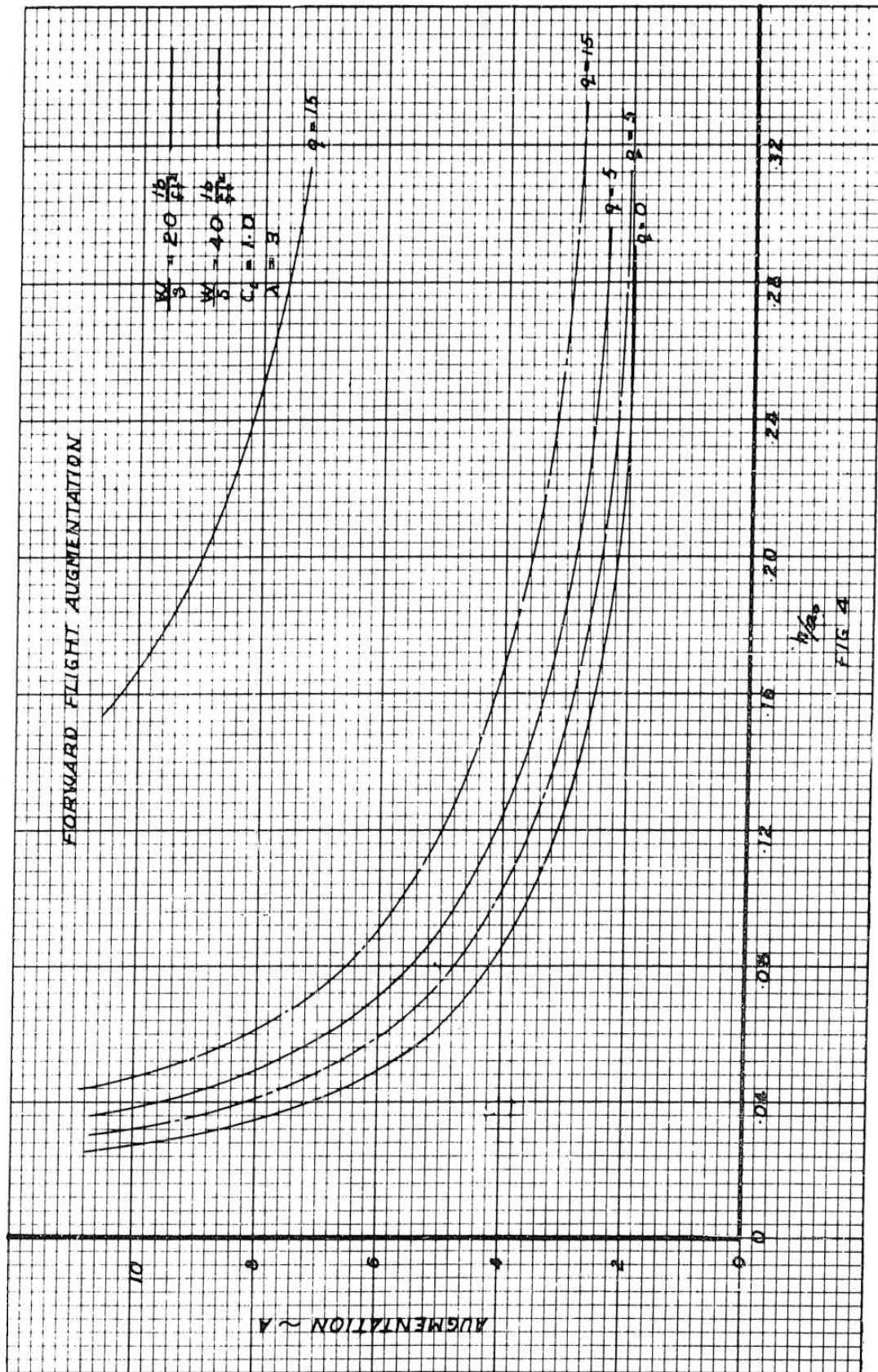


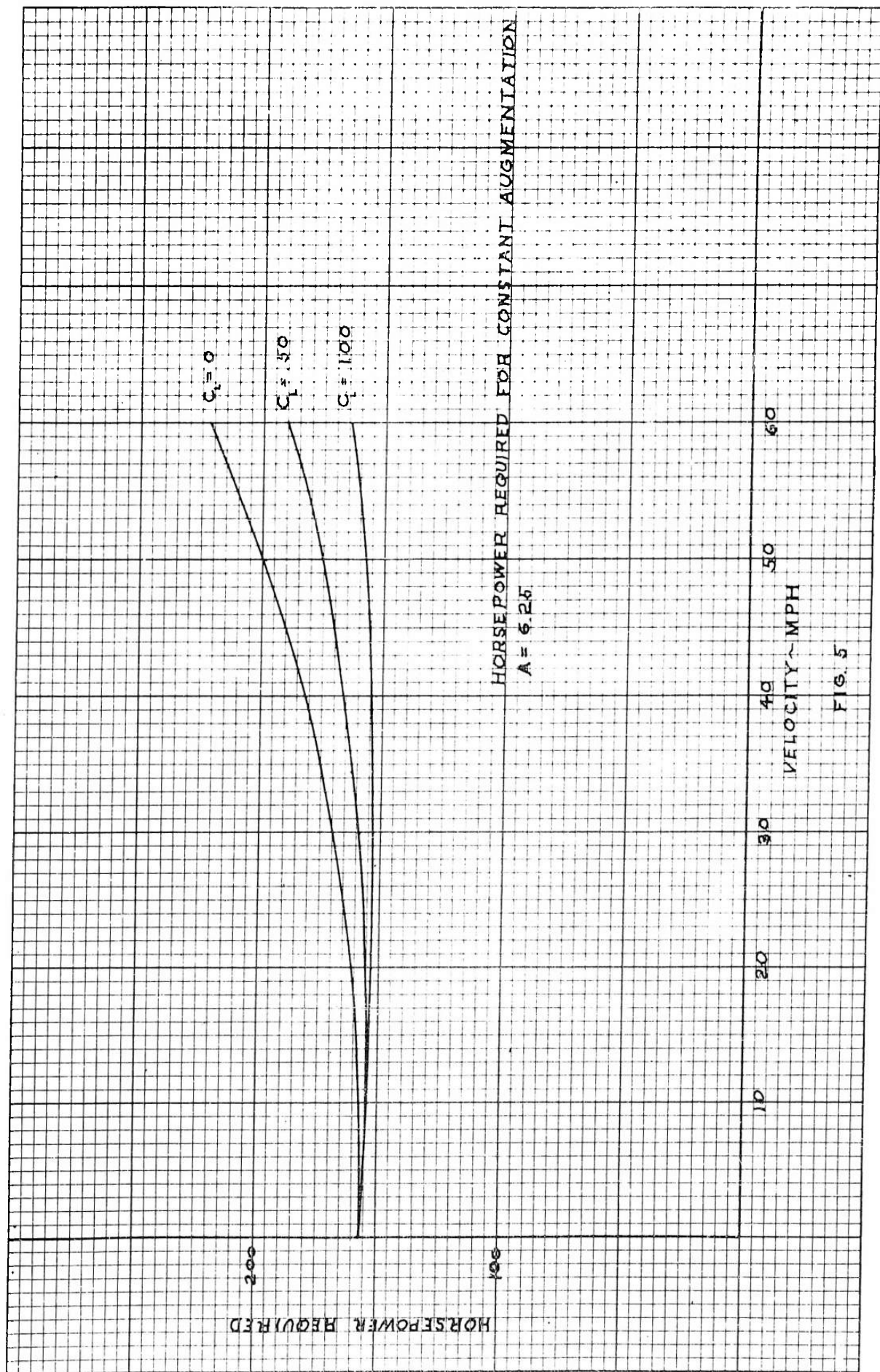
FIG. 2

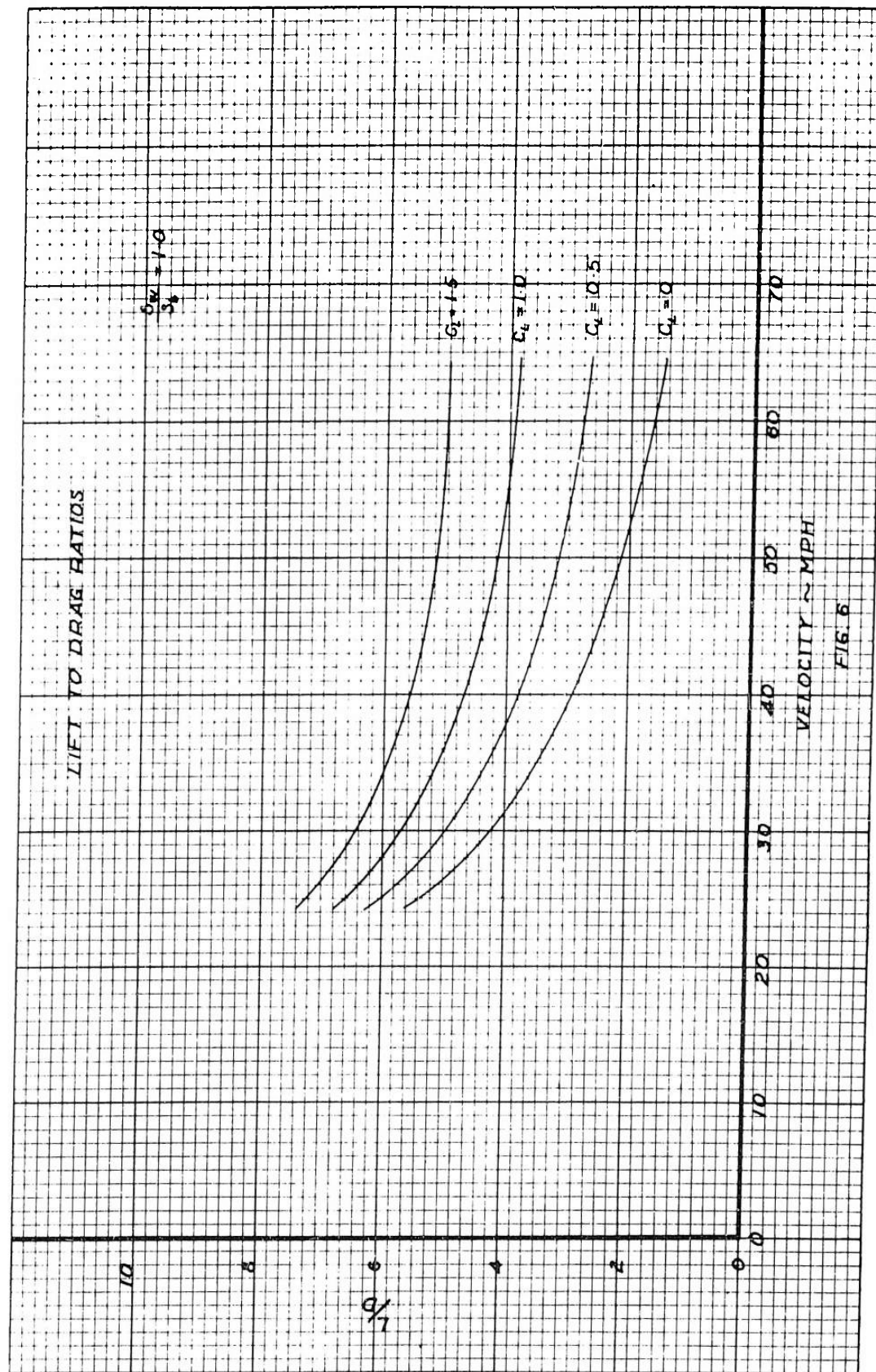


DEFINITION OF θ AND ϕ

FIG. 3







FORWARD FLIGHT AUGMENTATION
CURTISS-WRIGHT AIR CAR ACM6-1

$$\frac{W}{S} = 33.1 \frac{\text{lb}}{\text{ft}^2}$$

$$\frac{W}{S} = 16.7 \frac{\text{lb}}{\text{ft}^2}$$

$$C_L = 1.0$$

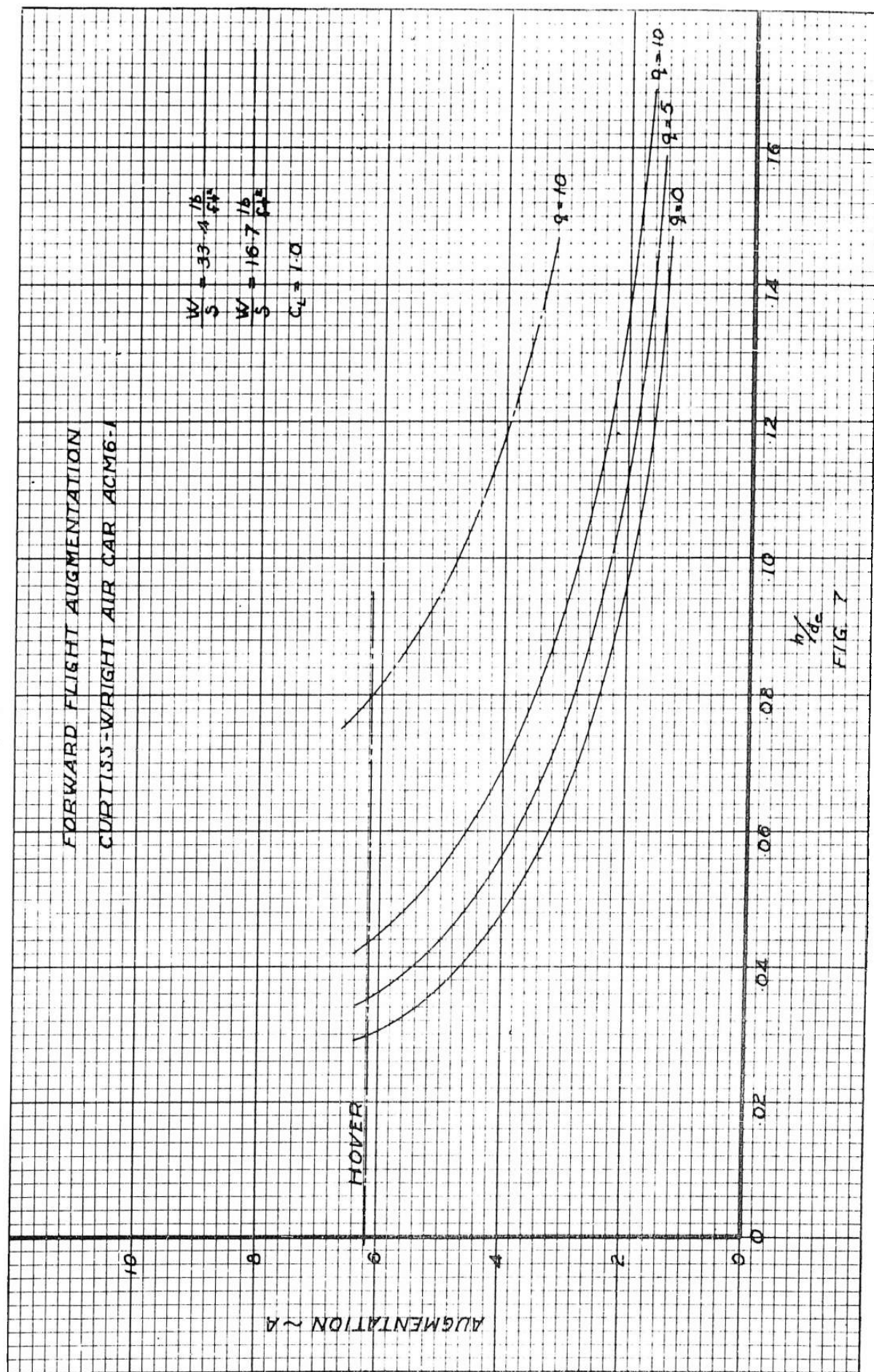


FIG. 7

FORWARD FLIGHT ALTITUDE
CURTISS-WRIGHT AIR CAR ACM6-1

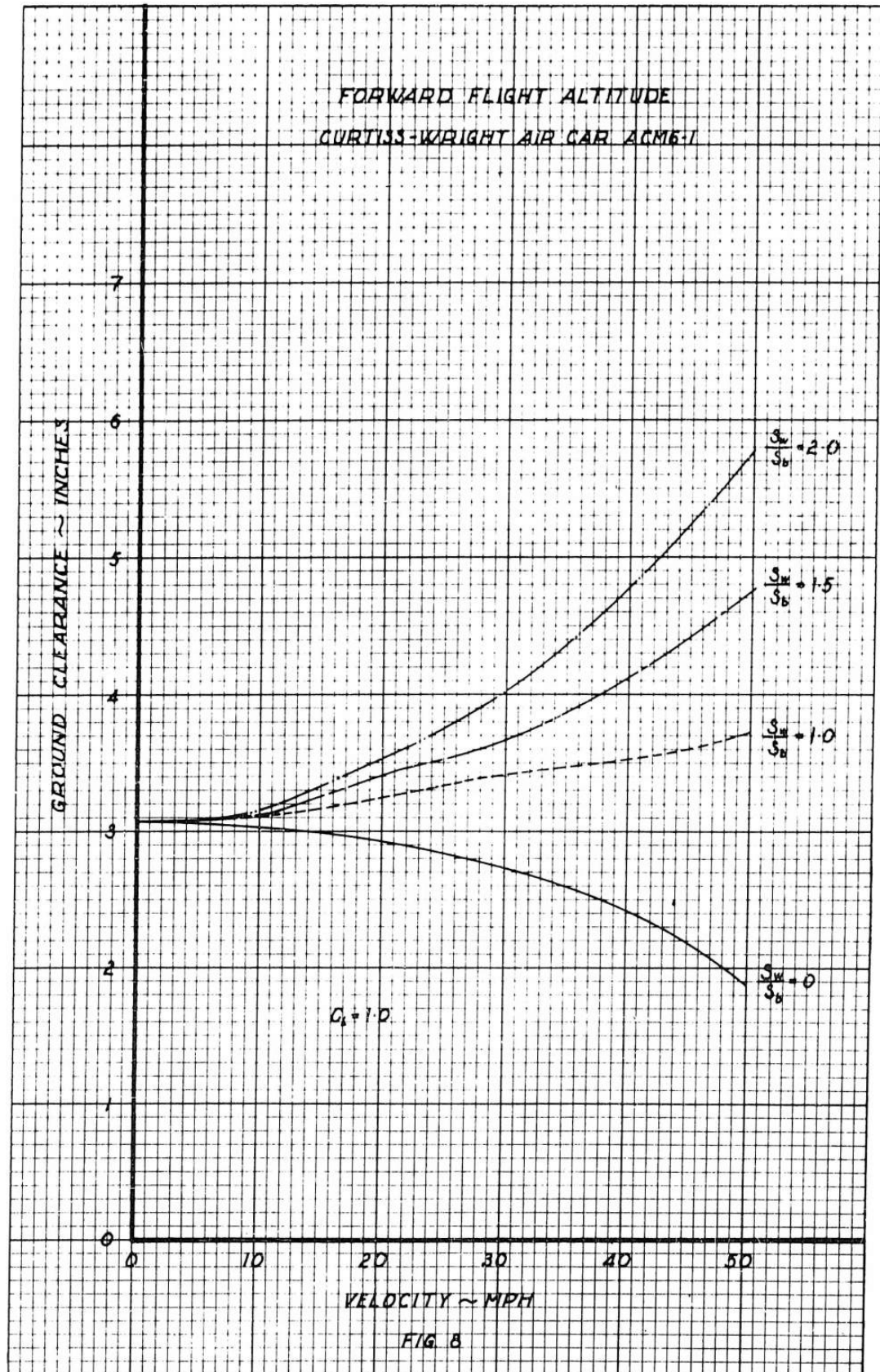
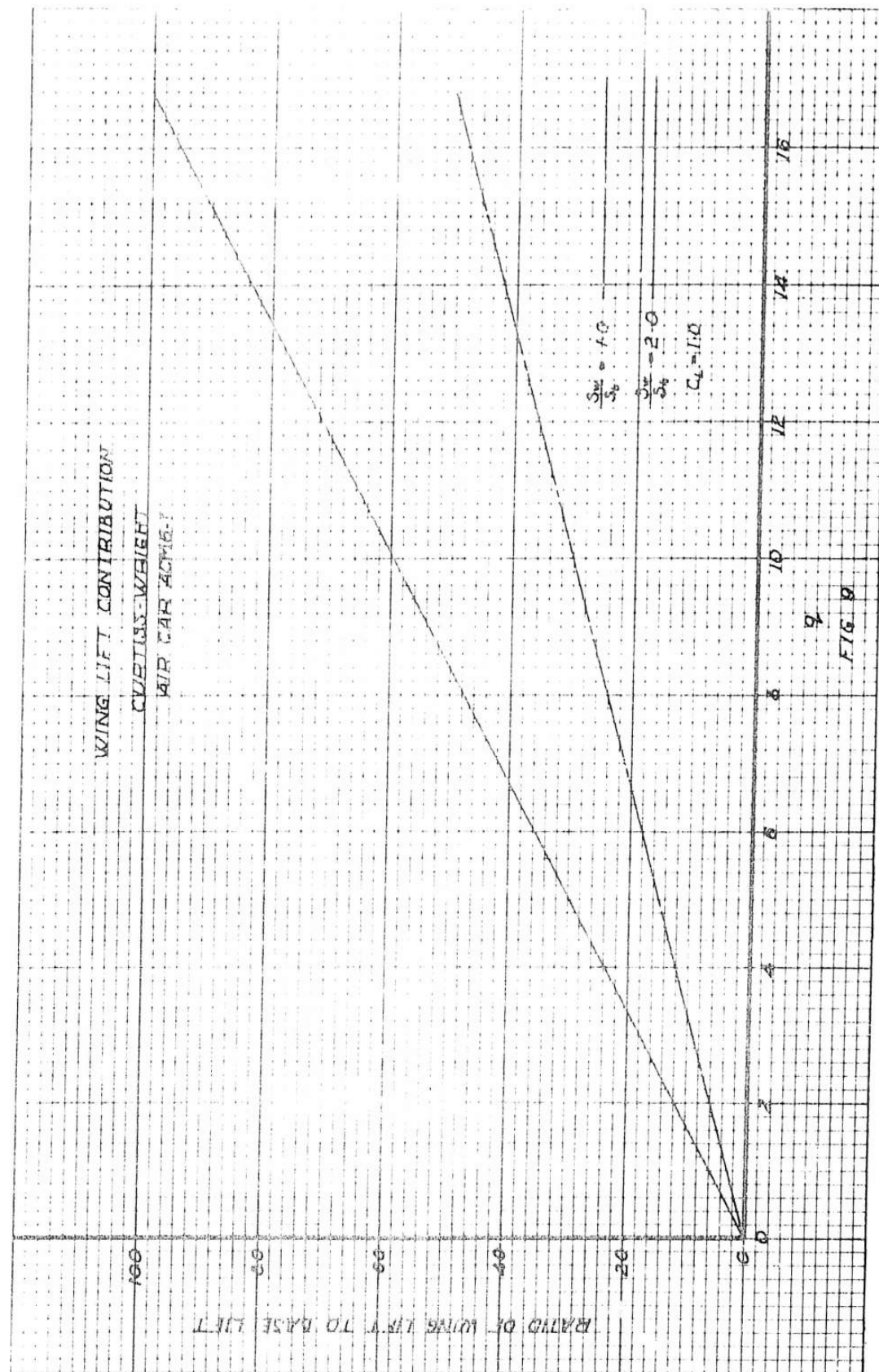
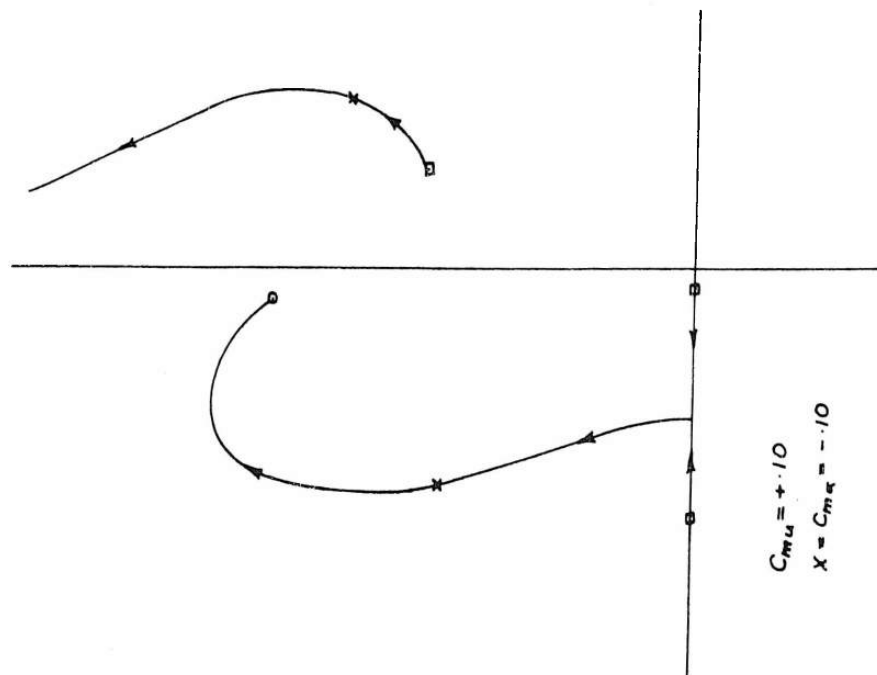
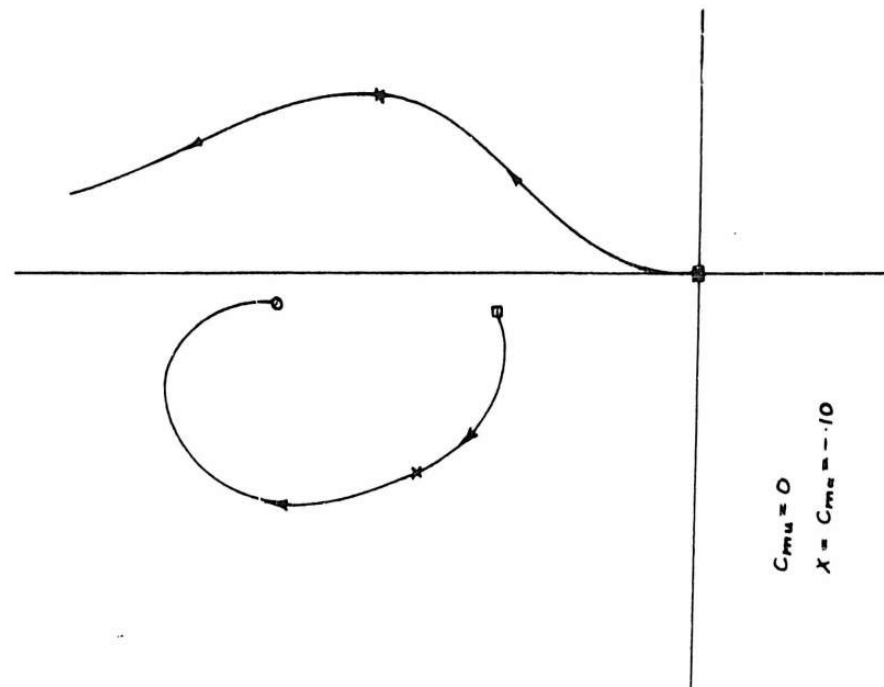


FIG. 8



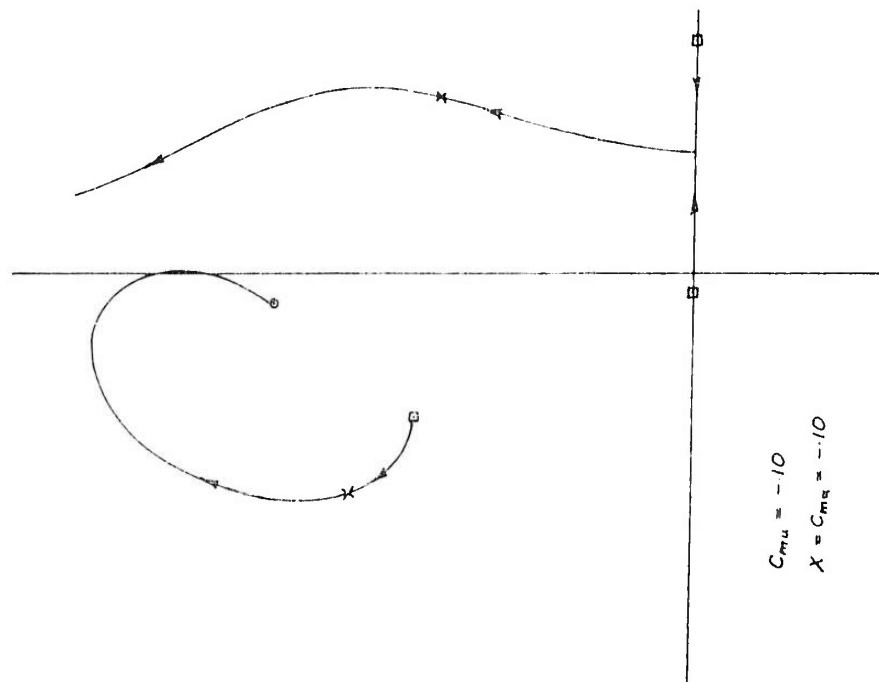


CASE I



CASE II

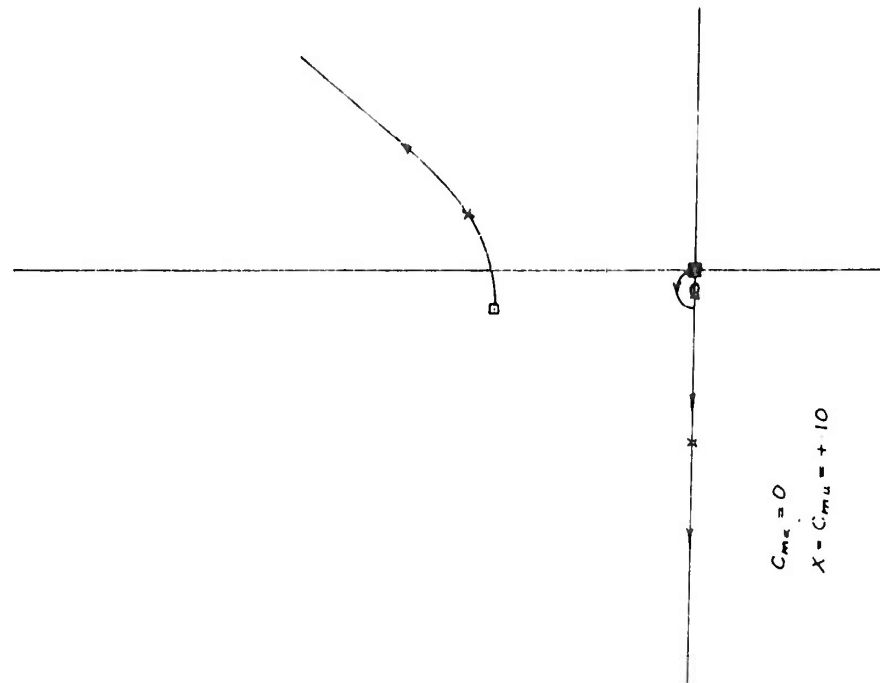
FIG. 10



$$C_{mu} = -10$$

$$X = C_{ms} = -10$$

CASE III



$$C_{ms} = 0$$

$$X = C_{mu} = +10$$

CASE IV

FIG. 11

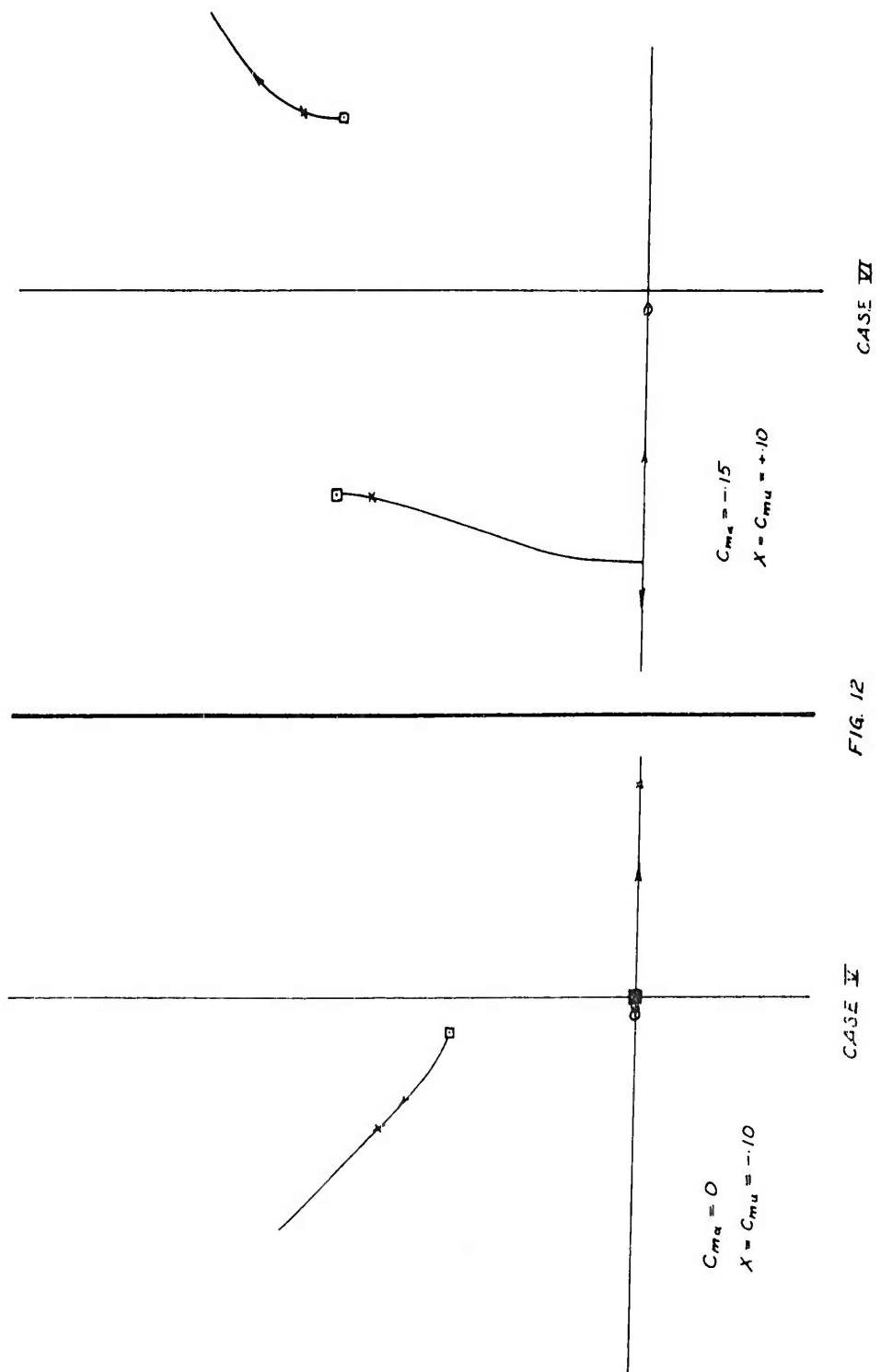
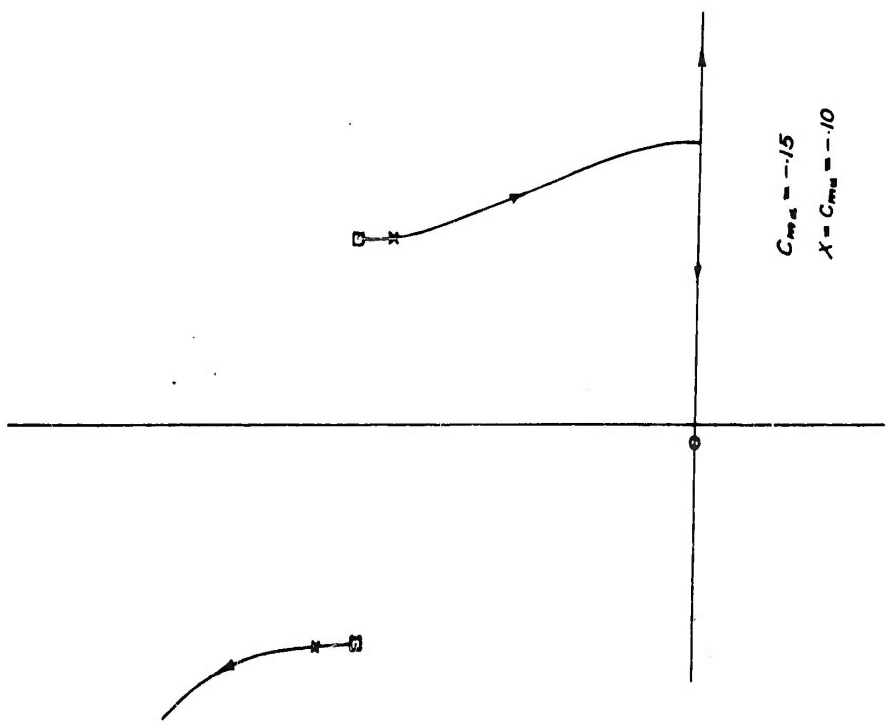
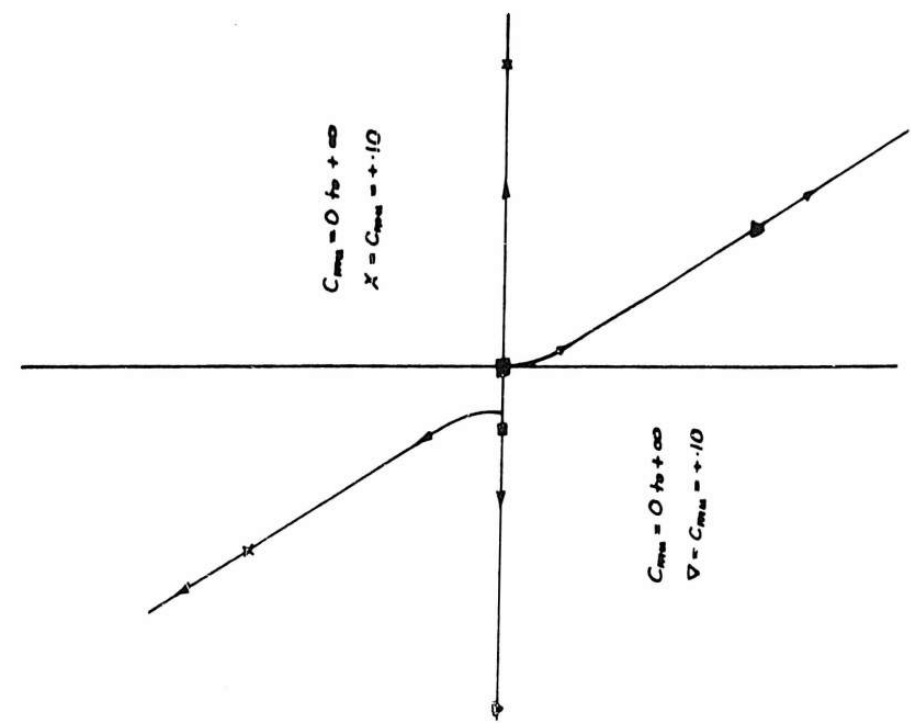


FIG. 12

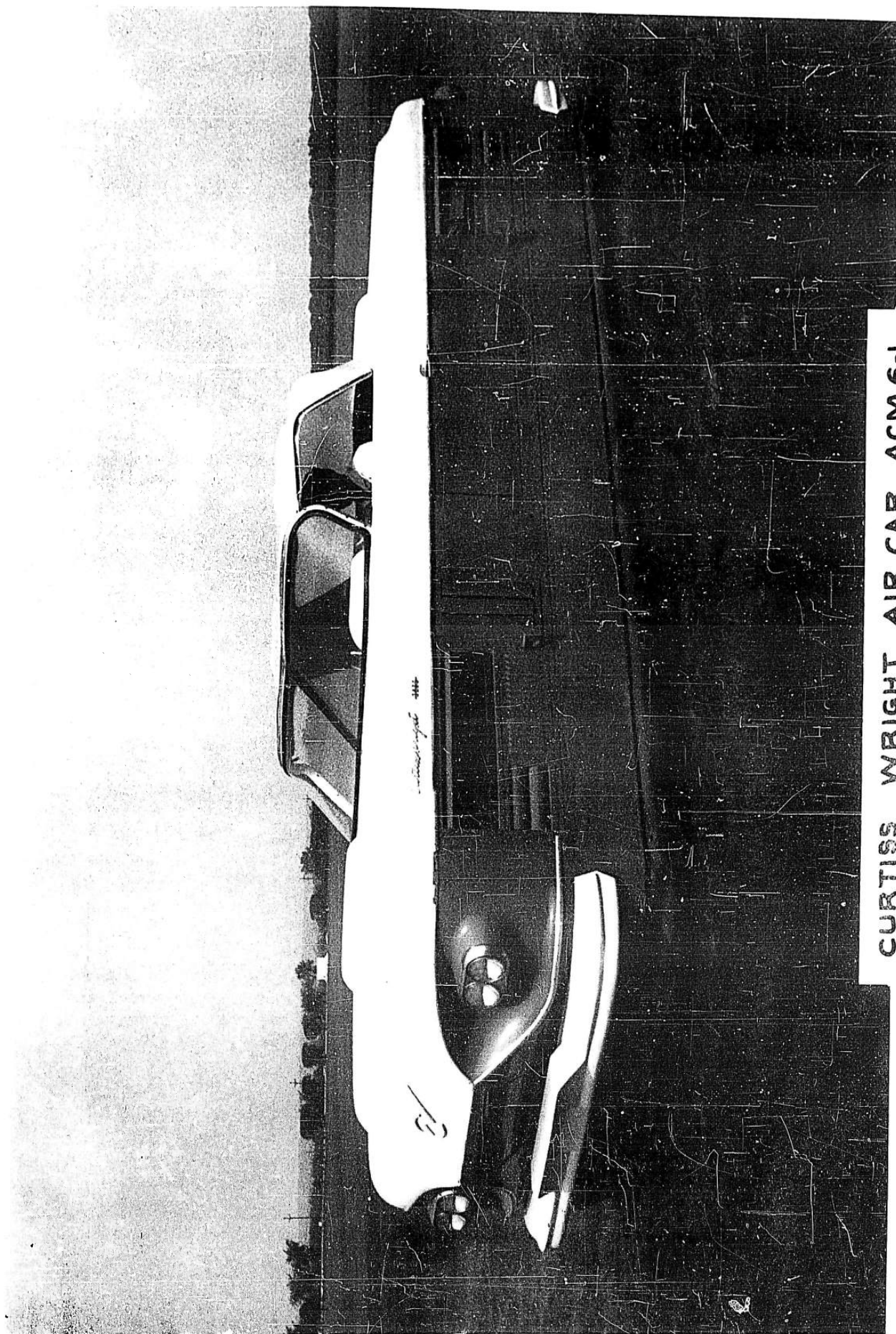


CASE VII



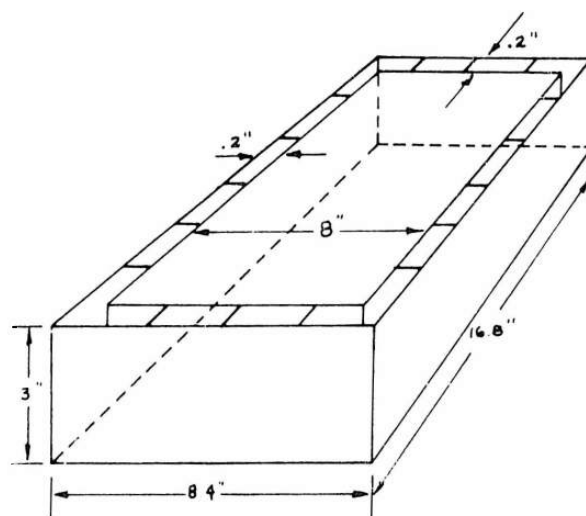
CASE VIII

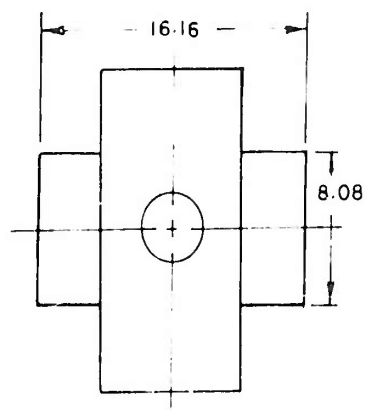
FIG. 13



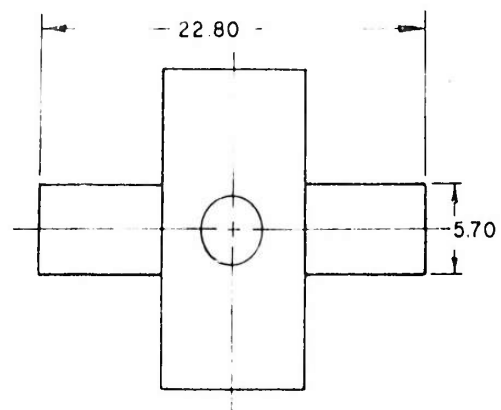
CURTISS WRIGHT AIR CAR ACM 6-1
FIG. 14

FIG. 15 - RECTANGULAR
ANNULAR JET MODEL

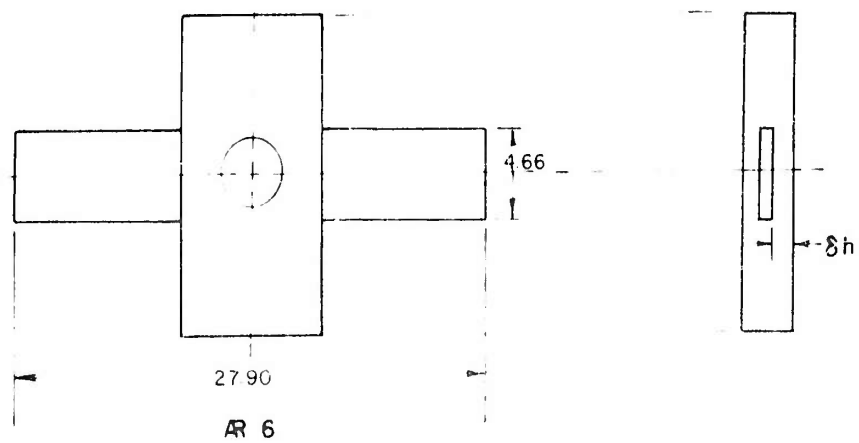




AR 2



AR 4



AR 6

RECTANGULAR MODEL SHOWING AR 2, 4, AND 6 WINGS
ALL DIMENSIONS IN INCHES

FIG. 16

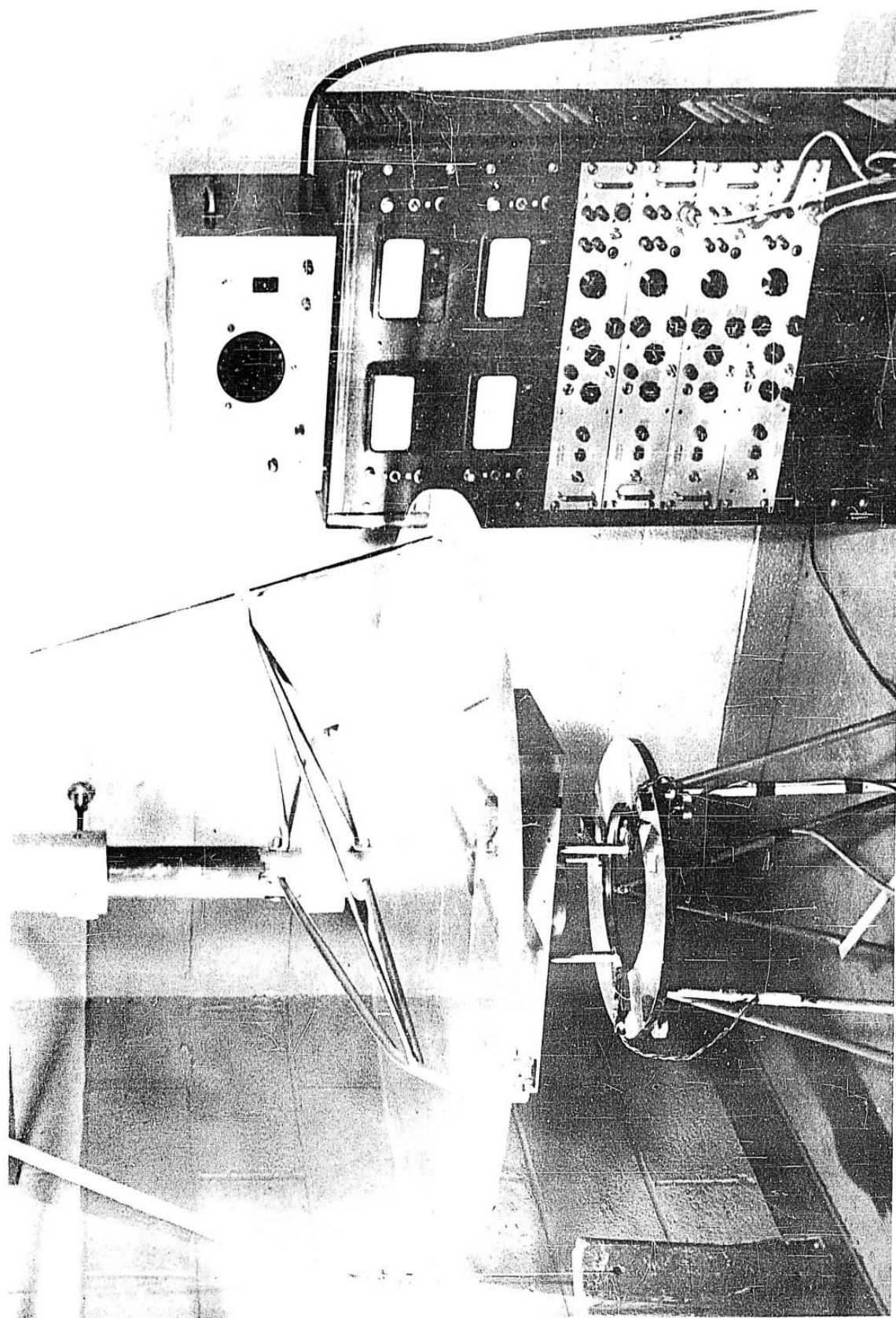


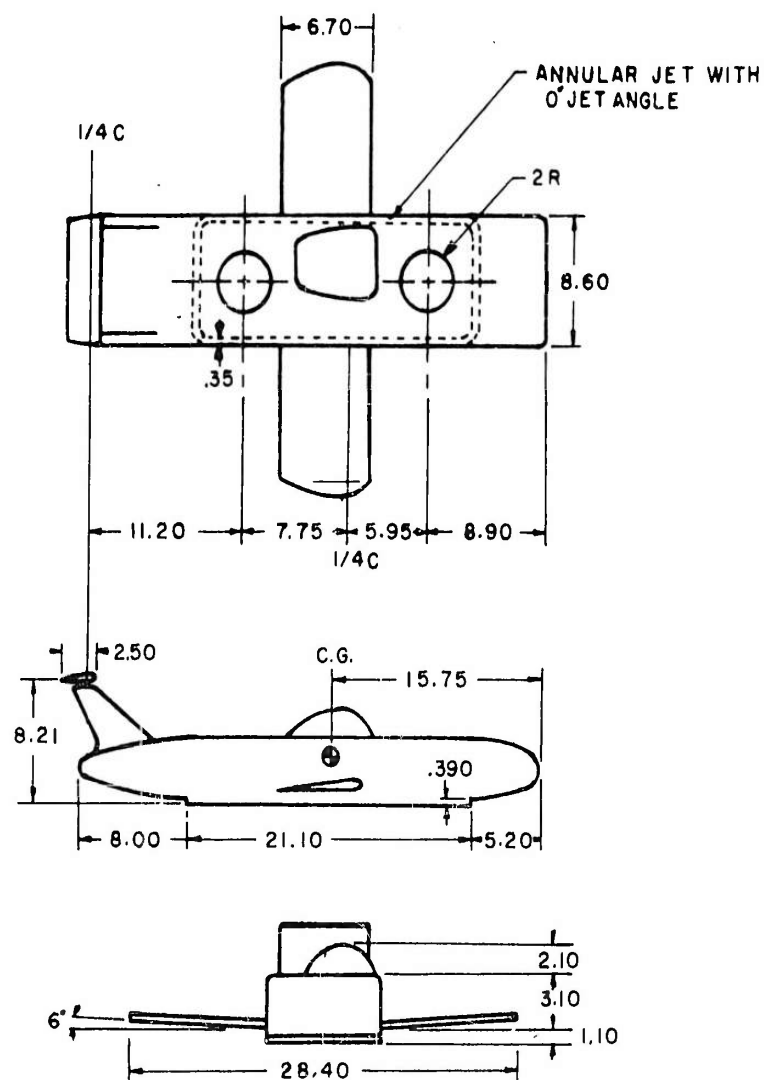
FIG. 17 STATIC HOVER TEST STAND



FIG. 18 MODIFIED C-W AIR CAR MODEL



FIG. 18 MODIFIED C-W AIR CAR MODEL



SCHEMATIC LAYOUT AND DIMENSIONS OF THE C-W
AIRCAR MODEL-ALL DIMENSIONS IN INCHES-WING
SHOWN IN THE FORWARD POSITION

FIG. 19

FIG. 20: HOVER PERFORMANCE OF
RECTANGULAR MODEL.

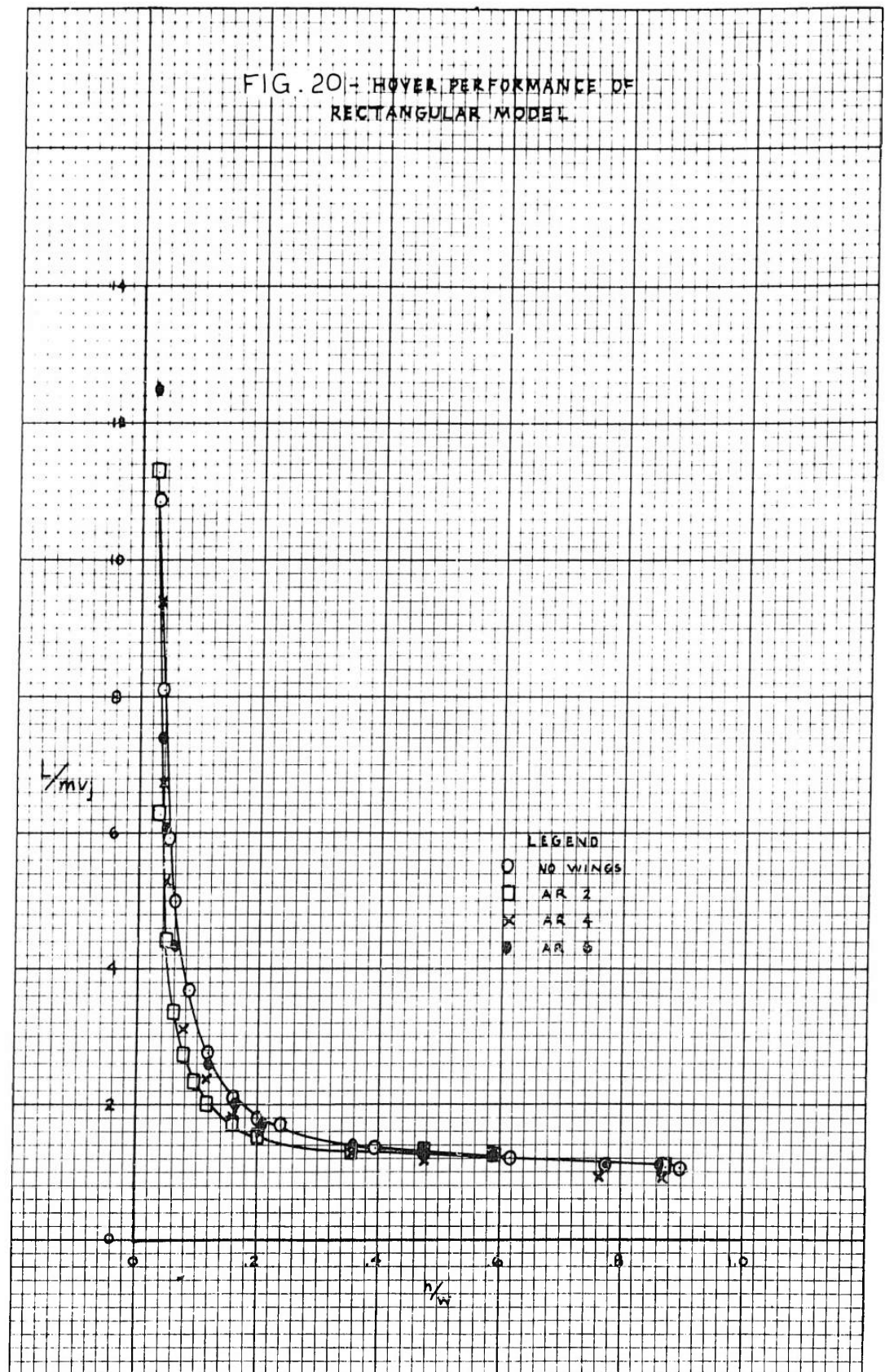


FIG. 21 - HOVER PERFORMANCE
OF RECTANGULAR MODEL

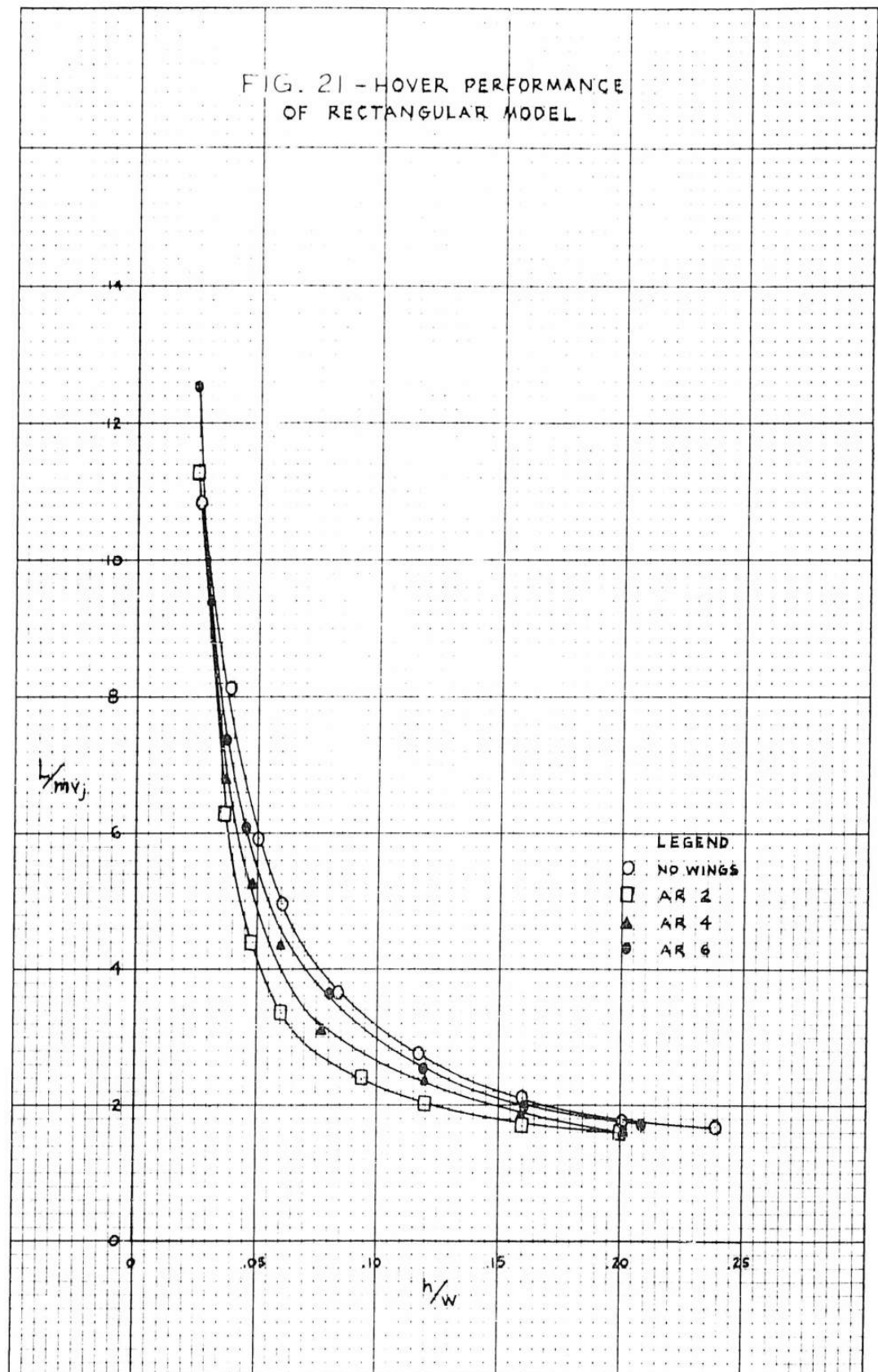


FIG. 22 - HOVER PERFORMANCE
OF RECTANGULAR MODEL WITH
WINGS ATTACHED AT DIFFERENT
HEIGHT INCREMENTS

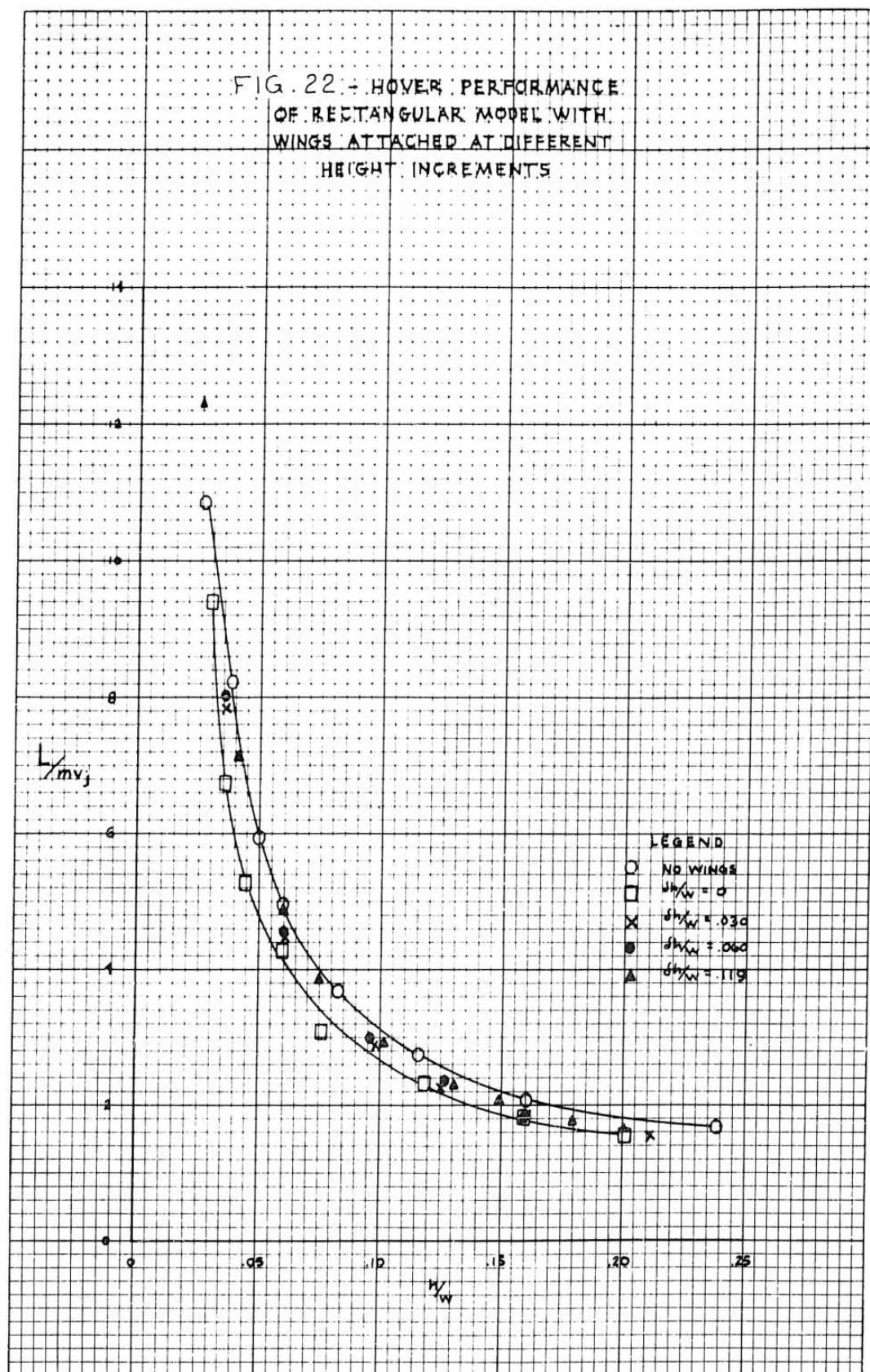


FIG. 23 - STATIC ROLL STABILITY
OF RECTANGULAR MODEL

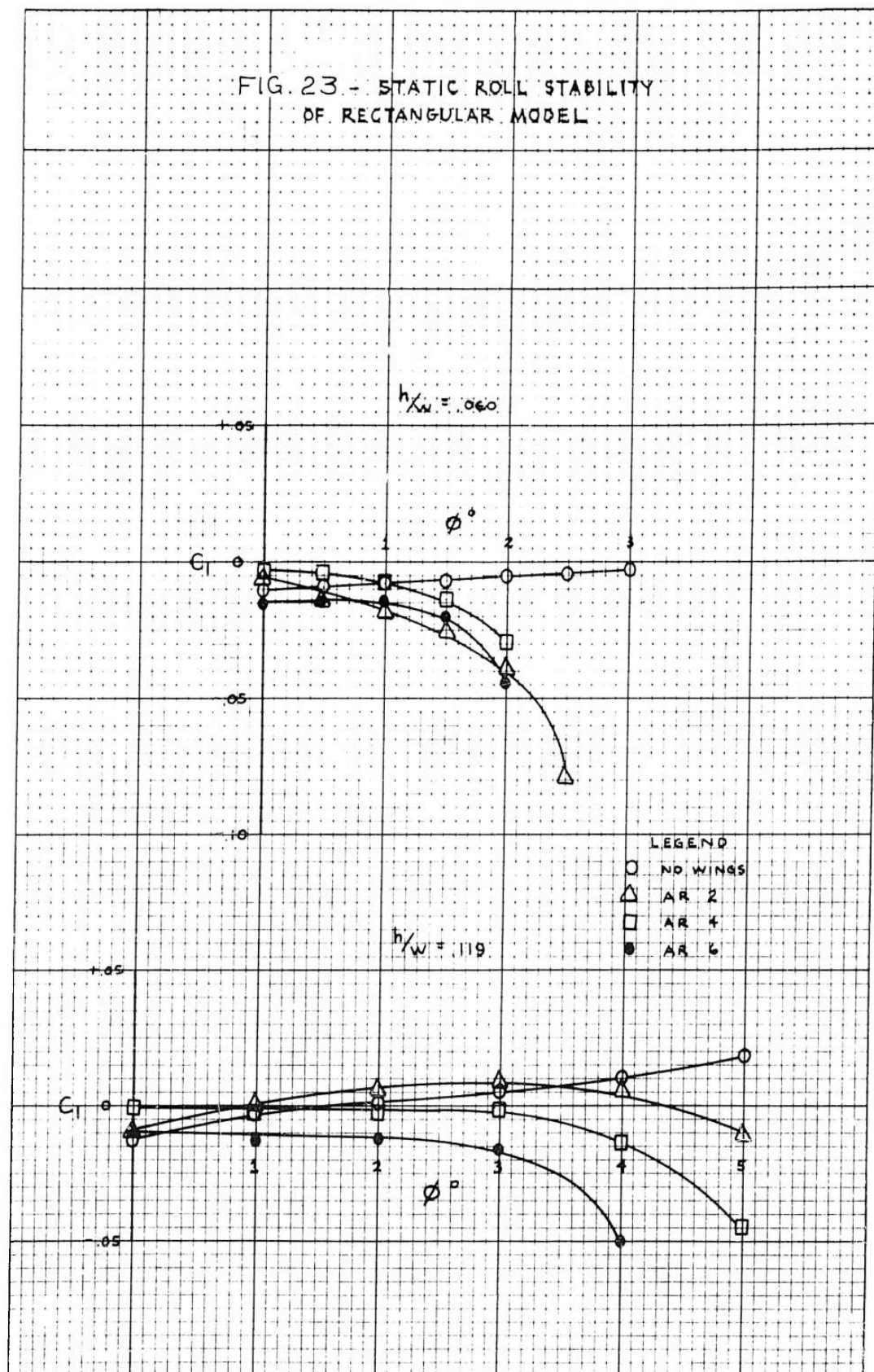


FIG. 24- STATIC ROLL STABILITY OF
RECTANGULAR MODEL AT $\mu/w = .559$

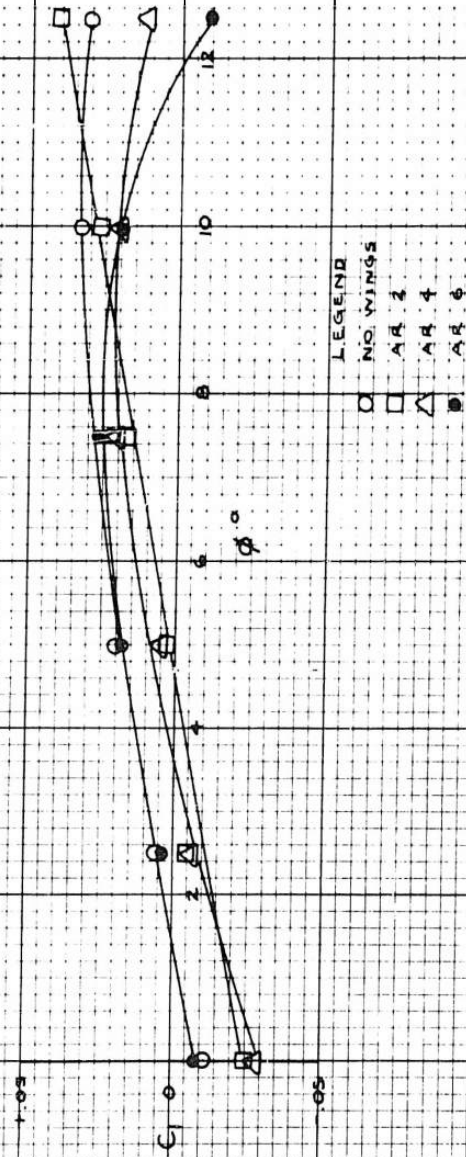


FIG. 25 - STATIC ROLL STABILITY OF
RECTANGULAR MODEL AT $M/W = 1.995$

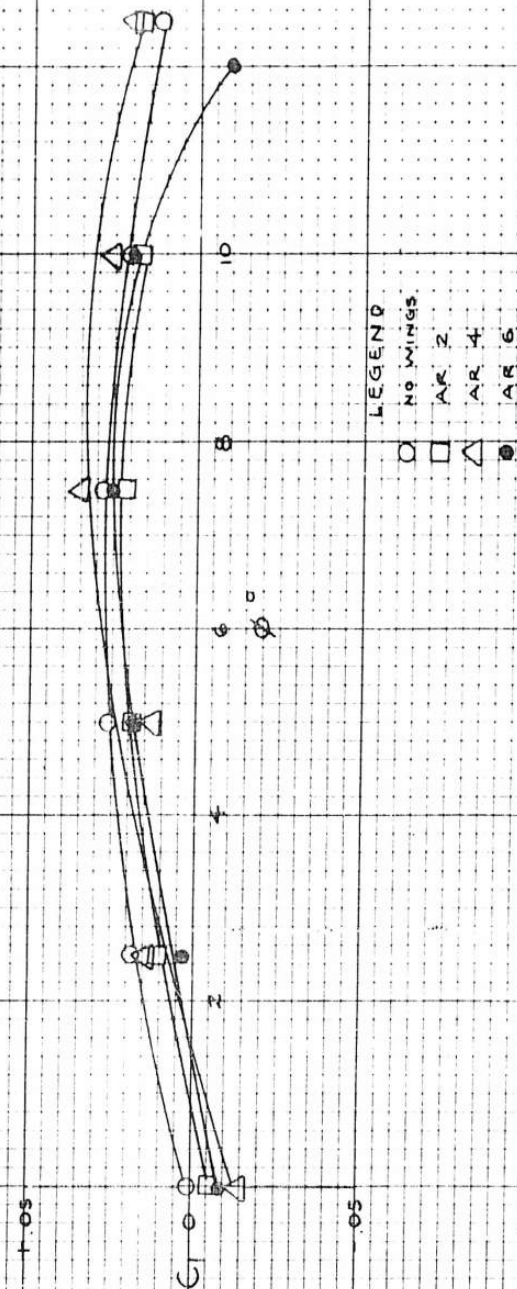


FIG. 26 - STATIC ROLL STABILITY
OF RECTANGULAR MODEL WITH WINGS
ATTACHED AT INCREMENTS ABOVE THE
BASE

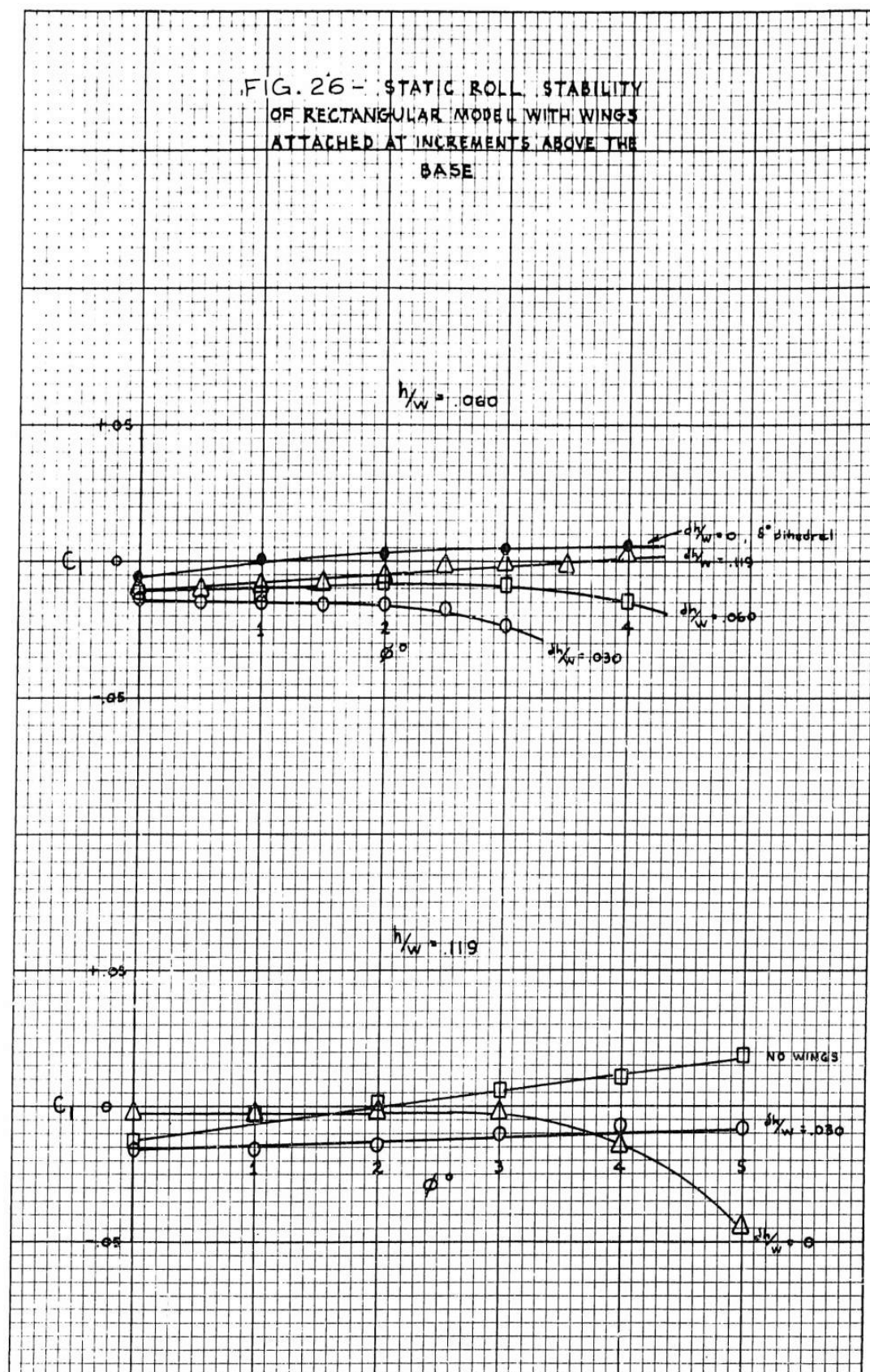


FIG. 27: COMPARISON OF STATIC
ROLL STABILITY AND HOVER
PERFORMANCE OF RECTANGULAR
MODEL WITH AR 2 AND AR 4
WINGS ATTACHED AT $h/w = .060$

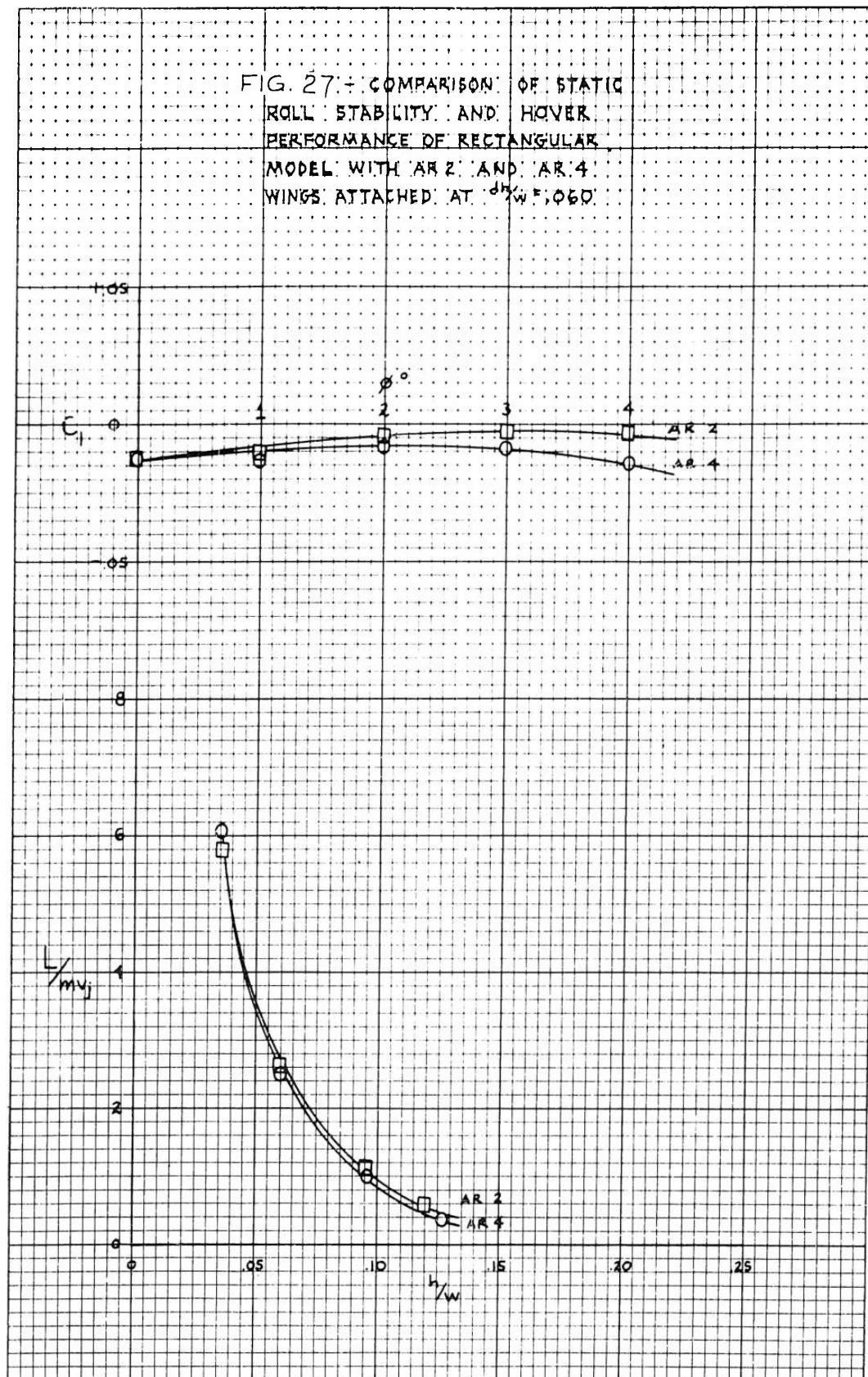


FIG. 2B - COMPARISON OF STATIC
ROLL STABILITY AND HOVER
PERFORMANCE OF RECTANGULAR
MODEL WITH AR 2 AND AR 4
WINGS ATTACHED AT $h/w = .030$

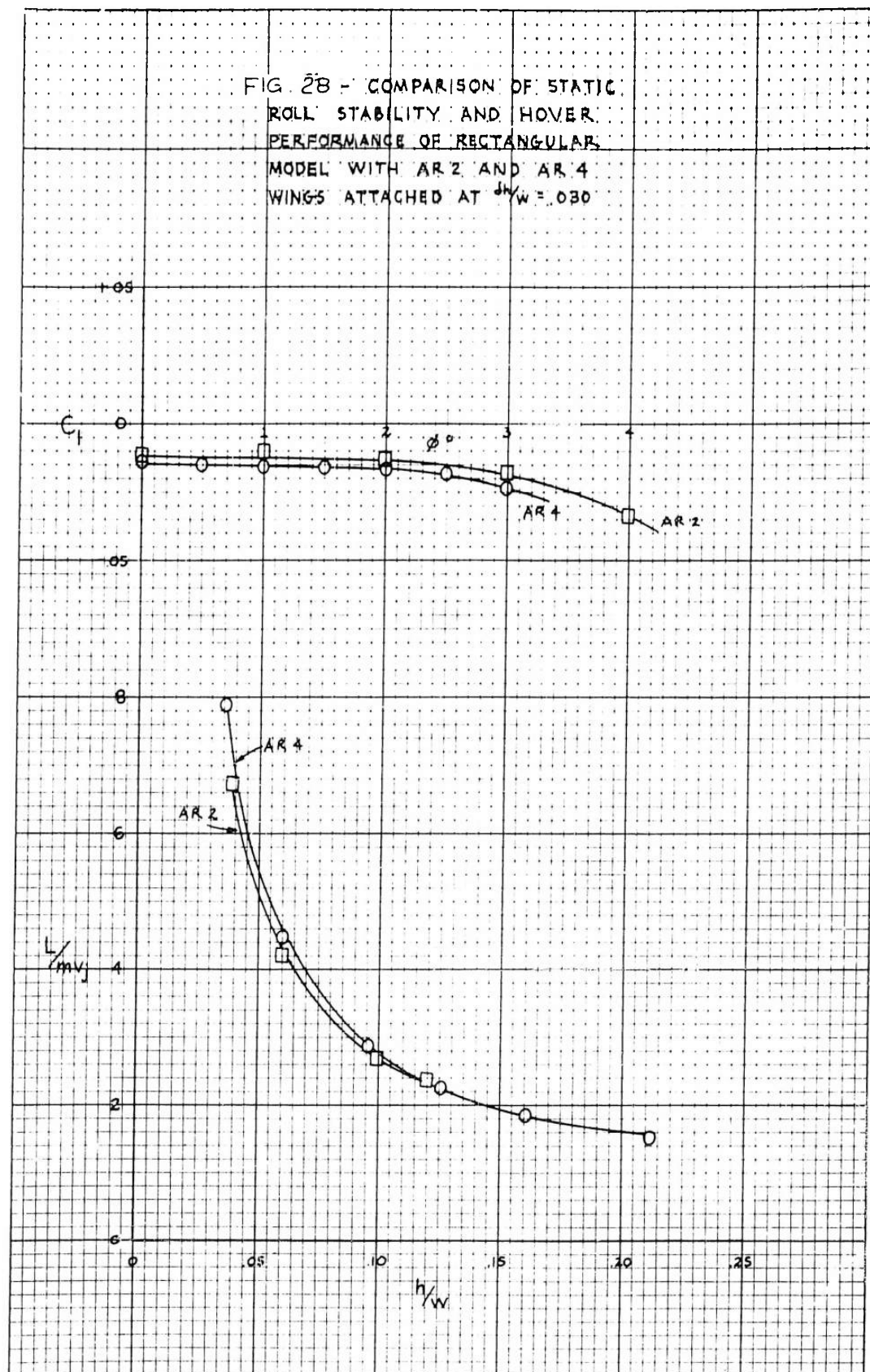


FIG. 29- HOVER PERFORMANCE OF
MODIFIED AND UNMODIFIED C-W
AIR CAR MODEL

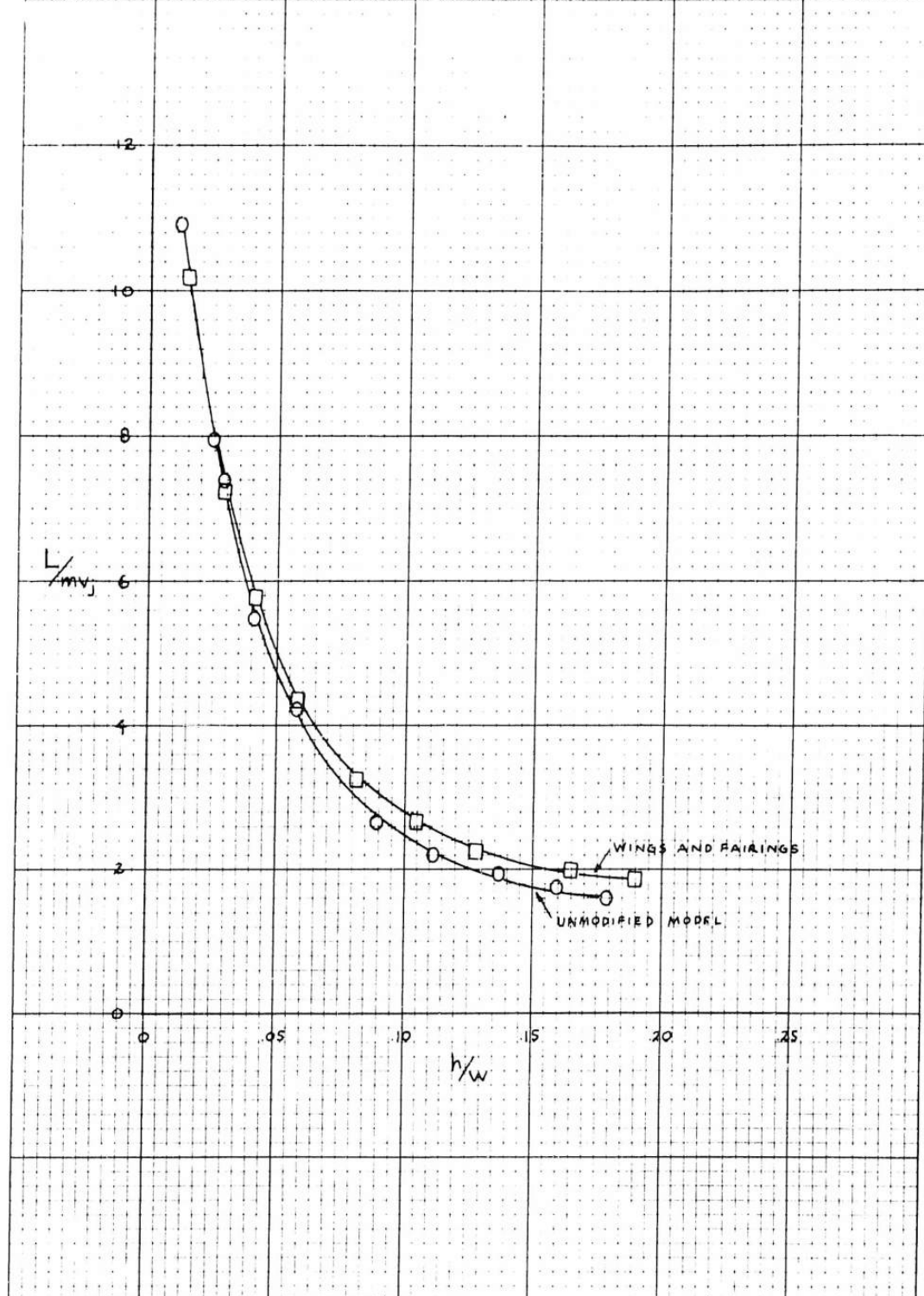


FIG. 30 - STATIC ROLL STABILITY
OF MODIFIED AND UNMODIFIED
C-W AIR CAR MODEL

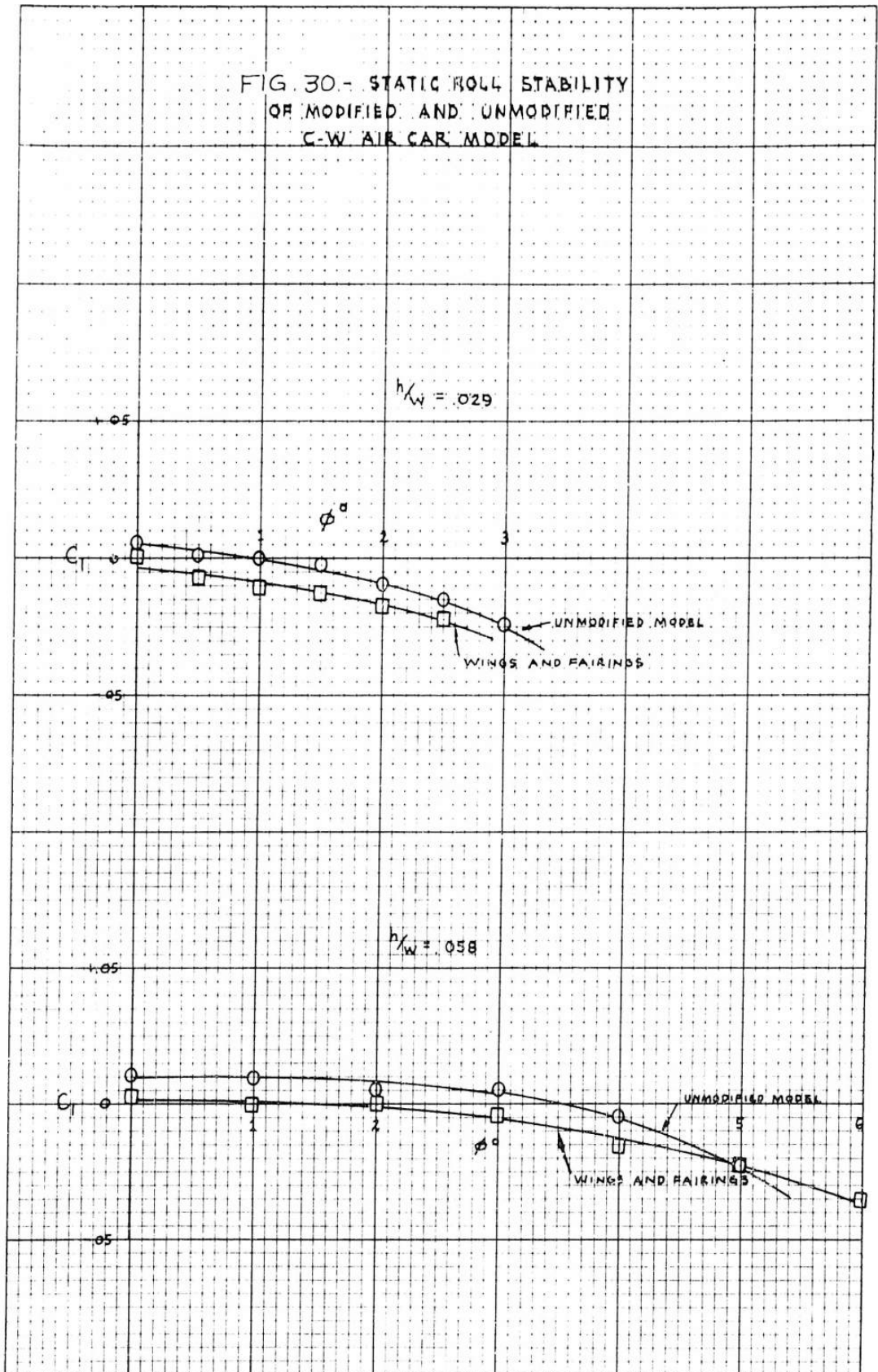


FIG. 31 - Modified GM Air Car model.
Lift & drag curves for various configurations.

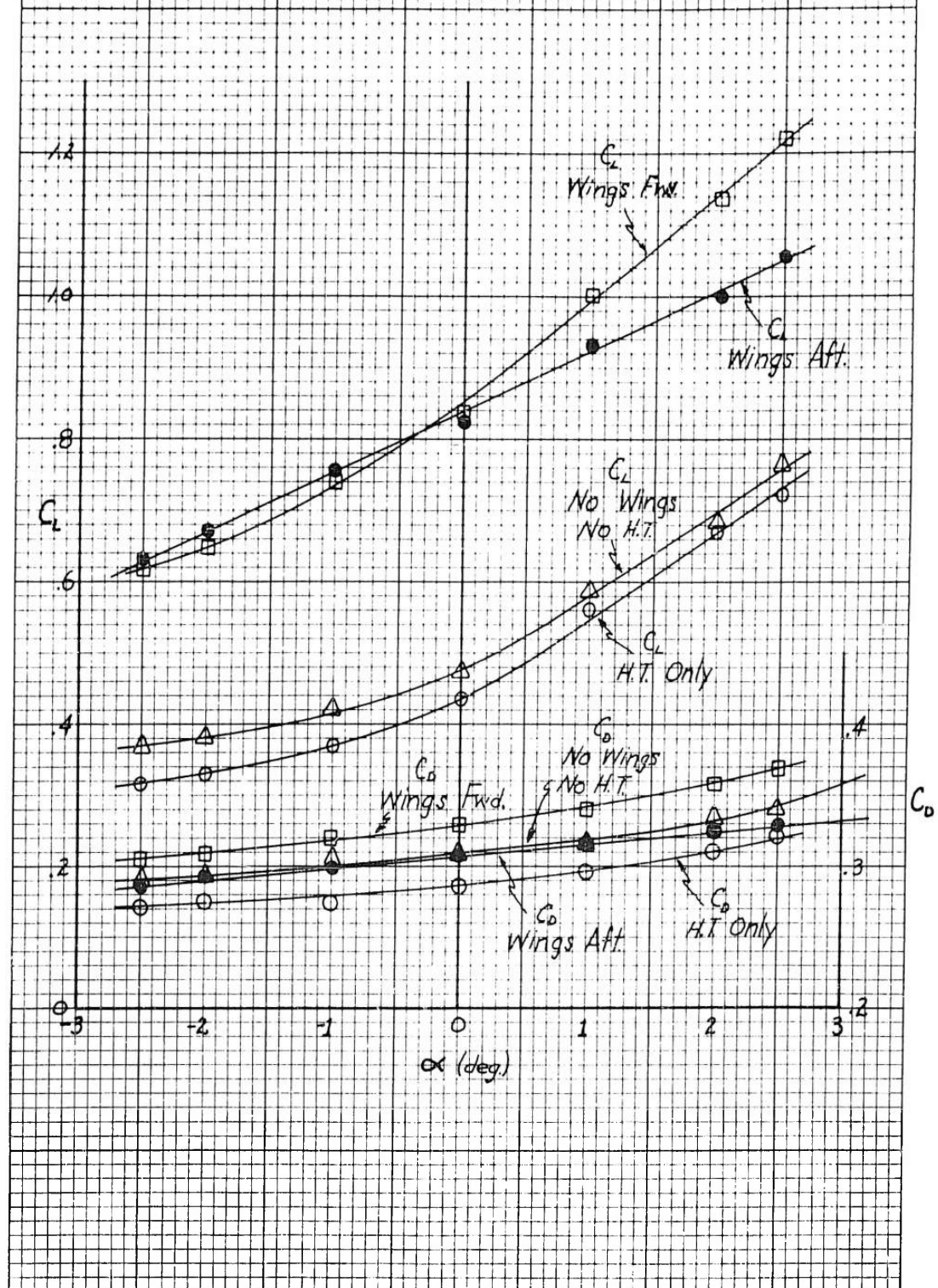


FIG. 32- Modified CW Air Car model.
 C_m vs. α for various configurations.

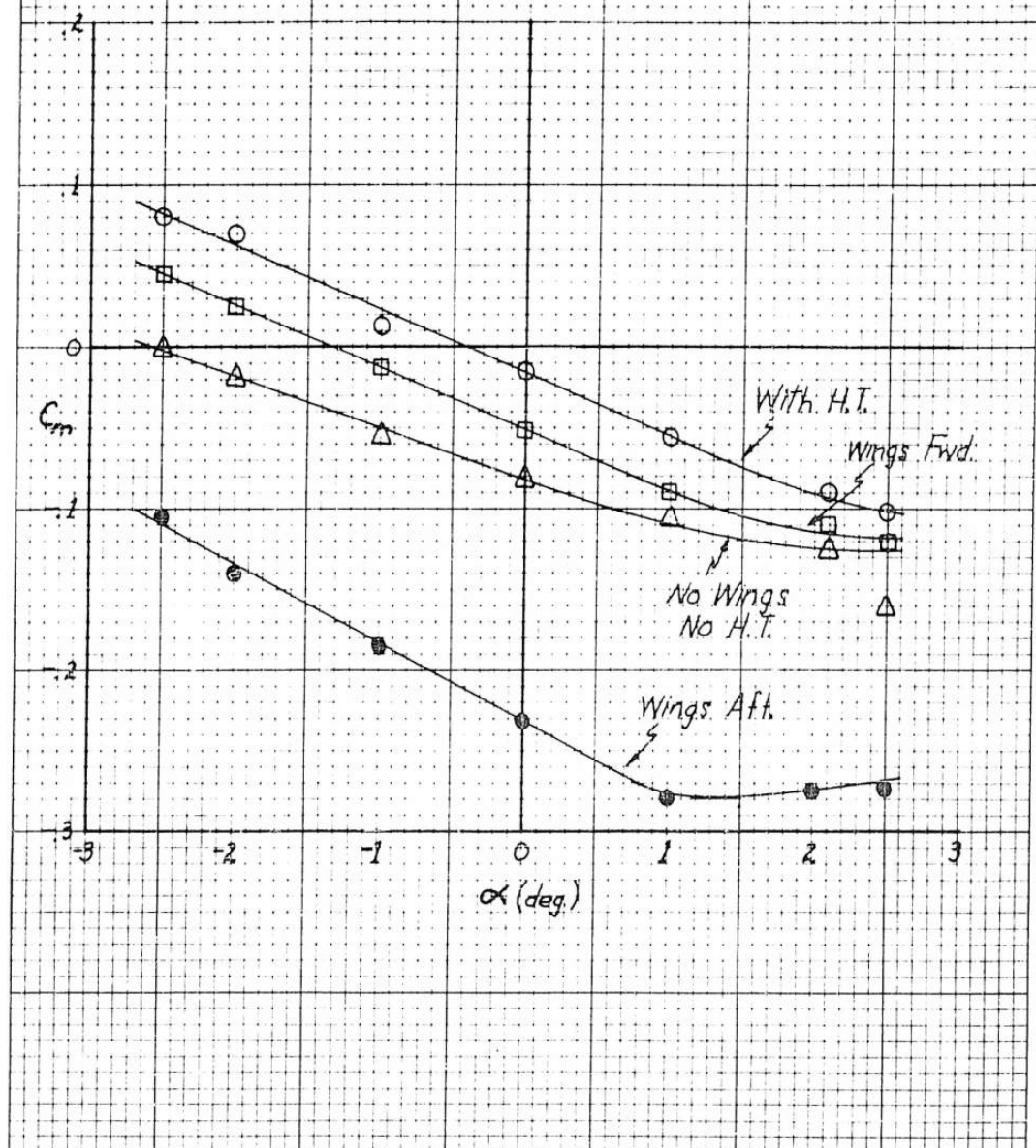


FIG. 33- Modified C-W Air Car model
Static stability for various configurations.

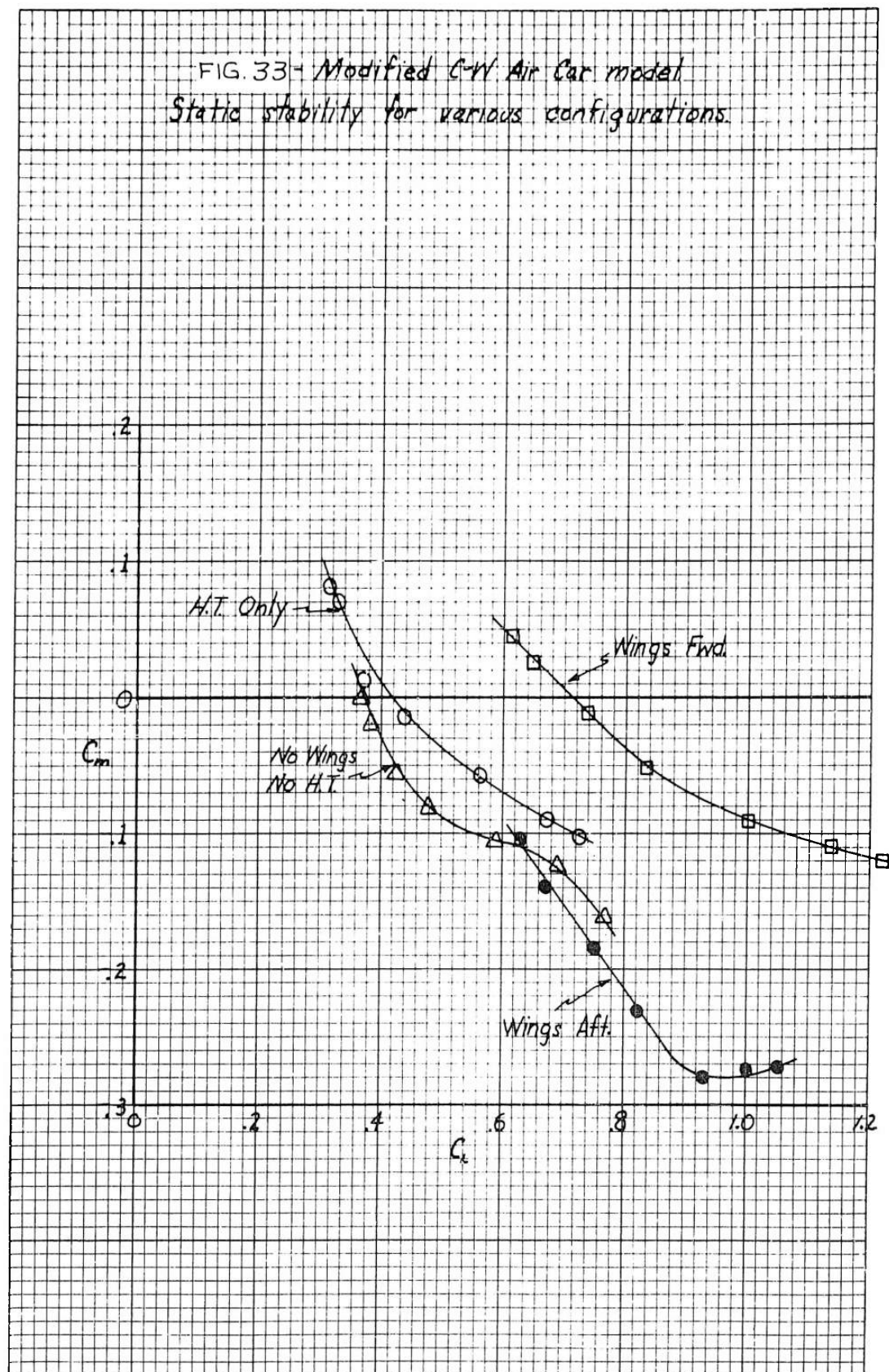


FIG. 34 • Modified C-W Air Car model.
Tail incidence effects.

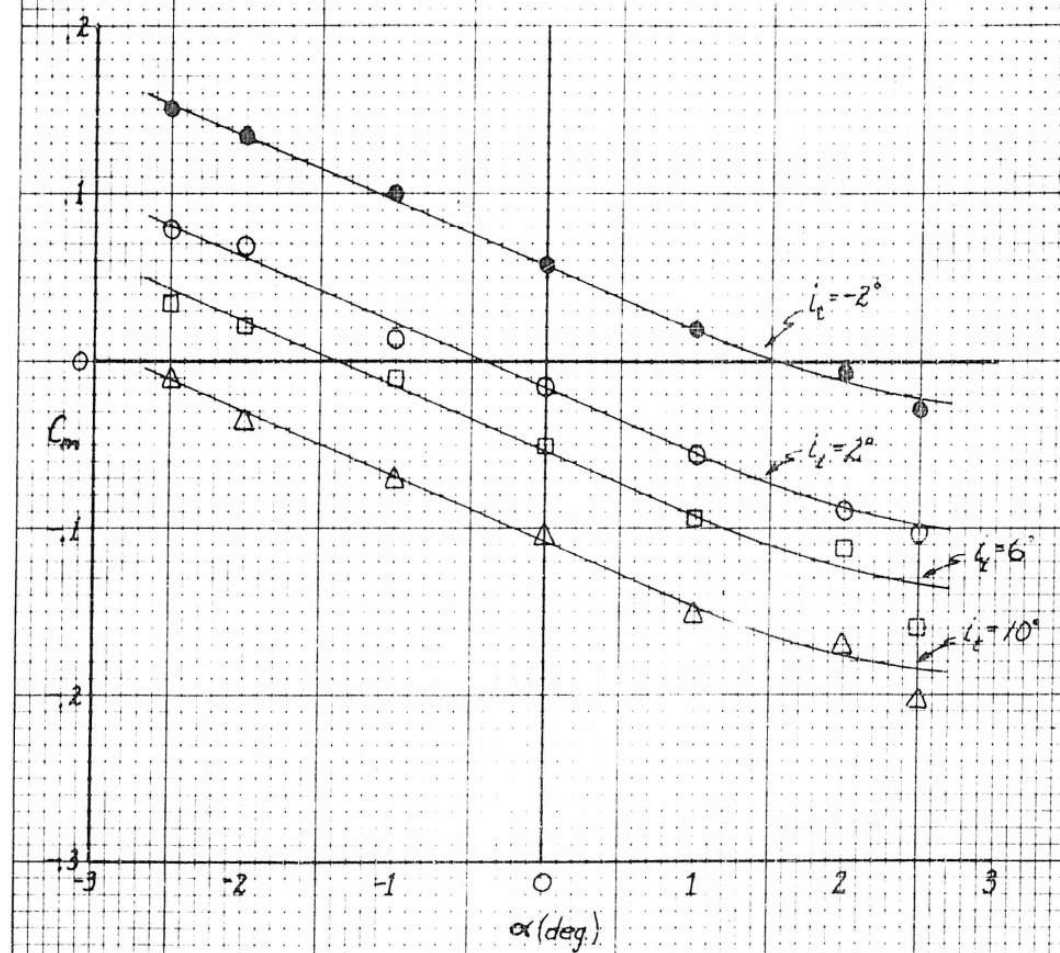


FIG. 35 - Modified C-W Air Car model.
Airspeed, model power, and wing
incidence effects on C_m .

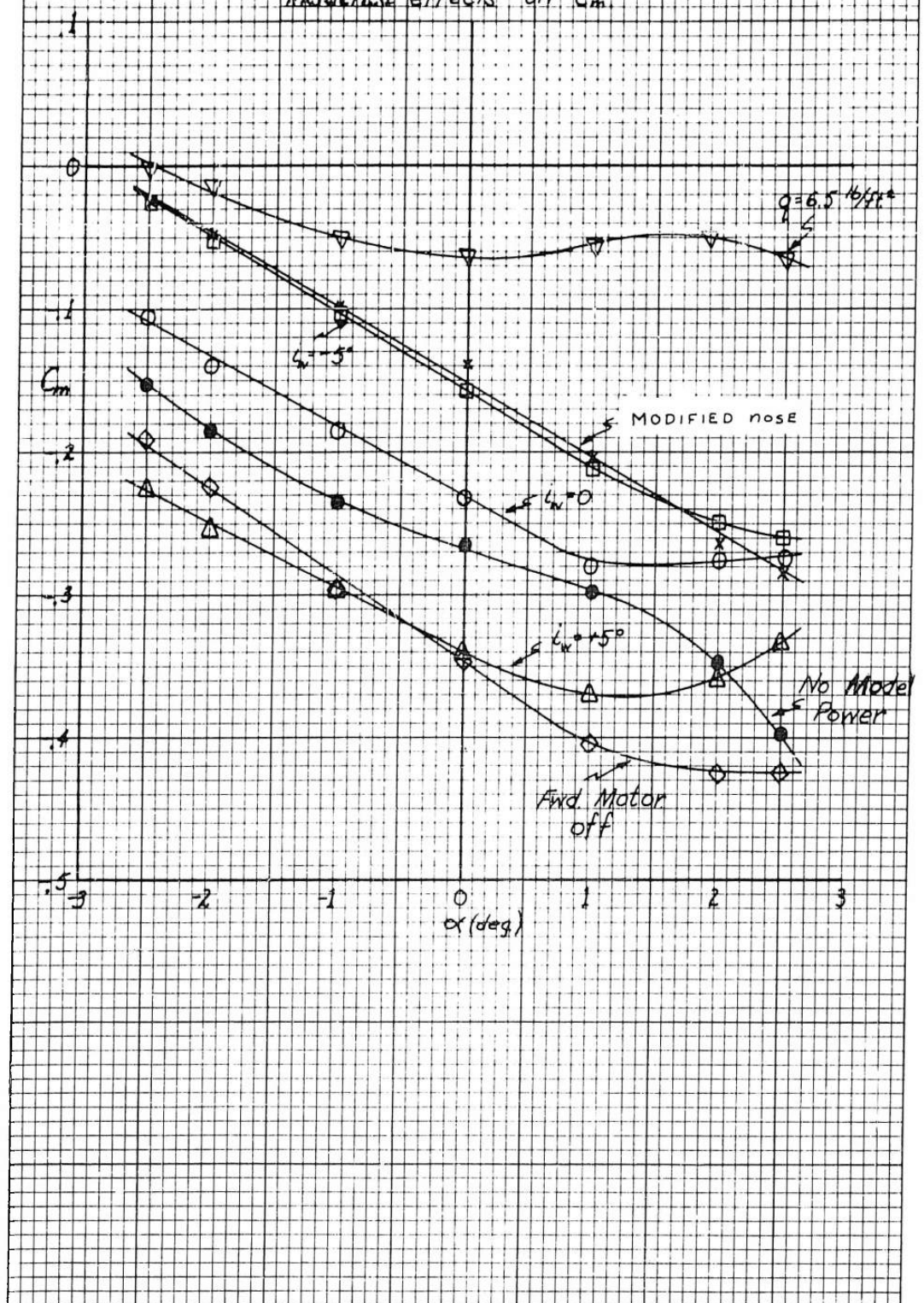


FIG 36 - Modified C-W Air Car model.
Lift & drag for various wing thicknesses
and modified nose.

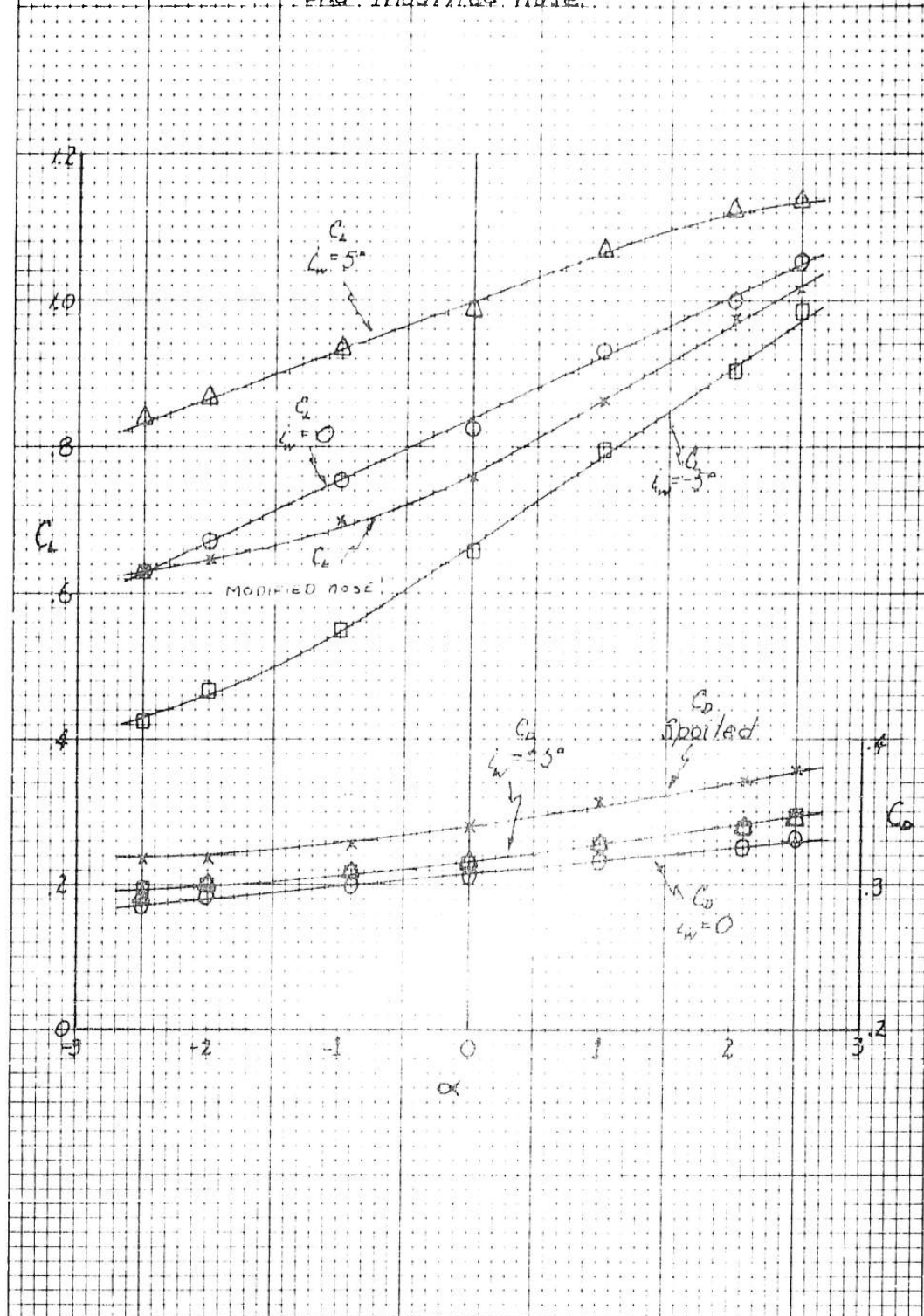


FIG. 37 Modified C-W Air Car model.
 Static stability for various wing incidences
 and modified nose.

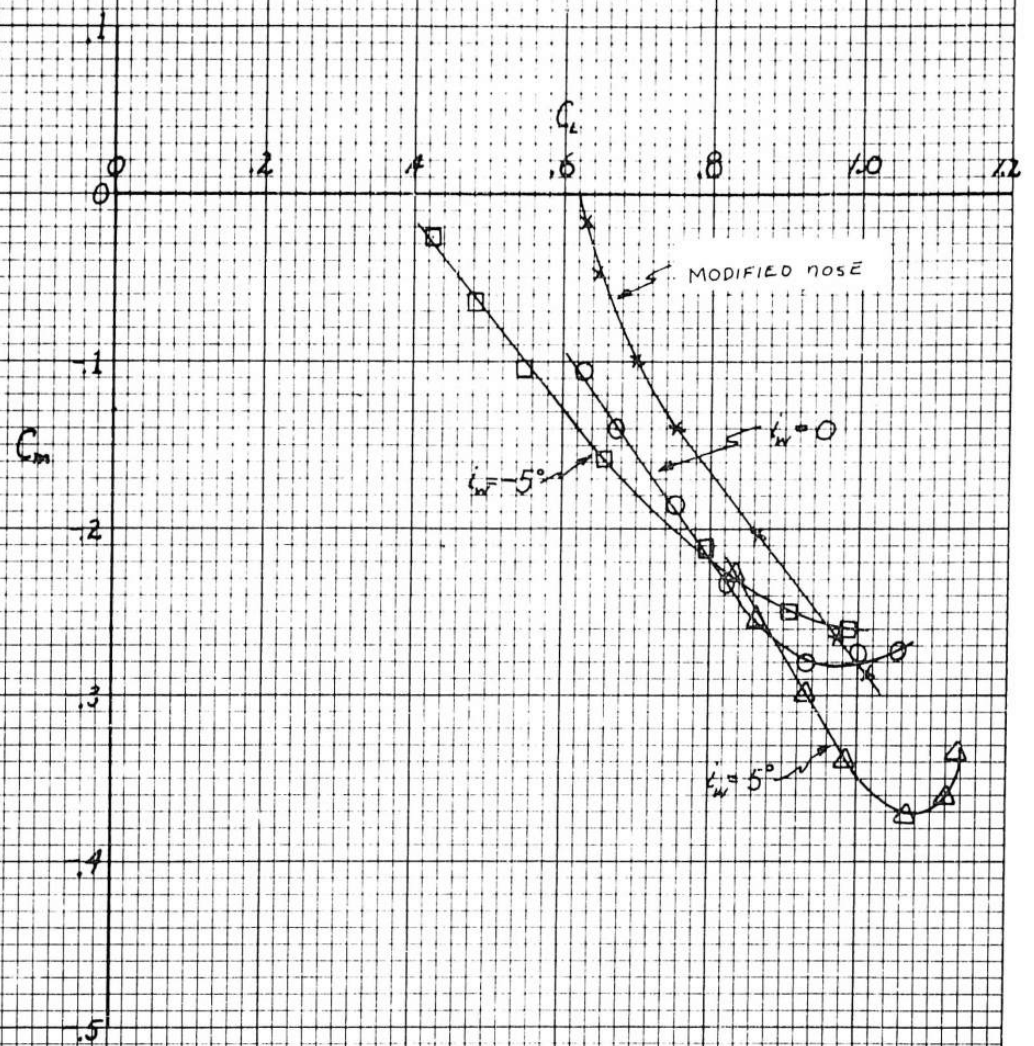
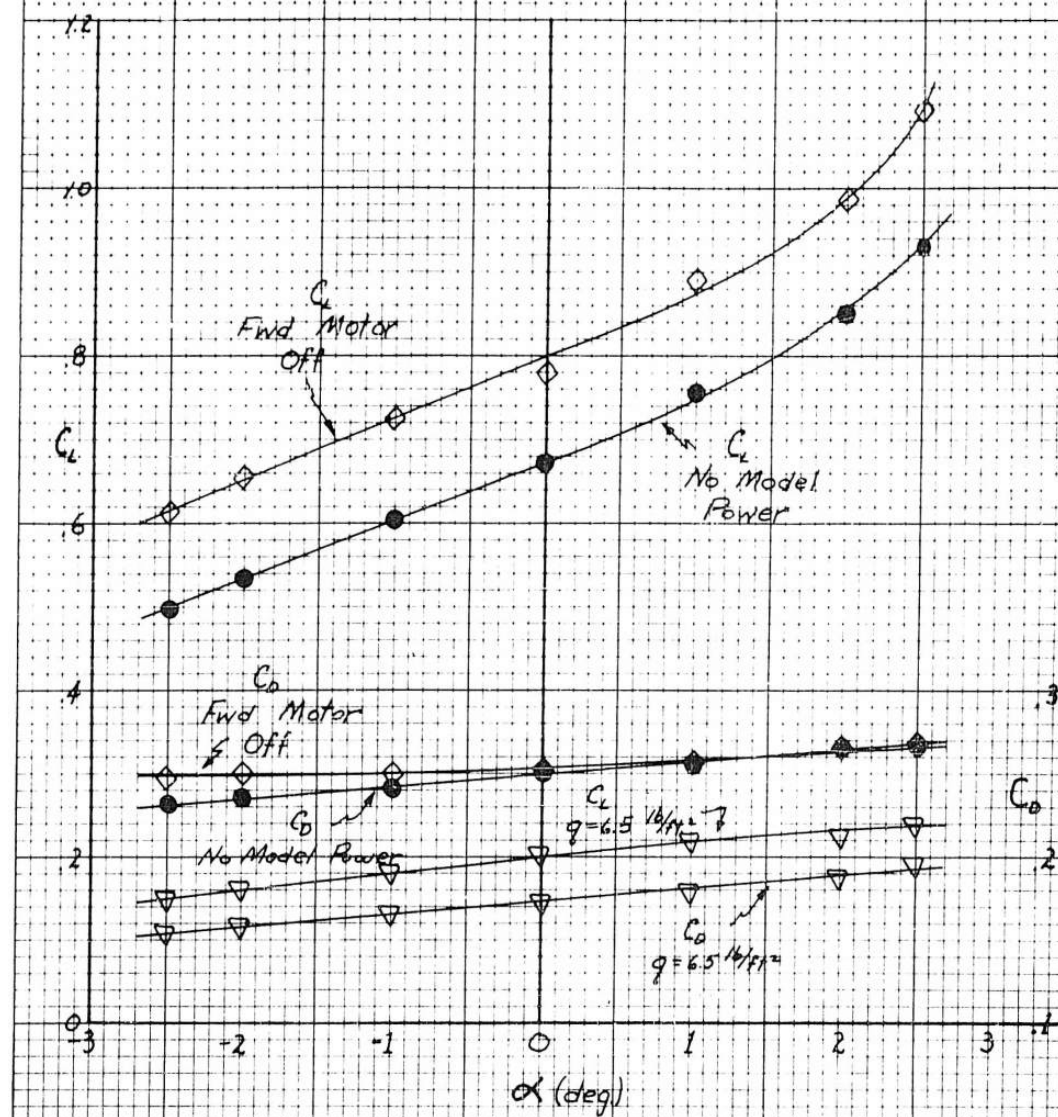


FIG. 38-Modified C_N Air Car model.
Lift & drag for varying model power
and airspeed.



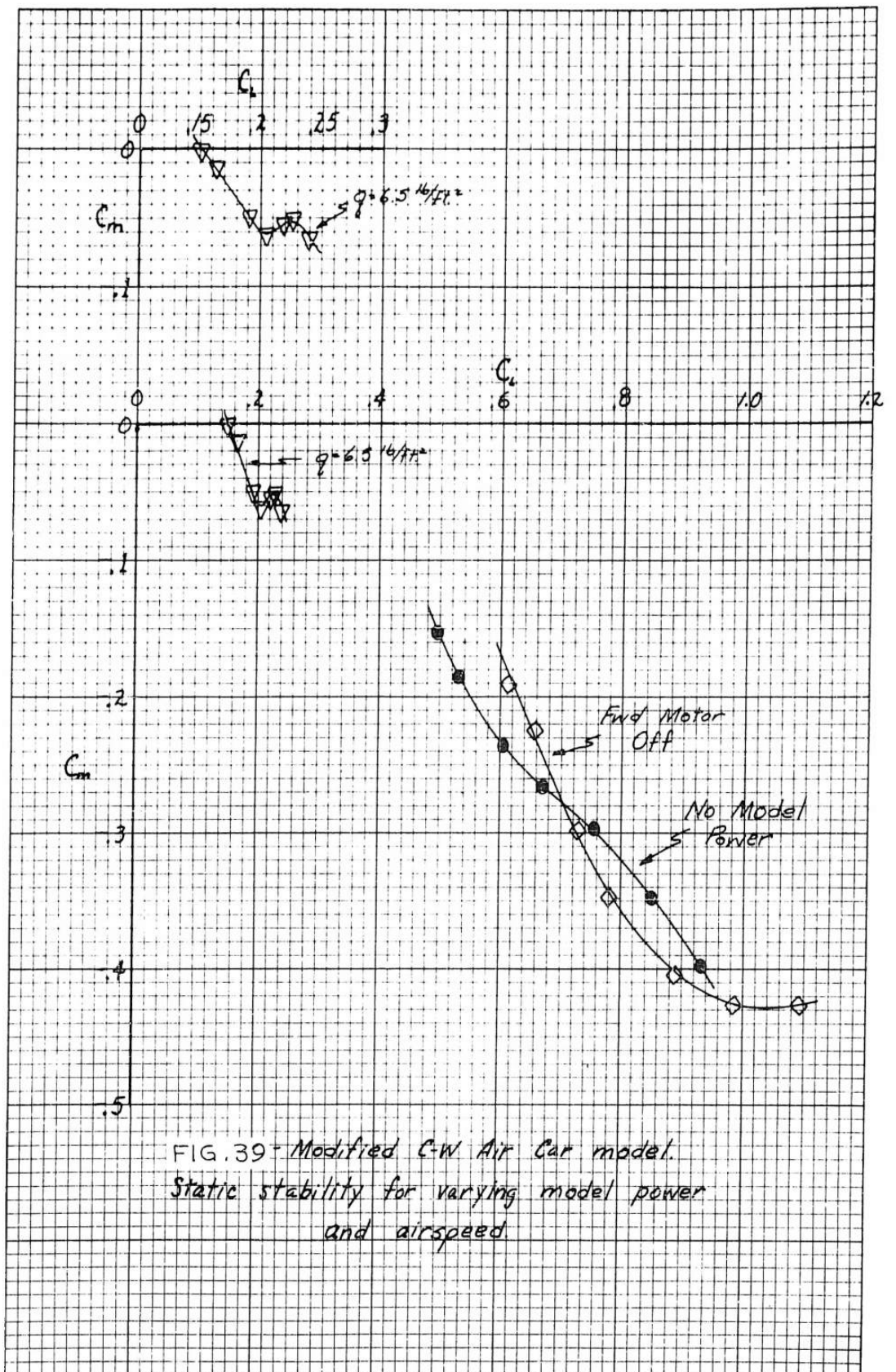
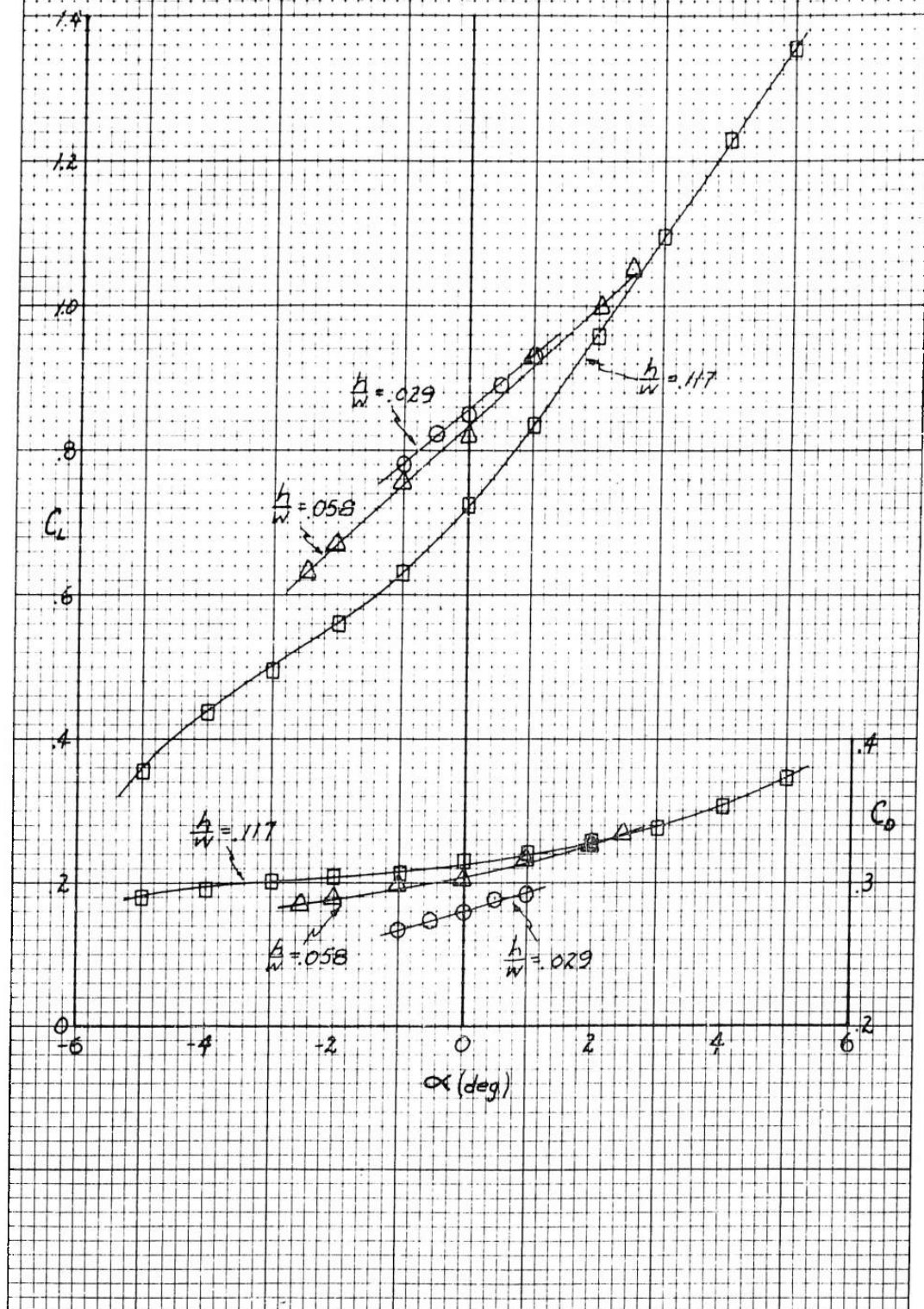


FIG. 39 - Modified C-W Air Car model.
Static stability for varying model power
and airspeed.

FIG. 40 - Modified G.M. Air Car model.
Lift & drag for various model heights.



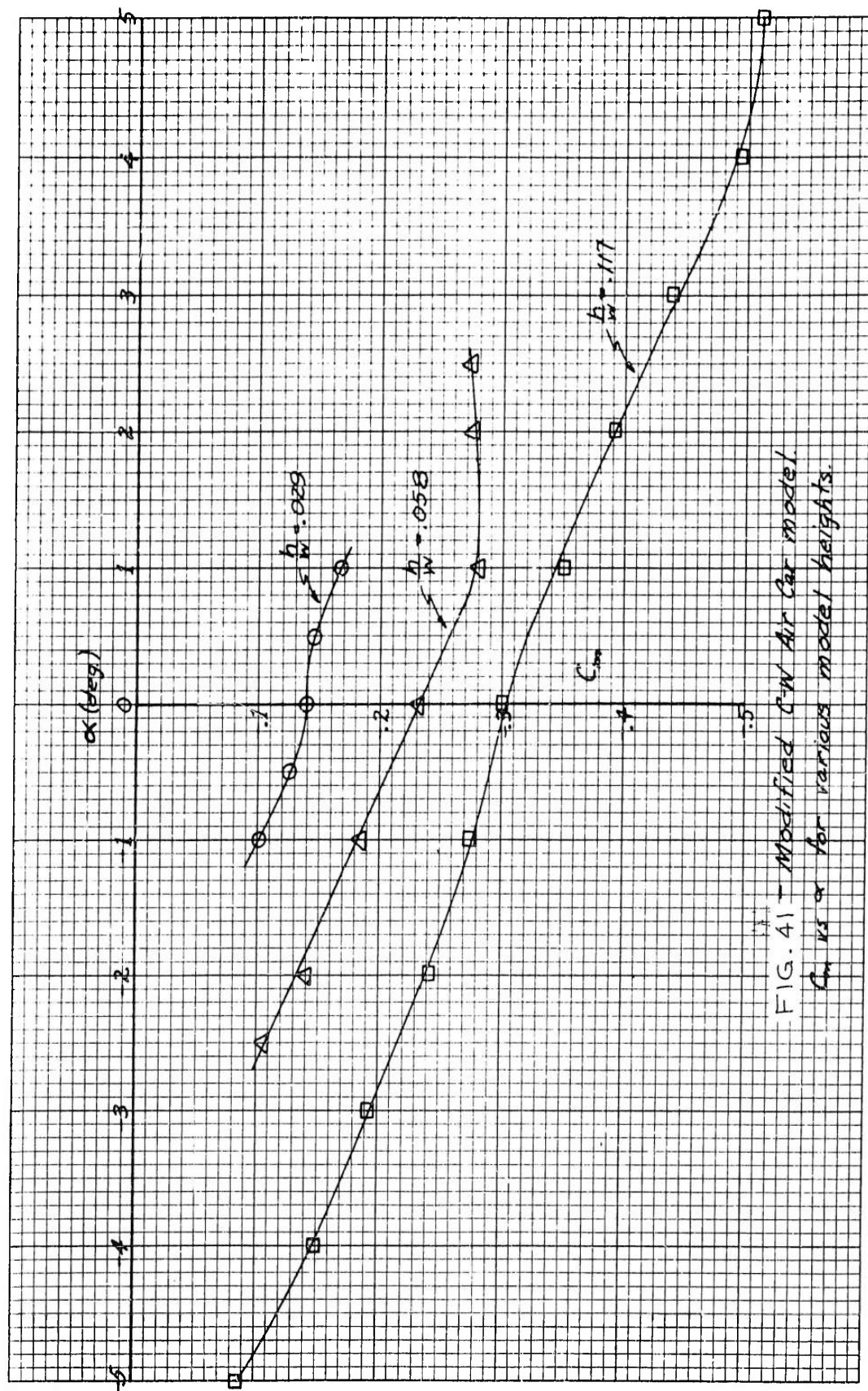


FIG. 41 - Modified C-W Air Car model.
 C_l vs α for various model heights.

FIG. 42-Modified C-N Air Car model.
Static stability for various model heights.

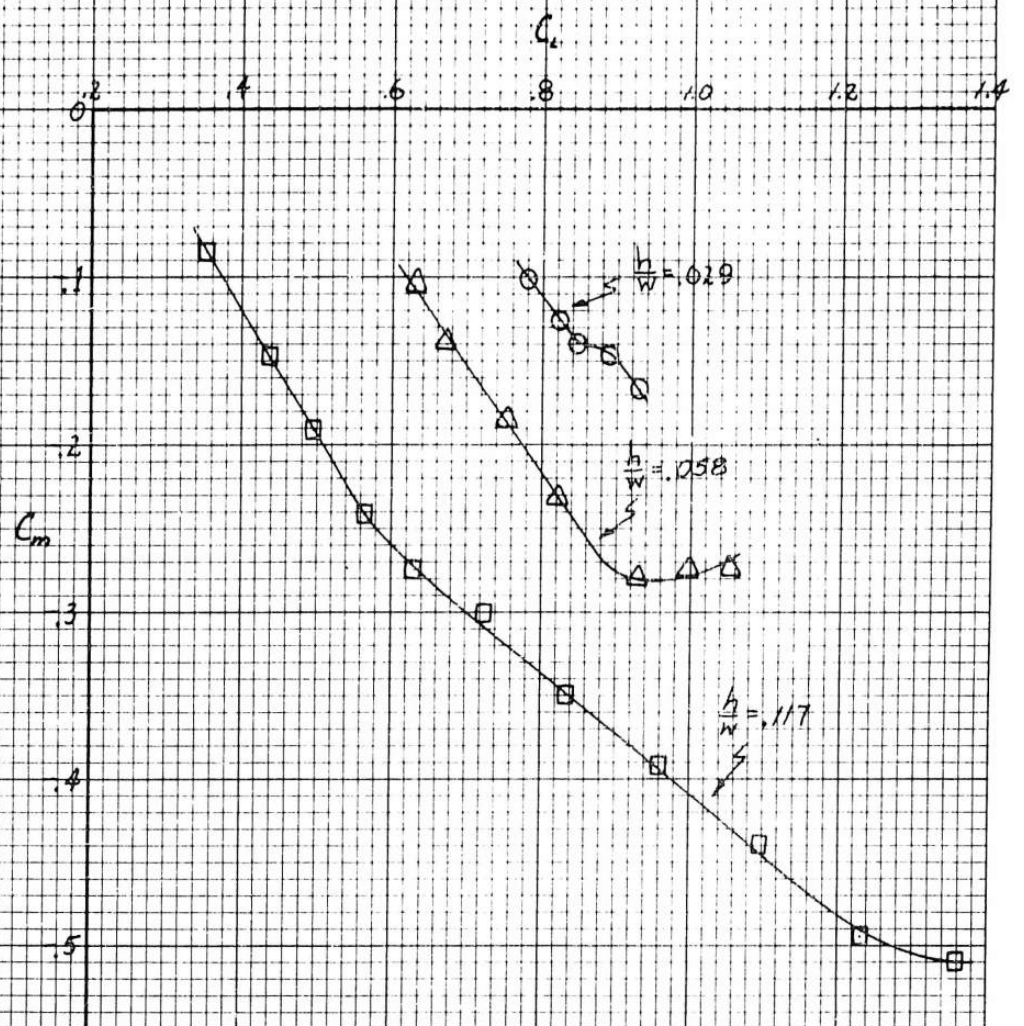
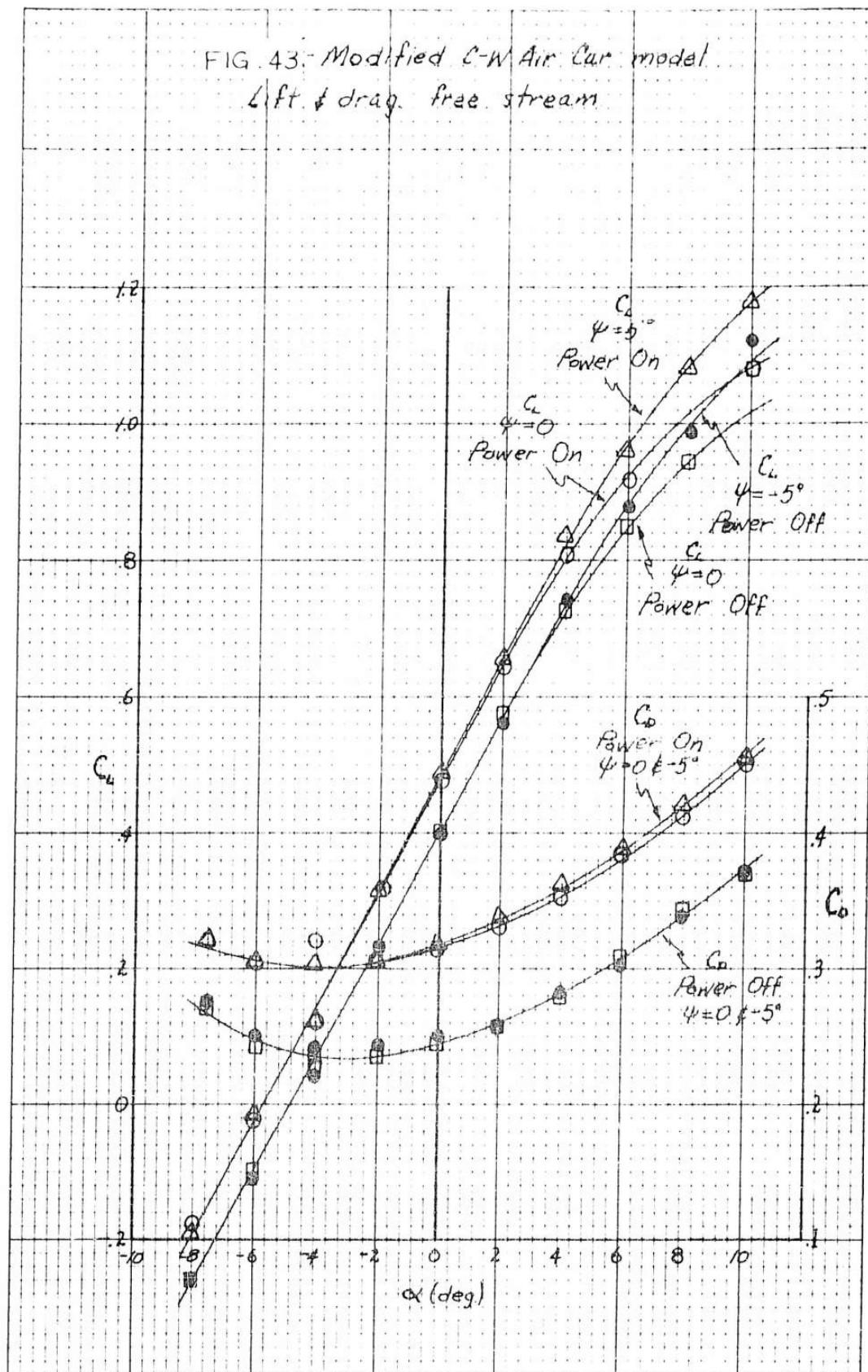


FIG. 43- Modified C-W Air Car model
Lift & drag free stream



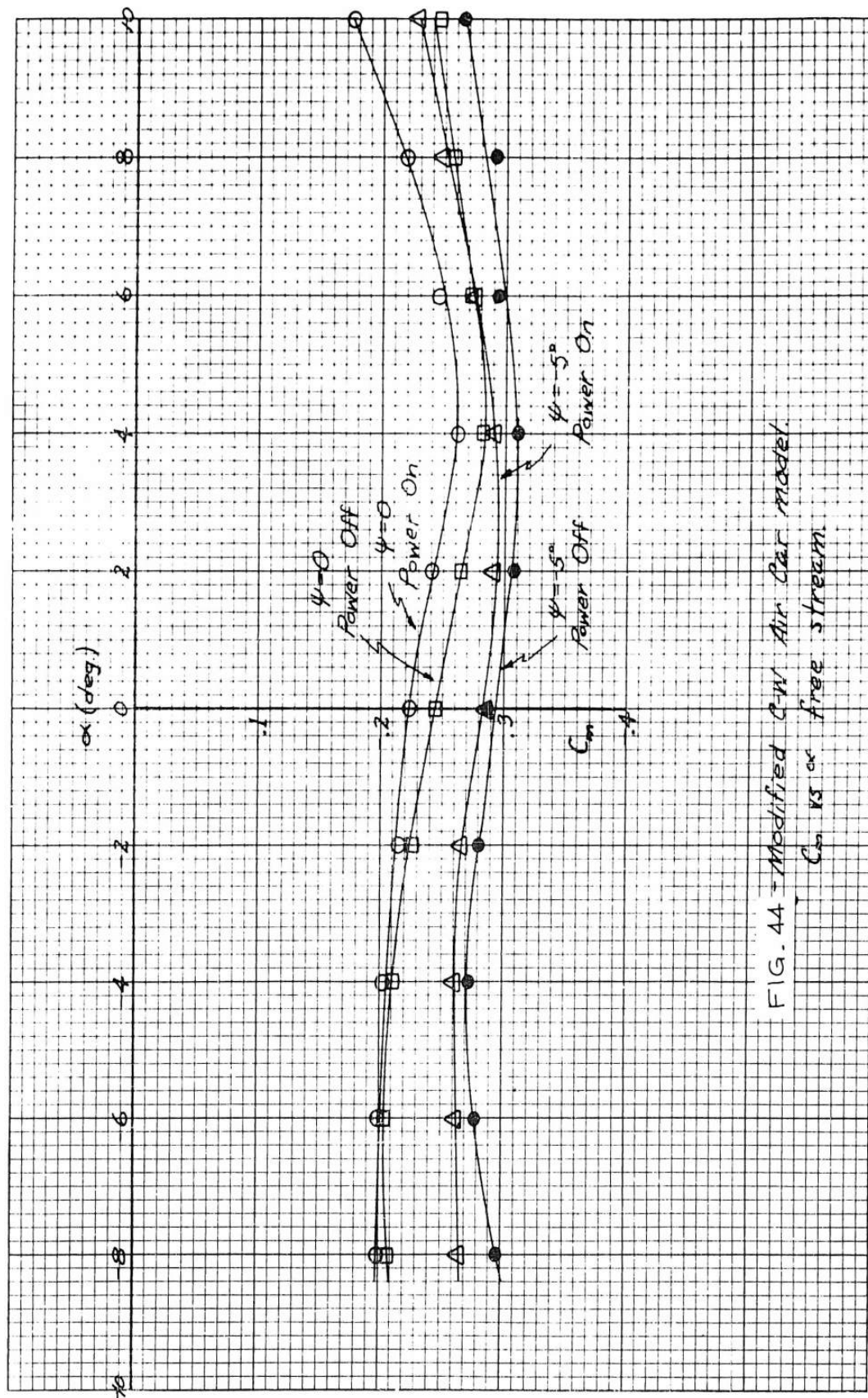


FIG. 44 - Modified C-W Air Car model.
 C_m vs α free stream.

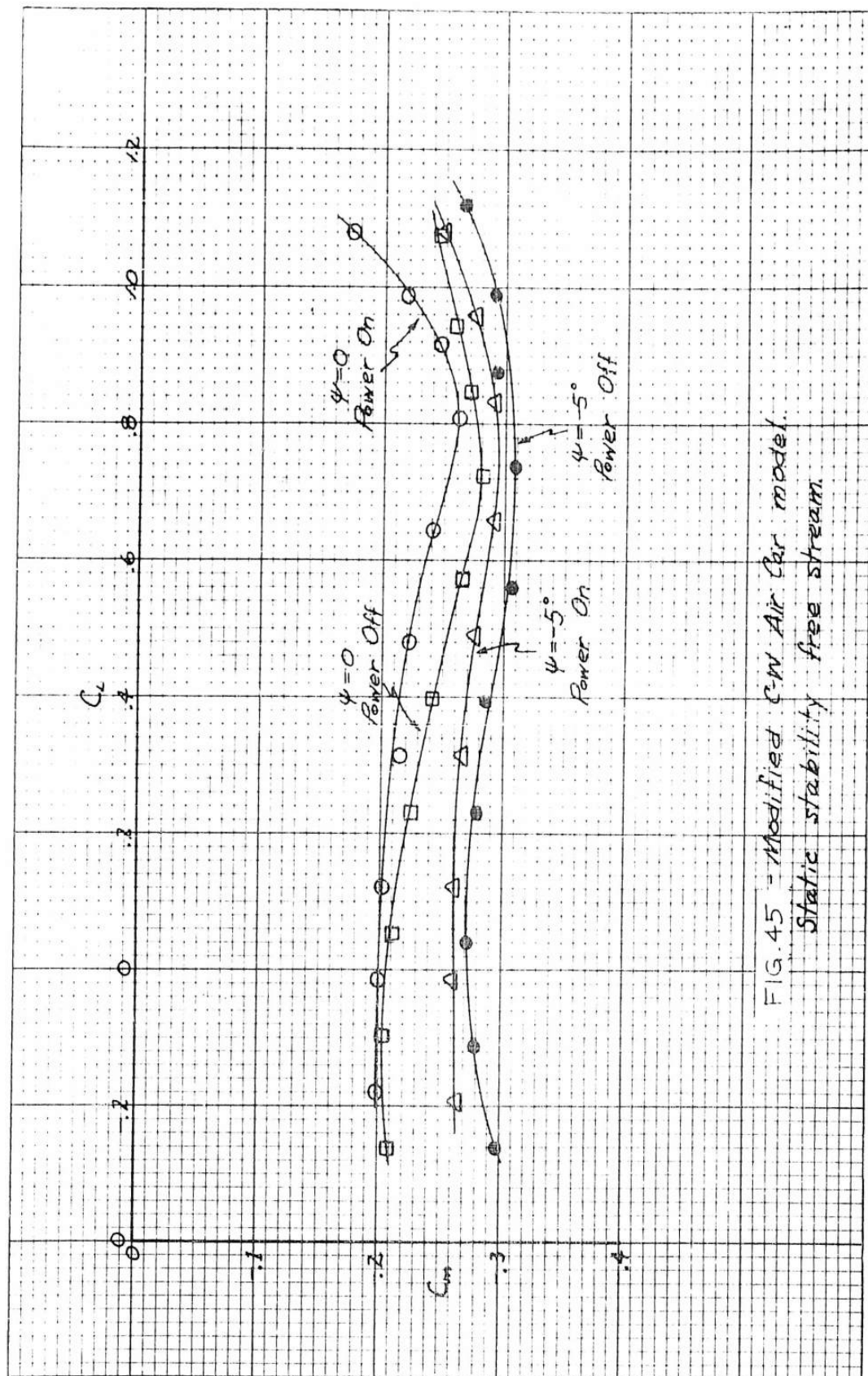
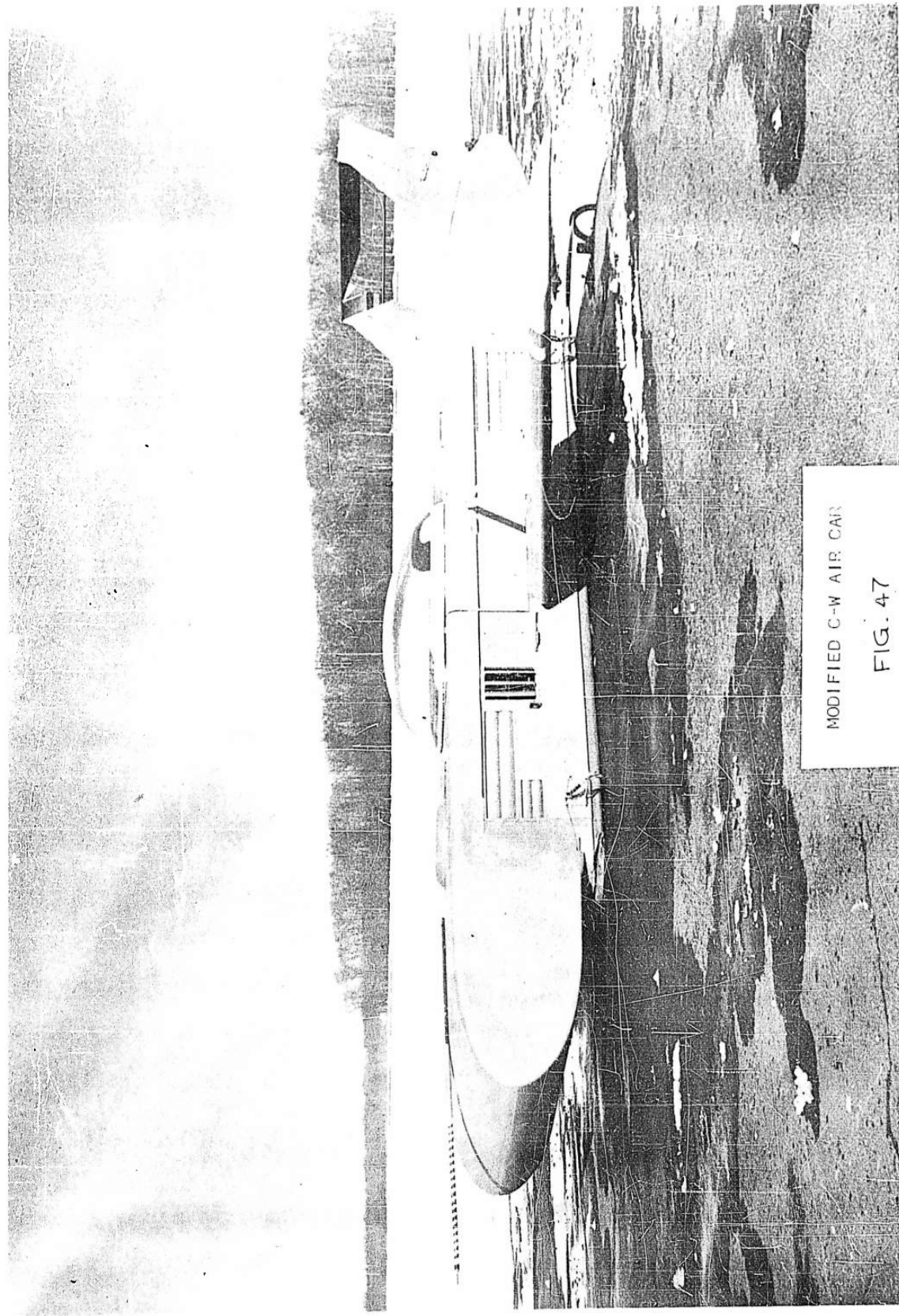


FIG. 45 - Modified CW Air Car model.
Static stability free stream.



CURTISS WRIGHT AIR CAR ACM6-1
FIG. 46



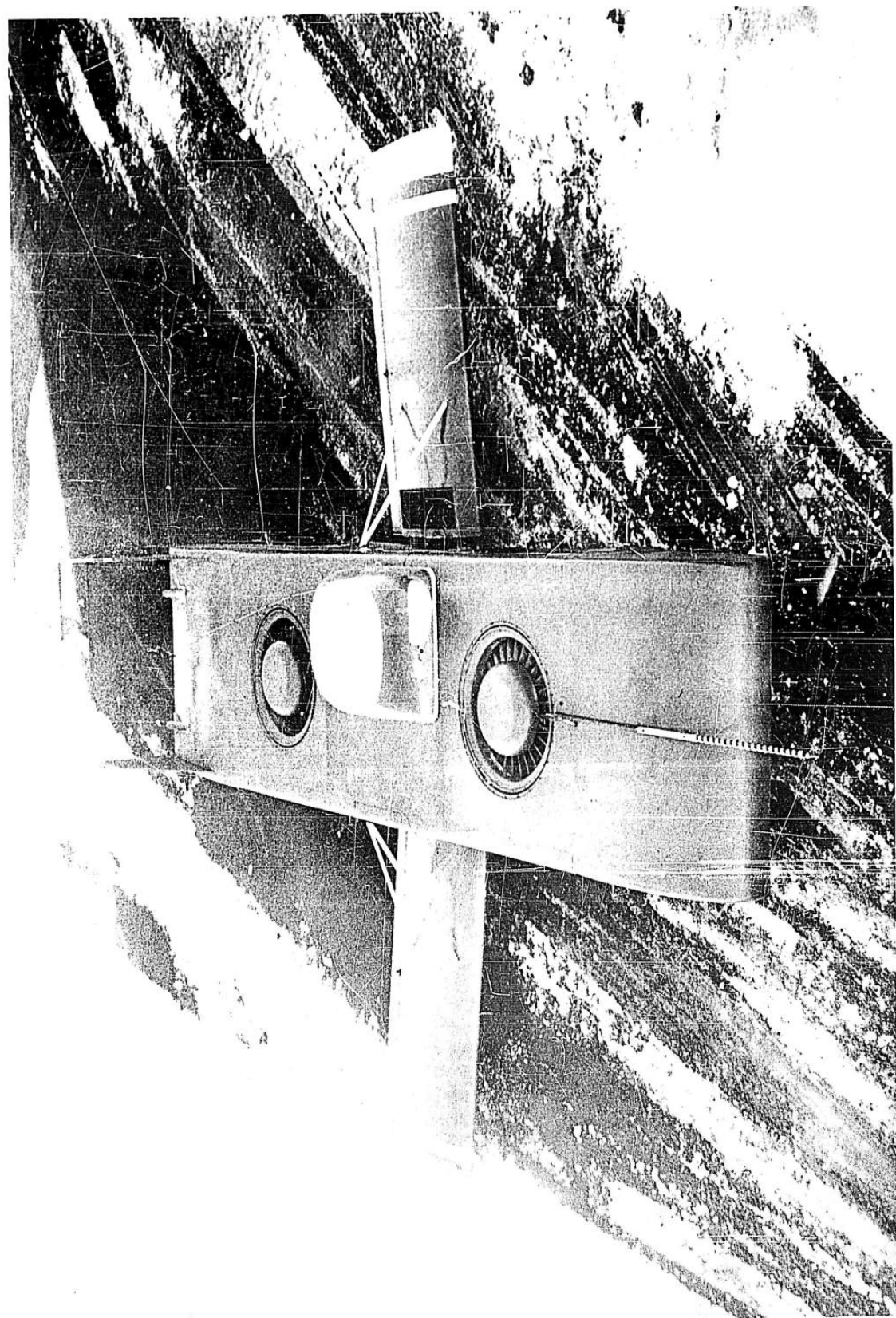
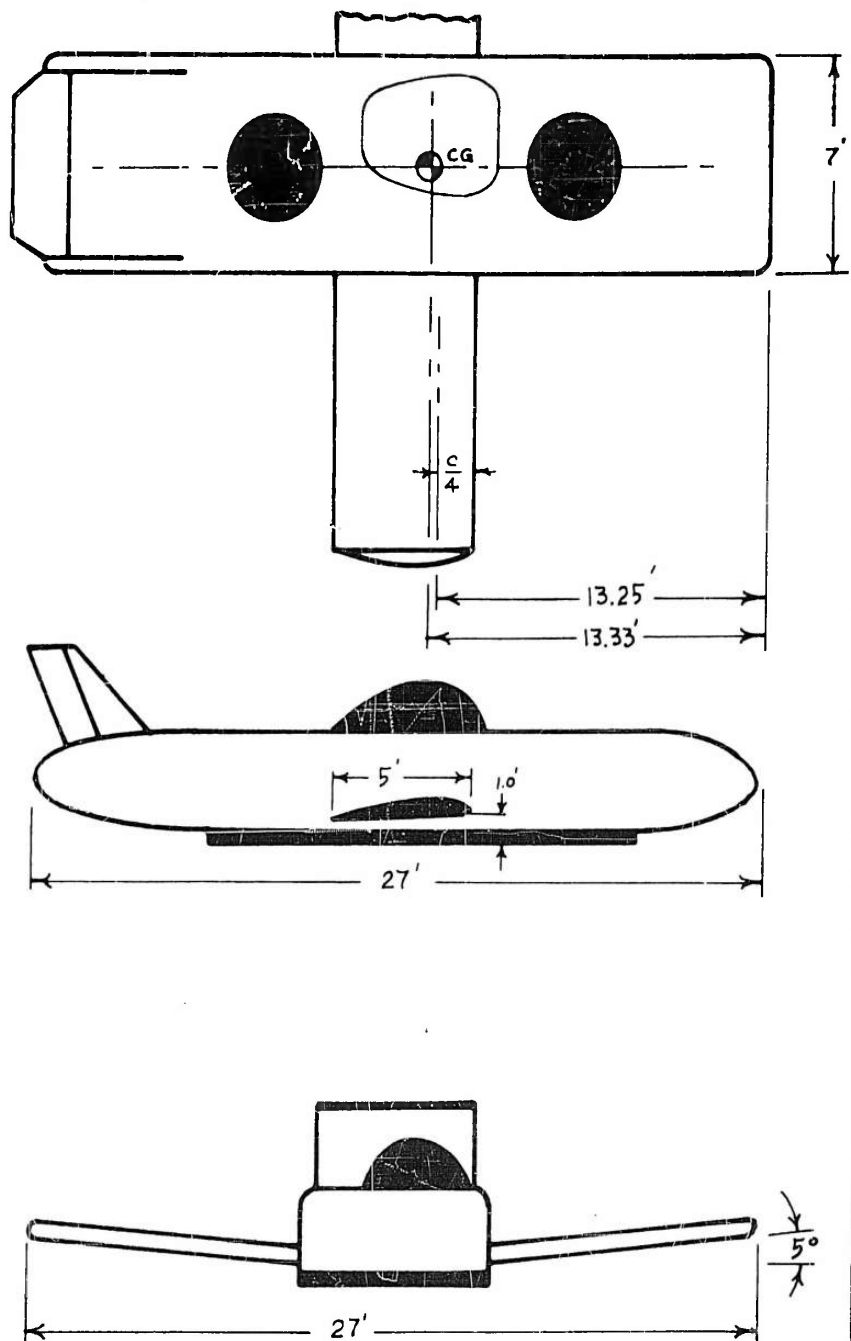
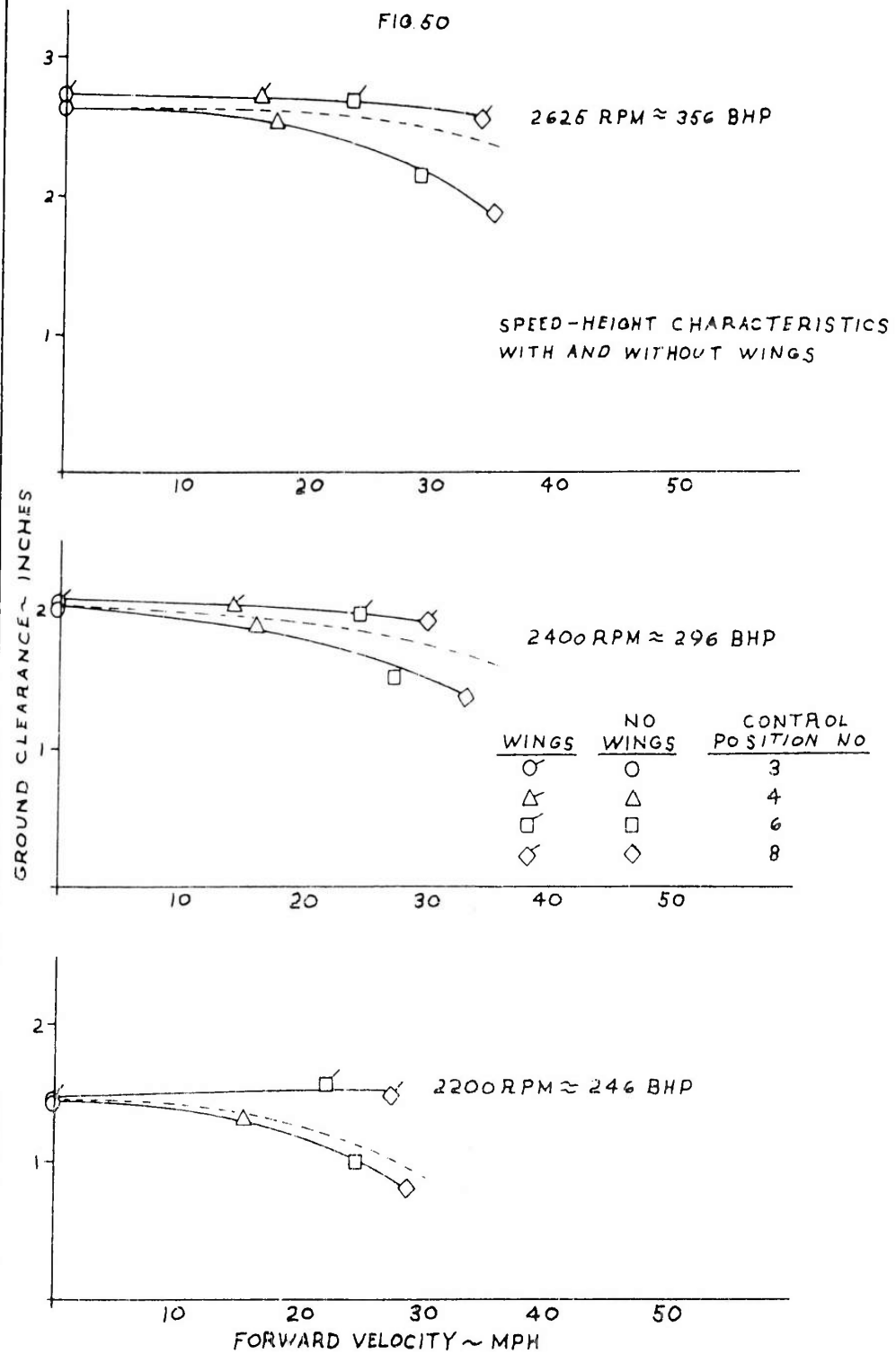


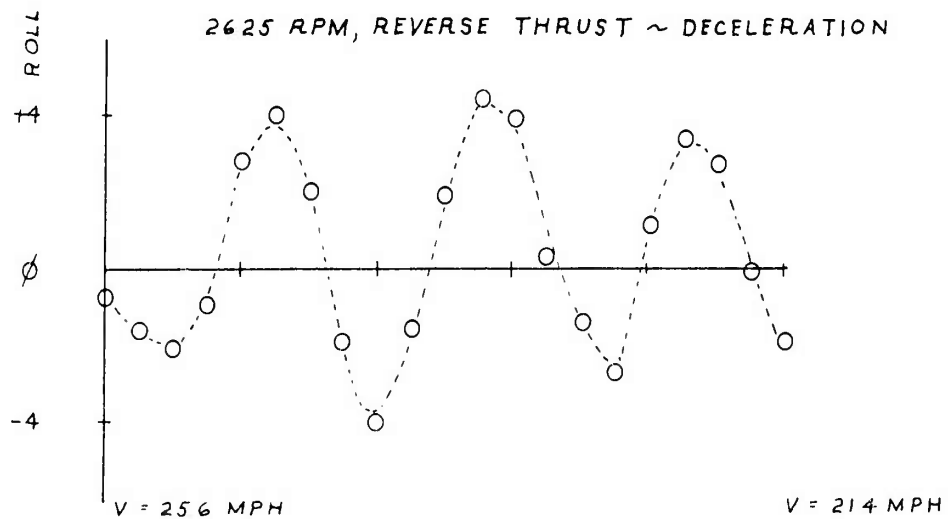
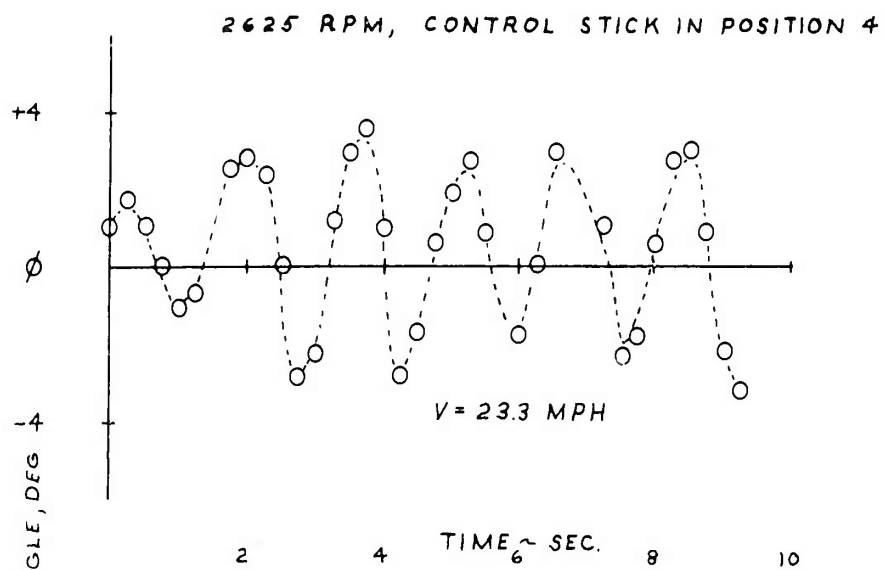
FIG. 48



GENERAL LAYOUT OF THE MODIFIED
C-W AIR CAR
FIG. 49

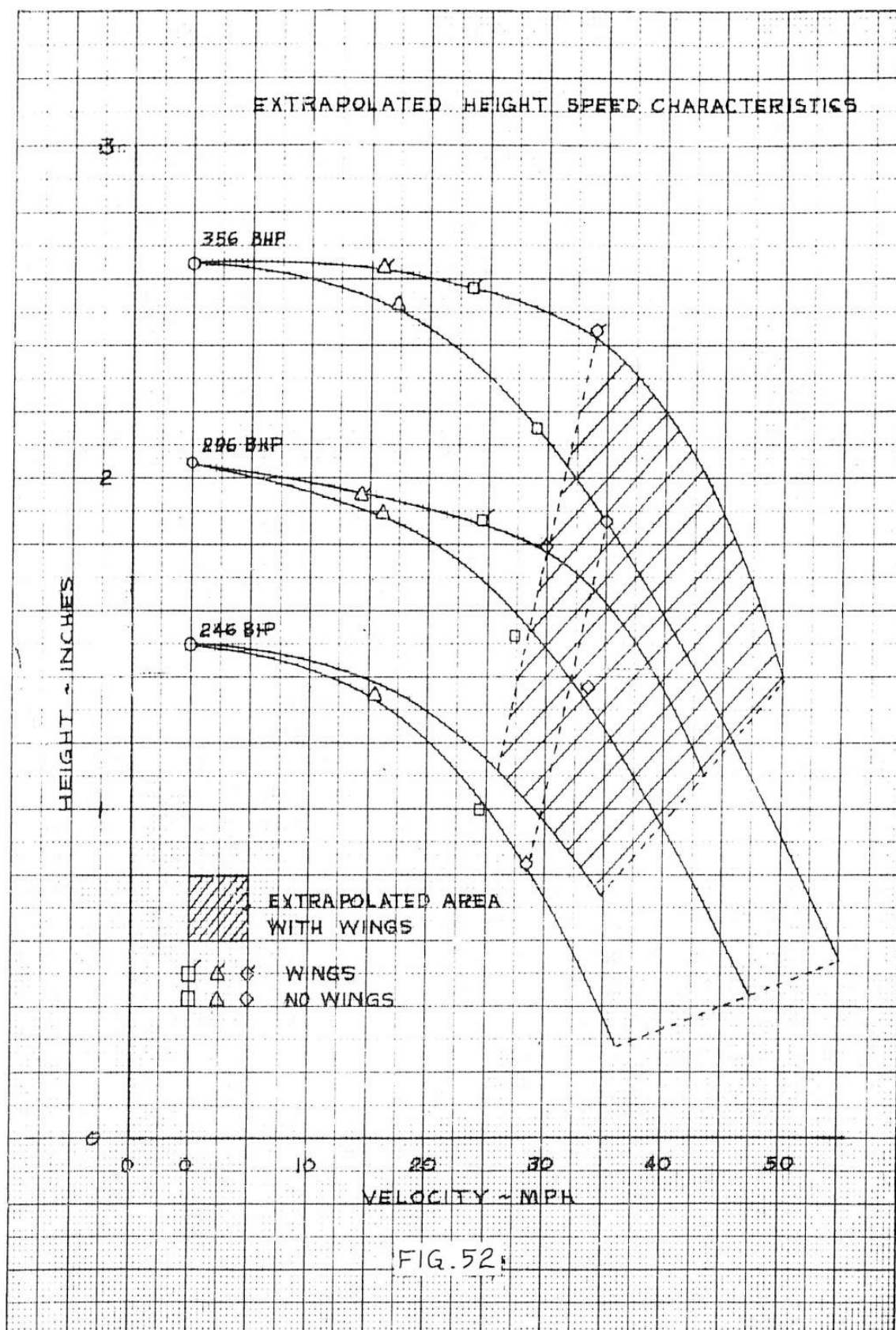
FIG. 50

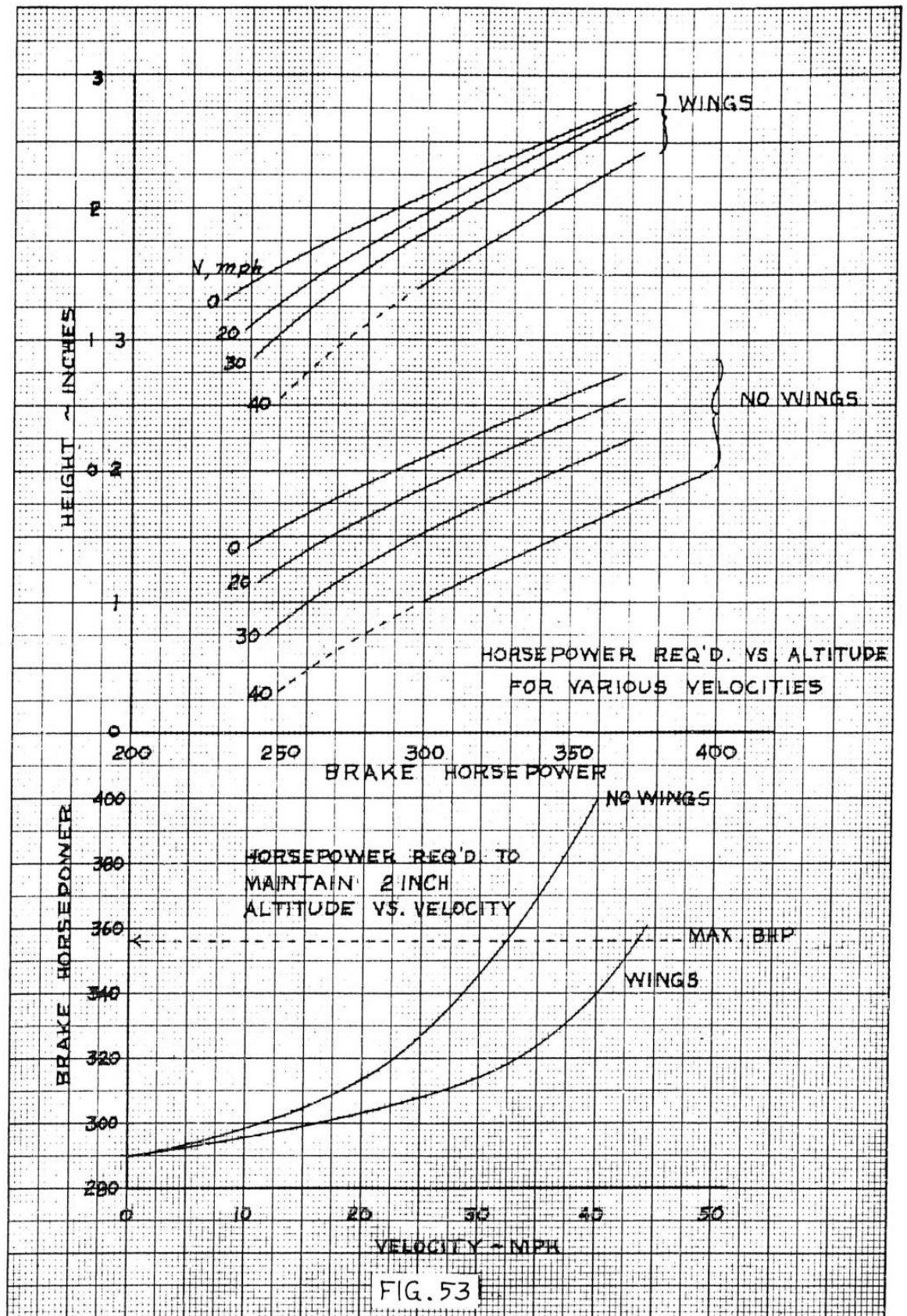




TYPICAL ROLL OSCILLATIONS

FIG 51





ALTITUDE CAPABILITIES OF THE SEPARATE
PROPULSION WINGED GEM

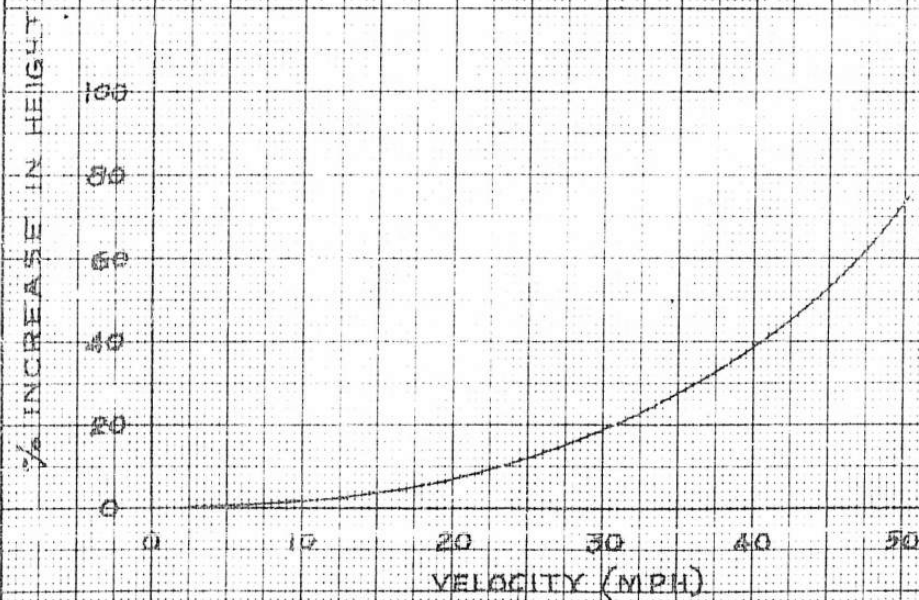
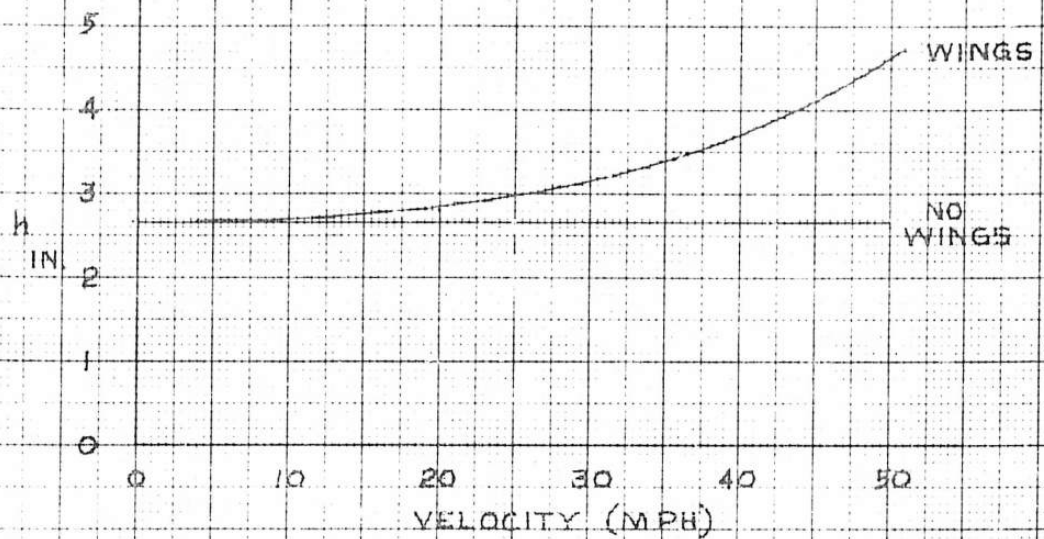
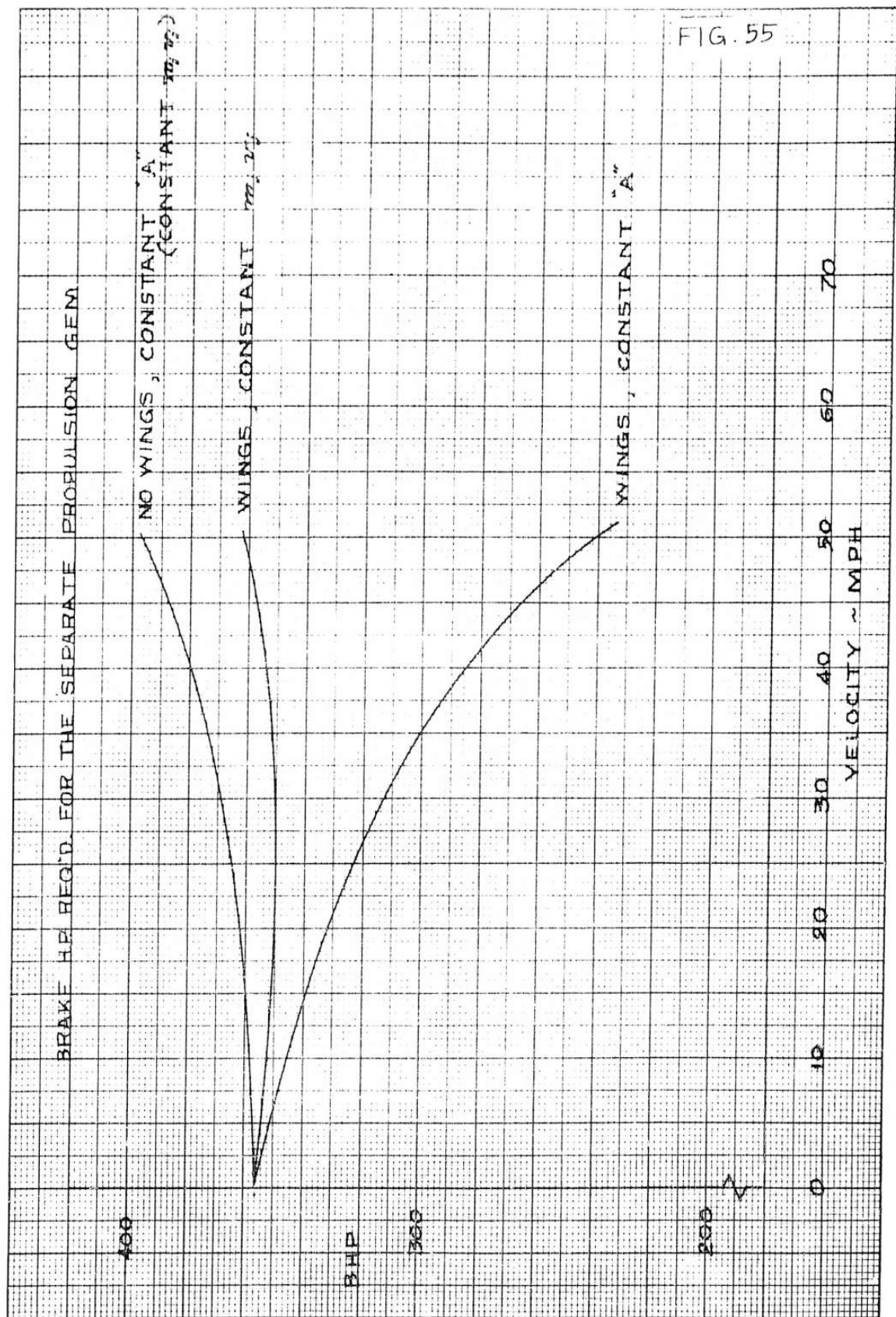


FIG. 54



DISTRIBUTION

Army War College	1
U. S. Army Aviation Test Activity	1
U. S. Army Polar Research and Development Center	1
Deputy Chief of Staff for Logistics, D/A	1
The Research Analysis Corporation	1
Army Research Office	2
Office of Chief of R&D, D/A	2
Naval Air Test Center	1
Army Research Office, OCRD	1
Deputy Chief of Staff for Military Operations, D/A	1
U. S. Army Engineer Research and Development Laboratories	2
U. S. Army Tank-Automotive Center	2
U. S. Army Combat Developments Command Transportation Agency	1
U. S. Army Aviation and Surface Materiel Command	2
U. S. Army Transportation Research Command	41
U. S. Army Transportation School	1
U. S. Army Airborne, Electronics and Special Warfare Board	1
U. S. Army Research and Development Group (Europe)	2
Chief of Naval Operations	1
Bureau of Naval Weapons	2
U. S. Naval Supply Research and Development Facility	1
U. S. Naval Postgraduate School	1
Bureau of Ships	1
U. S. Naval Ordnance Test Station	1
David Taylor Model Basin	1
Marine Corps Landing Force Development Center	1
Marine Corps Schools	1
U. S. Army Standardization Group, Canada	1
Canadian Army Liaison Officer, U. S. Army Transportation School	3
British Army Staff, British Embassy	4
U. S. Army Standardization Group, U. K.	1
NASA-LRC, Langley Station	2
Ames Research Center	2
Lewis Research Center	1
Scientific and Technical Information Facility	1
U. S. Government Printing Office	1

Defense Documentation Center	10
U. S. Army Medical Research and Development Command	1
Human Resources Research Office	2
U. S. Strike Command	1
U. S. Army Mobility Command	3
U. S. Army Materiel Command	6
U. S. Army Human Engineering Laboratories	1
U. S. Maritime Administration	1
Office of the Assistant Secretary of Defense for R&E	1

AD _____ Accession No. _____
Princeton University Aero. Eng. Dept.,
Princeton, New Jersey

THE GENERAL CHARACTERISTICS OF WINGED
GROUND EFFECT MACHINES
- D.R. Summers, G.P. Carr, J.J.Metzko,
W.B. Nixon and A.F.Wojciechowicz, Jr.

Report No. 657, June 1963
140 pp.

Contract No. DA44-177-TC-833
Project No. 9R38-11-009-03
Unclassified Report

UNCLASSIFIED

1. Ground Effect
Machines
2. Performance,
winged ground
effect machines
3. Stability,winged
ground effect
machines
4. D.R. Summers
G.P. Carr
J.J. Metzko
W.B. Nixon

THE GENERAL CHARACTERISTICS OF WINGED
GROUND EFFECT MACHINES
- D.R. Summers, G.P. Carr, J.J.Metzko,
W.B. Nixon and A.F.Wojciechowicz, Jr.

Report No. 657, June 1963
140 pp.

A.Wojciechowicz Contract No. DA44-177-TC-833
Project No. 9R38-11-009-03
DA44-177-TC-833 Unclassified Report

AD _____ Accession No. _____

1. Ground Effect
Machines
2. Performance,
winged ground
effect machines
3. Stability,winged
ground effect
machines
4. D. R. Summers
G. P. Carr
J. J. Metzko
W. B. Nixon
A.Wojciechowicz
5. Contract No.
DA44-177-TC-833

UNCLASSIFIED

AD _____ Accession No. _____
Princeton University Aero. Eng. Dept.,
Princeton, New Jersey

THE GENERAL CHARACTERISTICS OF WINGED
GROUND EFFECT MACHINES
- D.R. Summers, G.P. Carr, J.J.Metzko,
W.B. Nixon and A.F.Wojciechowicz, Jr.

Report No. 657, June 1963
140 pp.

Contract No. DA44-177-TC-833
Project No. 9R38-11-009-03
Unclassified Report

UNCLASSIFIED

1. Ground Effect
Machines
2. Performance,
winged ground
effect machines
3. Stability,winged
ground effect
machines
4. D.R. Summers
G.P. Carr
J.J. Metzko
W.B. Nixon

THE GENERAL CHARACTERISTICS OF WINGED
GROUND EFFECT MACHINES
- D.R. Summers, G.P. Carr, J.J.Metzko,
W.B. Nixon and A.F.Wojciechowicz, Jr.

Report No. 657, June 1963
140 pp.

A.Wojciechowicz Contract No. DA44-177-TC-833
Project No. 9R38-11-009-03
DA44-177-TC-833 Unclassified Report

AD _____ Accession No. _____

1. Ground Effect
Machines
2. Performance,
winged ground
effect machines
3. Stability,winged
ground effect
machines
4. D. R. Summers
G. P. Carr
J. J. Metzko
W. B. Nixon
A.Wojciechowicz
5. Contract No.
DA44-177-TC-833

UNCLASSIFIED

The purpose of the research reported upon herein was to determine the performance and stability advantages that could be obtained by the addition of wings to a ground effect machine. The work is both theoretical and experimental, the latter being accomplished both with models and a winged version of the full scale Curtiss-Wright Air Car.

Results indicate that substantial gains in both performance and stability are attainable by such a hybrid machine when compared to the pure GEM.

It is generally concluded that for the high speed cruise condition wings will be found most beneficial if the base loading of the craft is not excessive.

The purpose of the research reported upon herein was to determine the performance and stability advantages that could be obtained by the addition of wings to a ground effect machine. The work is both theoretical and experimental, the latter being accomplished both with models and a winged version of the full scale Curtiss-Wright Air Car.

Results indicate that substantial gains in both performance and stability are attainable by such a hybrid machine when compared to the pure GEM.

It is generally concluded that for the high speed cruise condition wings will be found most beneficial if the base loading of the craft is not excessive.

The purpose of the research reported upon herein was to determine the performance and stability advantages that could be obtained by the addition of wings to a ground effect machine. The work is both theoretical and experimental, the latter being accomplished both with models and a winged version of the full scale Curtiss-Wright Air Car.

Results indicate that substantial gains in both performance and stability are attainable by such a hybrid machine when compared to the pure GEM.

It is generally concluded that for the high speed cruise condition wings will be found most beneficial if the base loading of the craft is not excessive.

The purpose of the research reported upon herein was to determine the performance and stability advantages that could be obtained by the addition of wings to a ground effect machine. The work is both theoretical and experimental, the latter being accomplished both with models and a winged version of the full scale Curtiss-Wright Air Car.

Results indicate that substantial gains in both performance and stability are attainable by such a hybrid machine when compared to the pure GEM.

It is generally concluded that for the high speed cruise condition wings will be found most beneficial if the base loading of the craft is not excessive.

The purpose of the research reported upon herein was to determine the performance and stability advantages that could be obtained by the addition of wings to a ground effect machine. The work is both theoretical and experimental, the latter being accomplished both with models and a winged version of the full scale Curtiss-Wright Air Car.

Results indicate that substantial gains in both performance and stability are attainable by such a hybrid machine when compared to the pure GEM.

It is generally concluded that for the high speed cruise condition wings will be found most beneficial if the base loading of the craft is not excessive.

The purpose of the research reported upon herein was to determine the performance and stability advantages that could be obtained by the addition of wings to a ground effect machine. The work is both theoretical and experimental, the latter being accomplished both with models and a winged version of the full scale Curtiss-Wright Air Car.

Results indicate that substantial gains in both performance and stability are attainable by such a hybrid machine when compared to the pure GEM.

It is generally concluded that for the high speed cruise condition wings will be found most beneficial if the base loading of the craft is not excessive.

The purpose of the research reported upon herein was to determine the performance and stability advantages that could be obtained by the addition of wings to a ground effect machine. The work is both theoretical and experimental, the latter being accomplished both with models and a winged version of the full scale Curtiss-Wright Air Car.

Results indicate that substantial gains in both performance and stability are attainable by such a hybrid machine when compared to the pure GEM.

It is generally concluded that for the high speed cruise condition wings will be found most beneficial if the base loading of the craft is not excessive.

The purpose of the research reported upon herein was to determine the performance and stability advantages that could be obtained by the addition of wings to a ground effect machine. The work is both theoretical and experimental, the latter being accomplished both with models and a winged version of the full scale Curtiss-Wright Air Car.

Results indicate that substantial gains in both performance and stability are attainable by such a hybrid machine when compared to the pure GEM.

It is generally concluded that for the high speed cruise condition wings will be found most beneficial if the base loading of the craft is not excessive.

AD _____ Accession No. _____
Princeton University Aero. Eng. Dept.,
Princeton, New Jersey

THE GENERAL CHARACTERISTICS OF WINGED
GROUND EFFECT MACHINES
- D.R. Summers, G.P. Carr, J.J. Metzko,
W.B. Nixon and A.F. Wojciechowicz, Jr.

Report No. 657, June 1963
140 pp.

Contract No. DA44-177-TC-833
Project No. 9R38-11-009-03
Unclassified Report

UNCLASSIFIED
1. Ground Effect
Machines

2. Performance,
winged ground
effect machines

3. Stability, winged
ground effect
machines

4. D.R. Summers
G.P. Carr
J.J. Metzko
W.B. Nixon

A. Wojciechowicz
Contract No. DA44-177-TC-833
Project No. 9R38-11-009-03
Unclassified Report

AD _____ Accession No. _____

Princeton University Aero. Eng. Dept.,
Princeton, New Jersey

THE GENERAL CHARACTERISTICS OF WINGED
GROUND EFFECT MACHINES

- D.R. Summers, G.P. Carr, J.J. Metzko,
W.B. Nixon and A.F. Wojciechowicz, Jr.

Report No. 657, June 1963
140 pp.

Contract No. DA44-177-TC-833
Project No. 9R38-11-009-03
Unclassified Report

UNCLASSIFIED

1. Ground Effect
Machines

2. Performance,
winged ground
effect machines

3. Stability, winged
ground effect
machines

4. D. R. Summers
G. P. Carr
J. J. Metzko
W. B. Nixon

A. Wojciechowicz
Contract No.
DA44-177-TC-833

AD _____ Accession No. _____

Princeton University Aero. Eng. Dept.,
Princeton, New Jersey

THE GENERAL CHARACTERISTICS OF WINGED
GROUND EFFECT MACHINES

- D.R. Summers, G.P. Carr, J.J. Metzko,
W.B. Nixon and A.F. Wojciechowicz, Jr.

Report No. 657, June 1963
140 pp.

Contract No. DA44-177-TC-833
Project No. 9R38-11-009-03
Unclassified Report

UNCLASSIFIED
1. Ground Effect
Machines

2. Performance,
winged ground
effect machines

3. Stability, winged
ground effect
machines

4. D.R. Summers
G.P. Carr
J.J. Metzko
W.B. Nixon

A. Wojciechowicz
Contract No. DA44-177-TC-833
Project No. 9R38-11-009-03
Unclassified Report

AD _____ Accession No. _____

Princeton University Aero. Eng. Dept.,
Princeton, New Jersey

THE GENERAL CHARACTERISTICS OF WINGED
GROUND EFFECT MACHINES

- D.R. Summers, G.P. Carr, J.J. Metzko,
W.B. Nixon and A.F. Wojciechowicz, Jr.

Report No. 657, June 1963
140 pp.

Contract No. DA44-177-TC-833
Project No. 9R38-11-009-03
Unclassified Report

UNCLASSIFIED

1. Ground Effect
Machines

2. Performance,
winged ground
effect machines

3. Stability, winged
ground effect
machines

4. D. R. Summers
G. P. Carr
J. J. Metzko
W. B. Nixon

A. Wojciechowicz
Contract No.
DA44-177-TC-833

The purpose of the research reported upon herein was to determine the performance and stability advantages that could be obtained by the addition of wings to a ground effect machine. The work is both theoretical and experimental, the latter being accomplished both with models and a winged version of the full scale Curtiss-Wright Air Car.

Results indicate that substantial gains in both performance and stability are attainable by such a hybrid machine when compared to the pure GEM.

It is generally concluded that for the high speed cruise condition wings will be found most beneficial if the base loading of the craft is not excessive.

The purpose of the research reported upon herein was to determine the performance and stability advantages that could be obtained by the addition of wings to a ground effect machine. The work is both theoretical and experimental, the latter being accomplished both with models and a winged version of the full scale Curtiss-Wright Air Car.

Results indicate that substantial gains in both performance and stability are attainable by such a hybrid machine when compared to the pure GEM.

It is generally concluded that for the high speed cruise condition wings will be found most beneficial if the base loading of the craft is not excessive.

The purpose of the research reported upon herein was to determine the performance and stability advantages that could be obtained by the addition of wings to a ground effect machine. The work is both theoretical and experimental, the latter being accomplished both with models and a winged version of the full scale Curtiss-Wright Air Car.

Results indicate that substantial gains in both performance and stability are attainable by such a hybrid machine when compared to the pure GEM.

It is generally concluded that for the high speed cruise condition wings will be found most beneficial if the base loading of the craft is not excessive.

The purpose of the research reported upon herein was to determine the performance and stability advantages that could be obtained by the addition of wings to a ground effect machine. The work is both theoretical and experimental, the latter being accomplished both with models and a winged version of the full scale Curtiss-Wright Air Car.

Results indicate that substantial gains in both performance and stability are attainable by such a hybrid machine when compared to the pure GEM.

It is generally concluded that for the high speed cruise condition wings will be found most beneficial if the base loading of the craft is not excessive.